

Chapter 3

Turbulence Mixing

3.1 Introduction.

One of the most striking properties of turbulence is its ability to mix scalars (temperature, pollutants, chemical species) orders of magnitude faster than molecular diffusion alone. This enhanced mixing arises from the multi-scale structure of turbulent eddies. In nature, the dynamics of the atmosphere and oceans are strongly governed by scalar-mixing processes; similarly, phenomena ranging from stirring sugar into coffee, to industrial blending of fluids, to fuel–oxygen mixing in combustion chambers all rely on turbulent mixing.

Understanding mixing therefore requires more than the governing equations — it requires identifying the *characteristic scales and times* that describe how turbulent motions transport and dissipate scalar variance.

Turbulence is inherently multi-scale, no single length or time scale can capture its dynamics. In this chapter, we focus on the *physical interpretation* of these scales and their connection to mixing time-scales. Formal statistical definitions and derivations are presented in the following chapter Chapter 3; here, our aim is to build the intuition necessary for estimating how fast turbulence mixes scalars across a range of flows.

3.2 Why turbulent mixing matters.

1. **Climate and Atmosphere:** The Sun warms the tropics far more than the poles, creating a strong equator-to-pole temperature gradient. Without motion, this gradient would persist — tropics baking, poles freezing, mid-latitudes trapped in between. Instead, turbulent eddies and waves transport warm air poleward and cold air equatorward, blending them into the temperate conditions we know.
2. **Oceans:** Warm, light water overlies cold, dense water. Without turbulence, this stratification would persist indefinitely. Currents, winds, and tides inject turbulent motions that overturn layers, mixing heat, nutrients, and dissolved gases throughout the water column.
3. **Mixers** Pour cream into coffee and it will form slow, curling filaments; without stirring, they take minutes to blend. With a spoon, you inject turbulence — streaks stretch, fold, and fragment into ever finer scales until the drink is uniform.
4. **Combustion Systems:** Inject fuel into still air and it will form smooth plumes that mix slowly. Introduce turbulence — via swirl vanes, sharp velocity gradients, or sudden expansions — and the fuel sheet shreds into thin ribbons that wrap through the air, producing a nearly perfect mixture in milliseconds. Industrial burners, gas turbines, and refinery mixers use this principle deliberately: the faster and more uniformly fuel and oxidizer mix, the more efficient and cleaner the burn.

Whether in a coffee cup, a jet engine, or a chemical reactor, turbulence multiplies contact between components, accelerates the erosion of concentration gradients, and produces uniform mixtures in a fraction of the time molecular diffusion could

achieve.

Whether driven by shear or buoyancy, the root cause of turbulence production is a *gradient* in velocity, temperature, or density that injects energy into the flow. In shear-driven turbulence, velocity gradients create layers sliding past each other, producing fluctuating momentum transport known as *Reynolds stresses*. In buoyancy-driven turbulence, temperature or composition gradients cause lighter fluid to rise and heavier fluid to sink, producing fluctuating vertical motions and associated turbulent stresses. In both cases, these turbulent stresses transfer energy from the mean flow (or mean density distribution) into chaotic fluctuations, dramatically increasing effective mixing rates.

Large eddies carry fluid parcels across many gradient lengths in a single motion. As these eddies break down into smaller ones, the *turbulent cascade* passes energy to ever-finer scales until molecular diffusion finally completes the homogenization.

3.3 Characteristics of Turbulent Flows

Turbulent flows are marked by irregular, three-dimensional motions with strong velocity fluctuations across a wide range of scales. They typically arise at high Reynolds numbers, where inertial forces dominate viscous forces, and are a property of the *flow* rather than of the fluid itself. In everyday and engineering contexts, turbulence is the rule rather than the exception—present in atmospheric winds, ocean currents, combustion chambers, industrial mixers, and even the air moving around you now.

Key characteristics of turbulent flows include:

- **Irregularity and Chaos** Observe smoke rising from a chimney or measure velocity in a turbulent pipe: no exact pattern repeats itself. This apparent randomness means deterministic prediction of the exact motion is impractical.

However, statistical quantities such as mean velocities, variances, and correlations are repeatable and form the basis for turbulence modeling and theory.

- **Enhanced Mixing** Turbulent motions transport momentum, heat, and scalar quantities far more efficiently than laminar flows. In laminar wind over water, the surface may ripple but particles remain largely in place; in turbulence, eddies carry particles over large distances, blending temperature, momentum, and chemical species.
- **Flow Property, Not Fluid Property** Turbulence is a state of motion, not a property of the substance.
- **Three-Dimensionality and Vorticity** Turbulent flows contain complex vortex structures. Sustained turbulence requires *vortex stretching*, a process unique to three-dimensional flows, where vortices are elongated and intensified, feeding energy into smaller scales.
- **Large Reynolds Number** Most turbulent flows have high Reynolds numbers, indicating that inertial effects dominate over viscous effects. Stability theory seeks to determine the critical Reynolds number above which laminar flow transitions to turbulence—one of the central challenges of fluid mechanics.
- **Dissipation and Energy Cascade** Turbulence rapidly converts large-scale kinetic energy into smaller-scale motion via the cascade process, ultimately dissipating energy as heat through molecular viscosity at the smallest scales. The dissipation rate is much higher than in laminar flows, so without continuous energy input, turbulence decays.
- **Intermittency** Turbulent energy is not evenly distributed in space or time. Large eddies can produce bursts of intense small-scale activity, and the cascade process itself can amplify these fluctuations. Intermittency occurs across the energy-containing, inertial, and dissipation ranges, making the local turbulence intensity highly variable even in statistically steady flows.

In summary, turbulence is a multi-scale, three-dimensional, energy-dissipating process that enhances transport far beyond molecular diffusion. Its apparent randomness conceals an underlying statistical structure, which is why turbulence theory often combines physical reasoning with statistical and spectral descriptions.

3.4 Turbulence categories

Two broad classes of turbulence dominate how mixing occurs:

Mechanical Generation of Turbulence with scalars

Mechanical generation of turbulence occurs when a mean velocity gradient, such as $\frac{dU}{dz}$, acts as a source of turbulent energy. The velocity shear extracts energy from the mean flow and converts it into velocity fluctuations, denoted by u', v', w' . These velocity fluctuations interact with scalar fluctuations, such as temperature or concentration, and give rise to turbulent scalar flux terms like $\overline{w'\phi'}$. The scalar fluxes transport scalars from regions of high mean value to regions of low mean value, thereby enhancing mixing and homogenization within the flow. In this process, the mean shear drives velocity perturbations, the perturbations correlate with scalar variations, and the resulting turbulent fluxes redistribute the scalar field. The mixing is therefore a direct outcome of the coupling between mechanically generated turbulence and scalar transport, where the source of turbulence is the velocity gradient and the effect is the redistribution and smoothing of scalar gradients across the flow.

Buoyant Generation of Turbulence with Scalars

Buoyant generation of turbulence arises when density variations in a gravitational field lead to convective motions. A mean scalar gradient, such as a vertical temperature gradient $\frac{dT}{dz}$, produces regions of lighter, warmer fluid below heavier, cooler fluid. This unstable stratification generates buoyancy-driven velocity fluctuations, represented by w' , which in turn correlate with scalar fluctuations θ' . The resulting turbulent scalar flux, expressed as $\overline{w'\theta'}$, represents the vertical transport of heat or other scalars by turbulent eddies. Unlike mechanical generation, where turbulence extracts energy from mean shear, buoyant generation extracts energy from the available potential energy of the stratified fluid. The scalar fluxes transport scalars vertically, creating strong mixing and overturning that homogenizes the scalar field. Thus, buoyant turbulence is generated directly by the conversion of potential energy into kinetic energy, with scalar gradients serving as both the source of turbulence and the medium through which turbulent fluxes redistribute energy and matter.

3.5 Laminar mixing

Let us start the chapter by understanding what is mixing ? What are the differences between Laminar mixing and Turbulent mixing?

In laminar flows, the fluid moves in smooth, orderly layers. Molecules transfer mass, momentum, and energy through direct, orderly motion.

Fick's Second Law of Diffusion

The unsteady diffusion of a scalar (such as concentration or temperature) in one spatial dimension is governed by Fick's

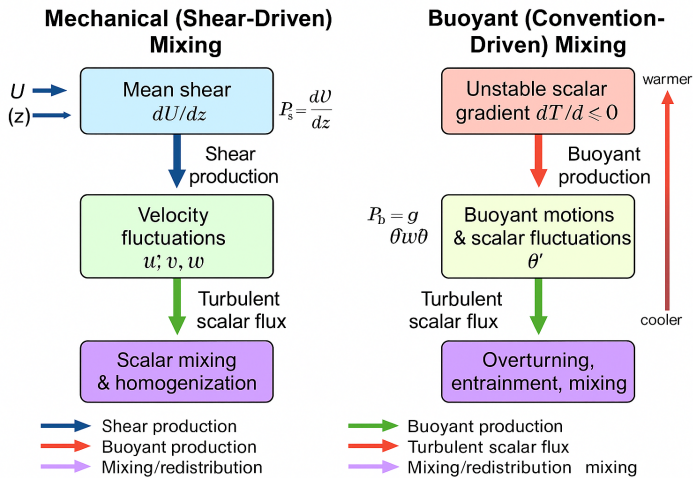


Figure 3.1: Mechanical and Buoyant generation of Turbulence with scalar.

second law:

$$\frac{\partial \phi}{\partial t} = \mu \frac{\partial^2 \phi}{\partial x^2} \quad (3.1)$$

Where, $\phi(x, t)$ is the scalar field (e.g., concentration), μ is the molecular diffusivity [units: m^2/s], x is the spatial coordinate and t is time.

Order-of-Magnitude Estimation

To estimate the characteristic time scale for diffusion over a length scale L , we apply dimensional (scaling) analysis to Eq. 3.2.

We define a time scale t_d and a length scale L , where we assume that the changes in ϕ occur. Let us assume that $t \sim t_d$, $x \sim L$

Then the terms in Eq. 3.2 scale as:

$$\underbrace{\frac{\partial \phi}{\partial t}}_{\sim \phi/t_d} = \mu \underbrace{\frac{\partial^2 \phi}{\partial x^2}}_{\sim \phi/L^2} \quad (3.2)$$

We obtain

$$\frac{\phi}{t_d} \sim \mu \frac{\phi}{L^2}.$$

Canceling ϕ (assuming it is non-zero) and rearranging gives

$$t_d \sim \frac{L^2}{\mu}. \quad (3.3)$$

Equation 3.3 provides the characteristic diffusion time over a distance L . The quadratic dependence on L demonstrates why diffusion is extremely slow across large distances.

Example: 3.1: Salt Dissolving in Still Water

Consider a small salt crystal is dropped into a quiescent tank of still water, the only mechanism available to mix the dissolved ions is through **molecular diffusion**. Because the surrounding fluid is initially at rest, there are no velocity gradients to generate shear or turbulence; therefore, the mass transfer process is *laminar* in the strictest sense.

The resulting mixing process is governed by Fick's second law; hence, we can assume that,

- Length scale: $L \sim 0.01$ m (1 cm),
- Diffusivity of salt in water: $\mu \sim 1 \times 10^{-9}$ m²/s.

$$t_d \sim \frac{(0.01)^2}{10^{-9}} = 1 \times 10^5 \text{ s} \approx 28 \text{ hours}$$

This simple estimate shows that, without stirring or turbulence, even small-scale diffusion is slow, highlighting the inefficiency of pure molecular diffusion for mixing in quiescent fluids.

3.6 Turbulent Mixing

Turbulent scalar mixing begins with a gradient of velocity, temperature, or concentration. This gradient acts as a source of instability, initiating fluctuations that lead to mixing. The consequences of mixing are a homogenous mixture where the gradients of temperature, concentration, or any other scalar will diminish. In the limit $t \rightarrow \infty$ the mean scalar becomes a spatial constant, all gradients vanish, and further transport proceeds only by molecular mixing. In particular, turbulent kinetic energy (TKE) is produced by velocity shear in the mean flow; the process is known as *mechanical generation* or *shear production*. When adjacent fluid layers move at different velocities, velocity gradients (shear) stretch and tilt turbulent eddies, transferring energy from the mean flow into turbulent fluctuations. This process is distinct from buoyant production, where turbulence arises from density or temperature differences.

We introduce the concept of Reynolds decomposition first.

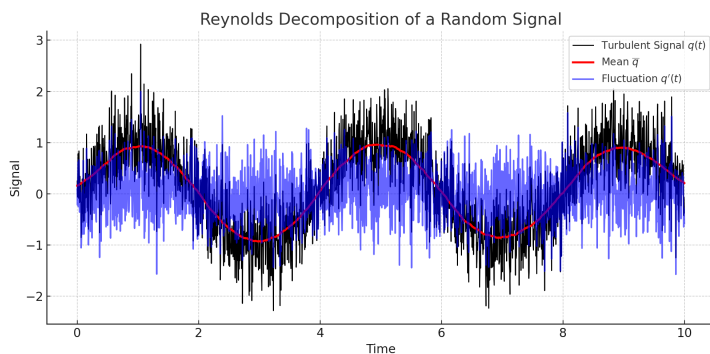


Figure 3.2: Reynolds decomposition of a random scalar signal $q(t)$. The curve $q(t)$ is split as $q(t) = \bar{q} + q'(t)$, where the running mean approximates the time average \bar{q} and the fluctuation is $q'(t) = q(t) - \bar{q}$.

Let $q(t)$ be a turbulent signal (scalar in this example).

We define the long-time average over a long time-period T as,

$$\bar{q}(t) = \frac{1}{T} \int_t^{t+T} q(\tau) d\tau, \quad (3.4)$$

for averaging window T large compared to turbulent timescales.

We define the *ensemble average* of a random turbulent signal $q(t)$ as:

$$\langle q(t) \rangle = \lim_{N \rightarrow \infty} \frac{1}{N} \sum_{n=1}^N q^{(n)}(t), \quad (3.5)$$

where

- $q^{(n)}(t)$ is the n^{th} realization (or outcome) of the random process q ,
- n is the index labeling each realization,
- N is the total number of realizations.

If we conduct 100 repeated wind-tunnel experiments under the same inlet and boundary conditions, then

$$q^{(1)}(t), q^{(2)}(t), \dots, q^{(n)}(t)$$

denote the measured velocity signals from the 1st, 2nd, ..., n^{th} runs, respectively. The ensemble average at time t is then

$$\langle q(t) \rangle = \frac{1}{N} \sum_{n=1}^N q^{(n)}(t).$$

In practice, repeated experiments may not be feasible. Instead, we often replace the ensemble average by a *time average*:

$$\bar{q}(t) = \lim_{T \rightarrow \infty} \frac{1}{T} \int_t^{t+T} q(\tau) d\tau.$$

The Reynolds averaging is defined as the process of decomposing any instantaneous turbulence quantity into a long-time averaged mean and a fluctuating component. This framework was

introduced by Osborne Reynolds. The Reynolds Decomposition is defined as follows:

$$q(t) = \bar{q} + q'(t), \quad \bar{q}' = 0. \quad (3.6)$$

The following are the properties of Reynolds Averaging. For any a, b and constant c ,

$$\begin{aligned} \overline{a+b} &= \bar{a} + \bar{b}, \\ \overline{ca} &= c\bar{a}, \\ \overline{ab} &= \bar{a}\bar{b} + \overline{a'b'}. \end{aligned} \quad (3.7)$$

3.6.1 Reynolds Averaged Scalar Transport Equation

For a passive scalar $\phi(\mathbf{x}, t)$ advected by a mean flow with uniform velocity $(U_1, 0, 0)$, the instantaneous scalar transport equation advected with mean velocity U_1 is:

$$\frac{\partial \phi}{\partial t} + U_1 \frac{\partial \phi}{\partial x_j} = \alpha \frac{\partial^2 \phi}{\partial x_j^2}, \quad (3.8)$$

where $\alpha = \mu/\rho$ is the molecular diffusivity of the scalar.

Reynolds Averaging: Applying Reynolds decomposition (Eq.3.6) for the ,

$$\phi = \bar{\phi} + \phi', \quad U_1 = \overline{U_1} + u'_1 \quad (3.9)$$

Here, $\bar{\phi}$ is the time-averaged mean concentration, and $\overline{U_1}$ is the mean velocity which is the same as the imposed uniform velocity U_1 in this problem; and ϕ' is the scalar fluctuations, and (u'_1, u'_2, u'_3) are the velocity fluctuations. Note that as we are writing the equation for advection with the mean velocity U_1 , the components u'_2, u'_3 do not appear in the equations. It should be noted that when we

Plug in Eq.3.9 in Eq.3.8,

$$\frac{\partial(\bar{\phi} + \phi')}{\partial t} + (\bar{U}_1 + u'_1) \frac{\partial(\bar{\phi} + \phi')}{\partial x_j} = \alpha \frac{\partial^2(\bar{\phi} + \phi')}{\partial x_j^2}. \quad (3.10)$$

,

We take a time-average of the above equation, and this is represented by the operator $\bar{()}$, resulting in,

$$\overline{\frac{\partial(\bar{\phi} + \phi')}{\partial t}} + \overline{(\bar{U}_1 + u'_1)} \frac{\partial(\bar{\phi} + \phi')}{\partial x_j} = \alpha \overline{\frac{\partial^2(\bar{\phi} + \phi')}{\partial x_j^2}}. \quad (3.11)$$

,

Recognizing the following: $\overline{\frac{\partial(\phi')}{\partial t}} = 0$, $\overline{\frac{\partial(\phi')}{\partial x_j}} = 0$, $\overline{\frac{\partial(U_1 \phi')}{\partial x_j}} = 0$, uniform mean velocity it does not vary spatially, the resultant equation is,

$$\frac{\partial \bar{\phi}}{\partial t} + \bar{U}_1 \frac{\partial \bar{\phi}}{\partial x_j} = \alpha \frac{\partial^2 \bar{\phi}}{\partial x_j^2} - \frac{\partial \bar{u}'_1 \phi'}{\partial x_j}. \quad (3.12)$$

The additional term $\overline{u'_1 \phi'}$ is the *turbulent scalar flux*.

3.7 Gradient-Diffusion Hypothesis (with a single local scale)

A *single* local turbulence scale (velocity u' and length ℓ) controls transport. The turbulent scalar flux is modeled analogously to Fick's law:

$$\overline{u'_1 \phi'} = -K_\phi \frac{\partial \bar{\phi}}{\partial x_j}, \quad (3.13)$$

where K_ϕ is the *eddy (turbulent) diffusivity* and κ is the molecular diffusivity.

Substituting (3.13) into (3.12) gives

$$\frac{\partial \bar{\phi}}{\partial t} + U_1 \frac{\partial \bar{\phi}}{\partial x_j} = \frac{\partial}{\partial x_j} \left[(\kappa + K_\phi) \frac{\partial \bar{\phi}}{\partial x_j} \right], \quad (3.14)$$

so the effective diffusivity is $\alpha_{\text{eff}} = \kappa + K_\phi$ with $K_\phi \gg \kappa$ in turbulence.

Scaling. Assuming $\phi' \sim \ell |\nabla \bar{\phi}|$ and a velocity scale u' , we obtain

$$K_\phi \sim C_\phi u' \ell, \quad C_\phi = \mathcal{O}(1), \quad (3.15)$$

and the mixing time over a layer of thickness L :

$$t_{\text{mix}} \sim \frac{L^2}{\kappa + K_\phi} \approx \frac{L^2}{u' \ell} \sim \frac{L}{u'} \text{ if } L \sim \ell. \quad (3.16)$$

3.8 Eddy Turnover time

Mixing in turbulent flows occurs over a wide range of time-scales. At one extreme, the integral scale represents the largest eddies in the flow. These large motions have sizes comparable to the characteristic dimension of the flow region (e.g., pipe diameter, boundary layer thickness, or stirred container size). The associated integral time-scale is

$$t_L \sim \frac{L}{u'}, \quad (3.17)$$

which is the time required for a large eddy to turn over. This sets the fastest effective stirring time, since these eddies sweep and fold scalar fields into smaller and smaller scales.

At the other extreme lies molecular diffusion, which operates at the smallest length scales where velocity fluctuations no longer dominate. The diffusive time-scale is

$$t_d \sim \frac{\ell^2}{\alpha}, \quad (3.18)$$

with ℓ the smallest scalar structures and α the molecular diffusivity. This represents the slowest possible mixing, since molecular transport alone is very inefficient compared to turbulent stirring.

Between these two extremes, turbulence provides a continuous

range of scales: large eddies stretch and fold scalar fields into smaller scales until the scalar gradients become so sharp that diffusion acts rapidly. Thus, turbulent mixing time-scales span from the relatively short eddy-turnover time at the integral scale to the very long diffusive time in the absence of stirring.

The key idea is that turbulence accelerates mixing by replacing the very slow diffusive time with a much shorter eddy-turnover time, effectively bridging the two ends of the spectrum.

Schematic Representation

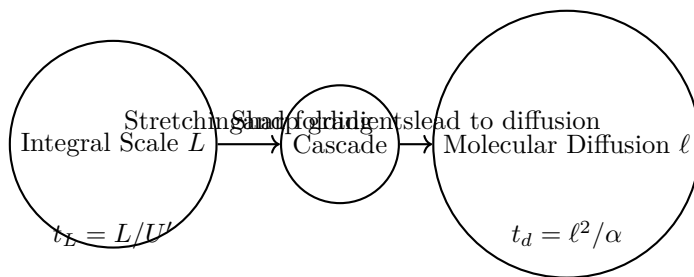


Figure 3.3: Schematic of turbulent mixing time-scales, with integral-scale eddy turnover time at one end and molecular diffusion time at the other. Turbulence bridges these extremes through a cascade of motions.

Eddy turnover time tells us how quickly large swirls can move fluid parcels around, fold them together, and promote mixing. Later, we will see how smaller and faster eddies emerge from these large motions, but for now the integral scale and its turnover time provide the fundamental reference for understanding turbulent mixing.

Key Concept: Turbulent Mixing Time-Scales

To understand turbulent mixing, it is essential to recognize the range of time-scales present in turbulent flows. At the upper end lies the **integral time-scale**, associated with the largest eddies that dominate stirring through vortex motion, stretching, and folding of fluid parcels. At the lower end are the **molecular diffusion time-scales**, where dissipation finally smooths out scalar gradients. Between these two extremes exists a continuum of eddy sizes, each with its own turnover time.

The central concept behind turbulent mixing is the **scalar turbulent flux term**, which represents the correlation between scalar fluctuations and velocity fluctuations. While each turbulent quantity:velocity, scalar, or pressure behaves as a seemingly random signal, their statistical correlations provide the organizing principle that governs mixing. These correlations are the defining characteristic of turbulence, enabling the transport and homogenization of momentum, heat, and scalars far more rapidly than molecular diffusion alone.

In the following chapters, we will analyze these correlations in greater depth and develop the statistical framework that explains how turbulent fluctuations combine to produce coherent fluxes and efficient mixing.

Example 3.3: Stirred Coffee Mixing Time

A typical mug has inner diameter $D \approx 9$ cm (radius $R \approx 4.5\text{--}5$ cm) and liquid depth $\approx 9\text{--}10$ cm. A teaspoon (or stirrer) has width $\approx 2\text{--}3$ cm. A gentle stir produces RMS fluctuations $u' \approx 0.10 \text{ m s}^{-1}$.

We need to estimate the *integral length scale* l , the *mixing length* L , turbulent fluctuation u' , the turbulent scalar diffusivity

$\alpha_t \sim u'l$ to calculate the mixing time $t_{\text{mix}} \sim \frac{L^2}{\alpha_t}$ (from Eq.??.

The dominant energy-containing eddies are set by the shear layer around the spoon/vortex core. A reasonable choice is the spoon width $l \approx 2$. We can assume the mixing length $L \approx R \approx 5$ cm.

We can assume u' to be of 30% of the mean fluid speed generated by the stirring motion. If the spoon moves at roughly 0.3 m/s (U_s) and imparts similar speeds to the surrounding fluid, the kinetic energy per unit mass introduced by stirring is $KE \sim \frac{1}{2}U_s^2$. Assuming this energy is cascaded into turbulent eddies, the characteristic velocity of turbulent fluctuations u' is 30% of the stirring velocity, $u' = k^{\frac{1}{2}} \sim 0.3U_s$.

With $u' = 0.10 \text{ m s}^{-1}$, $l = 0.02 \text{ m}$, $L = 0.05 \text{ m}$:

$$\alpha_t \approx u'l = (0.10)(0.02) = 2.0 \times 10^{-3} \text{ m}^2 \text{s}^{-1},$$

$$t_{\text{mix}} \approx \frac{L^2}{\alpha_t} = \frac{(0.05)^2}{2.0 \times 10^{-3}} = \frac{2.5 \times 10^{-3}}{2.0 \times 10^{-3}} \approx 1.25 \text{ s}.$$

Comparison to molecular diffusion. For heat in water, $\alpha \approx 1.4 \times 10^{-7} \text{ m}^2 \text{s}^{-1}$:

$$t_d \approx \frac{L^2}{\alpha} = \frac{2.5 \times 10^{-3}}{1.4 \times 10^{-7}} \approx 1.8 \times 10^4 \text{ s} \approx [5 \text{ h}].$$

Thus, turbulent stirring reduces the mixing time from hours to seconds.

Note that larger l (bigger spoon) or larger u' (faster stir) increases $\alpha_t = u'l$ and shortens t_{mix} .

Example 3.4 : Smoke Dispersal in Turbulent Air

Consider a turbulent atmospheric flow where the mean wind speed is approximately $U_s \sim 5 \text{ m/s}$. Smoke plume is released into the atmosphere. The plume spread is characterized by a

length scale of $L \sim 10$ m, while the integral length scale of the largest eddies is estimated as $l \sim 1$ m. Using these parameters, estimate the characteristic eddy turnover time, the ratio of large-eddy time scales to mean advection time, and discuss how turbulent mixing compares with advection by the mean flow.

In this example, we assume that the density of the smoke is only marginally different from that of the ambient air, hence the buoyancy forces are negligible. The dominant mechanism of mixing is by the turbulent velocity fluctuations.

Let: $U_s \sim 5\text{m/s}$ (Wind speed), $u' \sim 1.5\text{ m/s}$ (turbulent fluctuation velocity is 30% of the wind), $L \sim 10\text{ m}$ (plume spread), $l \sim 1\text{ m}$ (integral length scale).

Then, using Eq.??

$$\alpha_t \sim u'l = 1.5 \times 1 = 1.5 \text{ m}^2/\text{s}$$

$$t_t \sim \frac{L^2}{\alpha_t} = \frac{100}{1.5} = 66 \text{ s} \approx 1.1 \text{ minutes}$$

Thus, turbulence reduces the mixing time from months to minutes. The mixing is greatly accelerated by the turbulent eddies. Instead of taking hours or days as would be expected with molecular diffusion alone, the scalar becomes uniformly distributed throughout the domain in approximately one minute. This example highlights the efficiency of turbulent mixing and the importance of eddy diffusivity in scalar transport. This is a very simplistic approximation, where we have assumed there is a single eddy that is formed, and the mixing is at the scale of this eddy. However, turbulence results in a cascade of eddies. Energy is injected at the large scale L , transported down to smaller scales via nonlinear interactions, until it reaches the *Kolmogorov scale*, where viscosity dominates and energy is dissipated as heat. The cascade ensures that large-scale stirring rapidly produces small-scale eddies, which are most effective at homogenizing scalars like temperature, dye, or concentration.

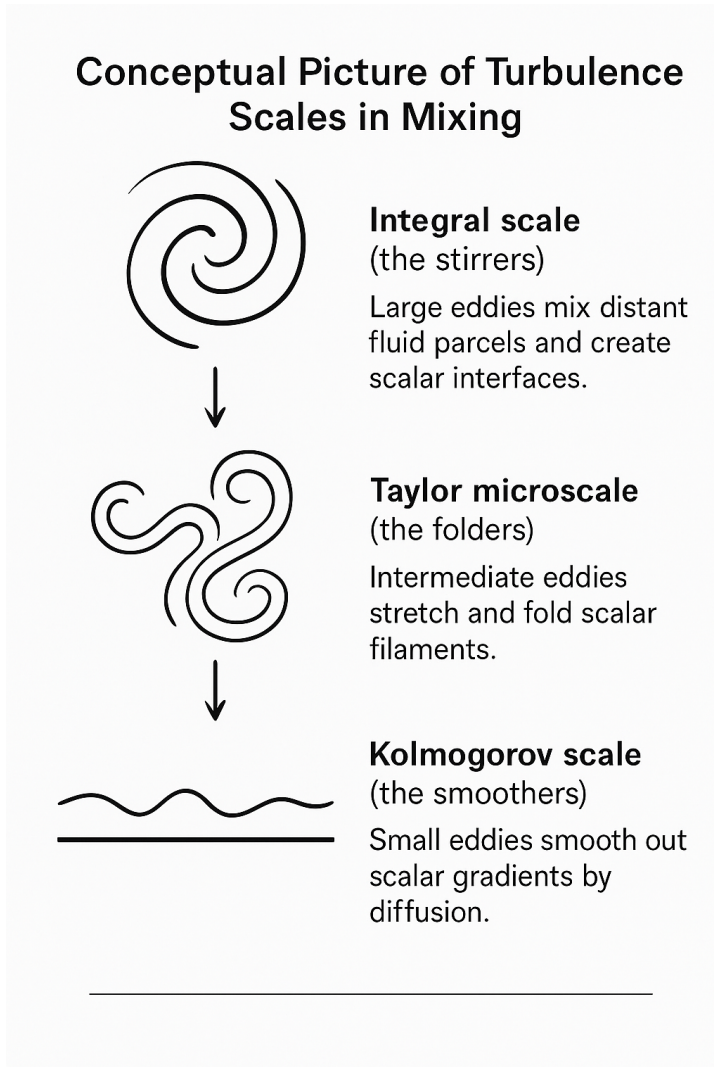


Figure 3.4: Conceptual picture of cascade model of turbulence in mixing: Large integral eddies (L), Intermediate eddies near the Taylor microscale (λ) and smallest Kolmogorov scale (η)

3.9 Buoyancy Generated Mixing

In addition to shear production, turbulence can also be generated through buoyancy. When the ground surface is heated, warmer and lighter air parcels rise while cooler parcels sink. This vertical motion couples temperature (or potential temperature θ) fluctuations directly to the turbulent velocity field. In the atmospheric boundary layer (ABL), turbulent exchange of heat and momentum is governed by surface fluxes and buoyancy generation. Unlike purely shear-driven turbulence, buoyancy couples scalar (temperature) fluctuations directly to turbulent kinetic energy (TKE) through vertical heat fluxes. Quantifying these fluxes and the associated similarity scales is essential for modeling surface-atmosphere exchange, atmospheric stability, and the relevant mixing time-scales.

3.9.1 Buoyancy-Driven Scalar Flux from a Heated Surface

Consider a uniformly heated horizontal plate that imposes a vertical mean thermal gradient. Let $\theta(x, y, z, t)$ denote potential temperature. Let the mean velocity be represented as u_j . In a thin surface layer above the plate, horizontal variations in mean fields are weak compared to vertical variations, so we assume horizontal homogeneity: $\partial_x(\cdot) = \partial_y(\cdot) = 0$ for mean quantities, with Boussinesq density variations and $\bar{w} = 0$.

We start with the Instantaneous scalar equation for potential temperature,

$$\frac{\partial \theta}{\partial t} + u_j \frac{\partial \theta}{\partial x_j} = \kappa \nabla^2 \theta + S, \quad (3.19)$$

where κ is the molecular diffusivity and S represents sources/sinks (often negligible in the surface layer away from the wall). Using the Reynolds decomposition Eq.3.6, we now decompose velocity and temperature into mean and fluctuating parts:

$$u_i = \bar{U}_i + u'_i, \quad \theta = \bar{\theta} + \theta'. \quad (3.20)$$

With horizontal homogeneity, $\bar{\theta} = \bar{\theta}(z, t)$ and $\bar{\mathbf{U}} = (\bar{U}(z, t), 0, 0)$. Where, S represents the sources/sinks and κ is the molecular diffusivity The Reynolds-averaged scalar equation is,

$$\begin{aligned} \frac{\partial \bar{\theta}}{\partial t} + \underbrace{\bar{u} \frac{\partial \bar{\theta}}{\partial x}}_{\approx 0} + \underbrace{\bar{v} \frac{\partial \bar{\theta}}{\partial y}}_{\approx 0} + \bar{w} \frac{\partial \bar{\theta}}{\partial z} \\ + \underbrace{\frac{\partial}{\partial x} \bar{u}' \bar{\theta}'}_{\ll \frac{\partial}{\partial z} \bar{w}' \bar{\theta}'} + \underbrace{\frac{\partial}{\partial y} \bar{v}' \bar{\theta}'}_{\ll \frac{\partial}{\partial z} \bar{w}' \bar{\theta}'} + \frac{\partial}{\partial z} \bar{w}' \bar{\theta}' = \kappa \nabla^2 \bar{\theta} + S. \end{aligned} \quad (3.21)$$

If we assume the mean subsidence $\bar{w} = 0$, the resultant equation is,

$$\frac{\partial \bar{\theta}}{\partial t} + \frac{\partial}{\partial z} \bar{w}' \bar{\theta}' = \kappa \frac{\partial^2 \bar{\theta}}{\partial z^2} + S. \quad (3.22)$$

Dominant vertical-flux assumption. In buoyancy-driven surface layers (heated from below), vertical motions dominate near the wall. Assume

$$w' \gg u', v' \quad (\text{for transport}), \quad \partial_z \bar{\theta} \neq 0, \quad \partial_x \bar{\theta} \approx \partial_y \bar{\theta} \approx 0.$$

Then the production of temperature fluctuations is primarily through the coupling term $w'(\partial \bar{\theta}/\partial z)$ in (??). Physically:

- Updrafts $w' > 0$ originating from the heated plate carry warmer-than-mean fluid ($\theta' > 0$).
- Downdrafts $w' < 0$ tend to carry cooler-than-mean fluid ($\theta' < 0$).

Both quadrants give a *positive* product $w' \theta'$, which builds a positive covariance $\bar{w}' \bar{\theta}'$ above a heated surface.

The measurable, mean turbulent flux is

$$q_z^{(\theta)} \equiv \overline{w'\theta'}. \quad (3.23)$$

In gradient-diffusion (eddy-diffusivity) form this is modeled as

$$\overline{w'\theta'} \approx -K_\theta \frac{\partial \bar{\theta}}{\partial z}, \quad (3.24)$$

with K_θ the eddy diffusivity for heat. Over a heated plate, $\partial \bar{\theta} / \partial z < 0$ (temperature decreases with height), so (3.24) gives $\overline{w'\theta'} > 0$, consistent with the quadrant argument above.

Surface heat and buoyancy flux. At the wall $z = 0$, the turbulent flux equals the imposed surface flux (to leading order in the roughness sublayer):

$$Q_H = \rho_0 c_p \overline{w'\theta'} \Big|_{z=0}, \quad B_0 = \frac{g}{\theta_0} \overline{w'\theta'} \Big|_{z=0}. \quad (3.25)$$

Here, Q_H is the sensible heat flux and B_0 is the surface buoyancy flux. Heating from below implies $Q_H > 0$ and $B_0 > 0$.

With w' dominating the turbulent transport, (3.22) reduces (steady, $\overline{S} \approx 0$) to

$$\frac{d}{dz} \overline{w'\theta'} \approx \kappa \frac{d^2 \bar{\theta}}{dz^2}. \quad (3.26)$$

A vertical mean thermal gradient over a heated plate generates temperature fluctuations θ' that are *correlated* with vertical velocity fluctuations w' . Under $w' \gg u', v'$, this produces a dominant, positive turbulent heat flux $\overline{w'\theta'}$ that carries heat upward. This is the key mechanism by which buoyancy generates scalar flux and drives turbulent mixing in the atmospheric surface layer.

Thus, just as mechanical shear produces scalar fluxes through $\overline{u'\phi'}$, buoyancy couples vertical motion and temperature fluctuations to produce $\overline{w'\theta'}$. In the ABL, this process controls the

growth of the convective boundary layer, sets characteristic velocity and temperature scales, and provides the essential input for similarity theory.

In later sections, we will use these fluxes to define convective scales such as the Deardorff velocity w_* and to establish the Monin-Obukhov framework for surface-layer similarity.

3.9.2 Convective Velocity and Temperature Scales

In a convective mixed layer of depth H (often denoted z_i), the Deardorff velocity scale is

$$w_* = (B_0 H)^{1/3}, \quad (3.27)$$

with a corresponding convective temperature scale

$$\theta_*^{(c)} = \frac{\overline{w'\theta'}|_0}{w_*}. \quad (3.28)$$

These give characteristic times for layer-scale transport:

$$\tau_* \sim \frac{H}{w_*}, \quad \tau_T \approx \frac{H \Delta\theta}{|\overline{w'\theta'}|}, \quad (3.29)$$

where $\Delta\theta$ is a representative mean temperature contrast across H .

3.9.3 Stratification and Brunt-Väisälä Frequency

Stratification is set by the vertical gradient of potential temperature. When $d\theta/dz > 0$ (air aloft is warmer in potential temperature sense), a vertically displaced parcel feels a restoring buoyancy force and oscillates about its original level; this is *stable* stratification. The oscillation rate is the Brunt-Väisälä frequency

$$N = \sqrt{(g/\theta) d\theta/dz}, \quad T_b = 2\pi/N \quad (3.30)$$

T_b is the time-period. For larger N means stronger resistance to vertical motion and suppressed turbulent mixing. When $d\theta/dz < 0$ (warmer near the surface), $N^2 < 0$ and N become imaginary: small vertical displacements grow rather than oscillate, signaling *unstable* stratification with buoyant convection, vigorous vertical transport, and typically positive $\overline{w'\theta'}$.

The *neutral* case has $d\theta/dz \approx 0$ (so $N \approx 0$), implying less buoyant effect and mixing governed primarily by shear.

Example 3.5: Density Currents

Lock Exchange Density Currents When two fluids of slightly different densities are initially separated and then allowed to interact (e.g., cold outdoor air entering a warm room through a gap under a door in winter), the denser fluid flows underneath the lighter fluid, with a well-defined gravity-current front. As the front advances, shear at the interface and buoyancy jointly produce turbulence, but the initial driving is from gravitational potential energy.

Problem (Convective room mixing). Consider a rectangular room of height $H = 2.5$ m in which a cold outdoor gravity current intrudes near the floor. From observations of the interior convective layer, the Deardorff velocity scale is estimated as $w_* \approx 0.33 \text{ m s}^{-1}$.

Given:

- Room height: $H = 2.5 \text{ m}$,
- Convective velocity: $w_* = 0.33 \text{ m s}^{-1}$,
- Reference potential temperature: $\theta_0 = 300 \text{ K}$,
- Air density: $\rho_0 = 1.2 \text{ kg m}^{-3}$,
- Specific heat (constant pressure): $c_p = 1005 \text{ J kg}^{-1} \text{ K}^{-1}$.

From the Deardorff relation (Eq. 3.25),

$$B_0 = \frac{w_*^3}{H} = \frac{(0.33)^3}{2.5} \approx 1.44 \times 10^{-2} \text{ m}^2 \text{ s}^{-3}. \quad (3.31)$$

Using $B_0 = \frac{g}{\theta_0} \overline{w'\theta'}$ (Eq. ??),

$$\overline{w'\theta'} = \frac{\theta_0}{g} B_0 \approx \frac{300}{9.81} (1.437 \times 10^{-2}) \approx 4.40 \times 10^{-1} \text{ K m s}^{-1}. \quad (3.32)$$

Define the convective temperature scale (Eq.3.28

$$\theta_*^{(c)} \equiv \frac{\overline{w'\theta'}}{w_*} \approx \frac{0.440}{0.33} \approx 1.33 \text{ K}. \quad (3.33)$$

The (dynamic) sensible heat flux (Eq.3.25) is

$$Q_H = \rho_0 c_p \overline{w'T'} \approx \rho_0 c_p \overline{w'\theta'} \approx (1.2)(1005)(0.440) \approx 5.31 \times 10^2 \text{ W m}^{-2}. \quad (3.34)$$

Convective (eddy-turnover) time (Eq. 3.27):

$$\tau_* = \frac{H}{w_*} = \frac{2.5}{0.33} \approx 7.6 \text{ s}. \quad (3.35)$$

Example 3.7: Convective Atmospheric Boundary Layer

On a warm summer afternoon over flat terrain, surface sensible-heat fluxes can reach

$$Q_0 \approx 500 \text{ W m}^{-2}.$$

For air at $T_0 \approx 300 \text{ K}$ and density $\rho \approx 1.2 \text{ kg m}^{-3}$, the corresponding *buoyancy flux* (Eq.3.25) is

$$B = \frac{g}{T_0 \rho c_p} Q_0 = \frac{9.81}{300} \frac{500}{(1.2)(1005)} \approx 1.35 \times 10^{-2} \text{ m}^2 \text{s}^{-3}.$$

If the mixed-layer depth is $H \approx 1200 \text{ m}$, the Deardorff convective velocity scale is

$$w_* = (B H)^{1/3} = [(1.35 \times 10^{-2})(1200)]^{1/3} \approx 2.6 \text{ m s}^{-1}.$$

The turnover time of the largest eddies spanning the ABL depth is calculated using Eq.3.27

$$\tau_{\text{turn}} = \frac{H}{w_*} \approx \frac{1200}{2.6} \approx 460 \text{ s} (\sim 8 \text{ min}).$$

This means that within about 8 minutes, a parcel can traverse the full ABL depth. Several such turnovers are typically needed for complete homogenization of heat, moisture, and tracers in the boundary layer.

In this convective ABL, turbulence is generated primarily by buoyancy due to surface heating. The energy-containing eddies span the entire mixed-layer depth, efficiently redistributing scalars. Small UAVs flying at 50–200 m altitude may encounter vertical gusts approaching $\pm w_*$, making stable flight control challenging.

Nomenclature

ϕ	Scalar quantity (e.g., temperature, concentration, salinity)
$\bar{\phi}$	Mean (time-averaged) scalar
\mathbf{u}	Instantaneous velocity vector
$\bar{\mathbf{u}}$	Mean velocity vector
u'_i	Fluctuating velocity component in the i direction
u'	Root-mean-square (RMS) turbulent velocity fluctuation
l	Integral length scale (size of the largest eddies)
L	Characteristic length scale of the mixing region
μ	Molecular diffusivity
μ_t	Eddy diffusivity (turbulent diffusivity)
k	Turbulent kinetic energy, $u' = \sqrt{k}$
t_{eddy}	Eddy turnover time
t_{mix}	Turbulent mixing time scale
t_d	Molecular-diffusion time scale
ε	Turbulent kinetic energy dissipation rate
u_l	Velocity fluctuation at scale l
t_l	Turnover time at scale l
g	Acceleration due to gravity
T'	Temperature fluctuation
w'	Vertical velocity fluctuation
T_0	Reference temperature
C	Scalar concentration (generic)
Q	Source strength or flux (when used in examples)
ρ	Density
Pr_t	Turbulent Prandtl number, $Pr_t = \mu_t/\alpha_t$
α_t	Turbulent thermal diffusivity

End-of-Chapter Problems

- Mixing-length baseline.** For a scalar with molecular diffusivity α in a turbulent region of size L , assume $\alpha_t \approx u'l$ with u' and l known. Show that $t_{\text{mix}} \sim L^2/(u'l)$. Evaluate t_{mix} and the ratio t_d/t_{mix} for $L = 0.05$ m, $u' = 0.10$ m s $^{-1}$, $l = 0.02$ m, and (i) heat in water $\alpha = 1.4 \times 10^{-7}$ m 2 s $^{-1}$, (ii) mass diffusion in water $D = 1 \times 10^{-9}$ m 2 s $^{-1}$.
- Stirred cup variants.** Using the stirred-coffee model, recompute t_{mix} for (a) a larger spoon $l = 0.03$ m, (b) faster stirring $u' = 0.2$ m s $^{-1}$, and (c) vertical mixing limited by depth $L = 0.10$ m with the baseline u', l . Comment on which change most reduces t_{mix} .
- Convective ABL scaling.** Given surface heat flux $Q_0 = 500$ W m $^{-2}$, air density $\rho = 1.2$ kg m $^{-3}$, $c_p = 1005$ J kg $^{-1}$ K $^{-1}$, $T_0 = 300$ K, and mixed-layer depth $H = 1200$ m: (a) compute the buoyancy flux $B = (g/T_0) Q_0 / (\rho c_p)$; (b) find the Deardorff velocity $w_* = (BH)^{1/3}$; (c) estimate the turnover time $\tau_{\text{turn}} = H/w_*$; (d) using $\mu_T \approx 0.1 w_* H$, estimate $t_{\text{mix}} \approx H^2/(2\mu_T)$.
- Rayleigh–Bénard convection.** For water at 30°C with $\beta = 2.1 \times 10^{-4}$ K $^{-1}$, $\nu = 1.0 \times 10^{-6}$ m 2 s $^{-1}$, $\alpha = 1.4 \times 10^{-7}$ m 2 s $^{-1}$, layer depth $H = 0.10$ m, and $\Delta T = 10$ K: (a) compute Ra and state the regime; (b) estimate $w_* = (g\beta\Delta TH)^{1/3}$; (c) compute $\tau_{\text{turn}} = H/w_*$; (d) estimate $\mu_T \approx 0.1 w_* H$ and $t_{\text{mix}} \approx H^2/(2\mu_T)$.
- Door-gap density current.** Cold air at $T_{\text{ext}} = 278$ K intrudes under a door into a room at $T_{\text{room}} = 298$ K. Gap depth $h = 0.02$ m. (a) Compute reduced gravity $g' = g\Delta T/T_0$ with $T_0 = 298$ K. (b) Estimate the front speed using $\text{Fr}_d \approx 1$: $U \approx \sqrt{g'h}$. (c) If the measured $w_* = 0.33$ m s $^{-1}$ and $H = 2.5$ m, estimate

- $\overline{w'T'} \approx w_*^3/[(g/T_0)H]$ and $P_b = (g/T_0)\overline{w'T'}$. (d) Compute $\tau_* = H/w_*$ and discuss mixing time compared with (b).
6. **Fuel-air premixing (jet in crossflow).** A jet of diameter $h = 0.02$ m injects fuel into air with $\Delta U = 40$ m s^{-1} , air density $\rho = 1.18$ kg m^{-3} , viscosity $\mu = 1.8 \times 10^{-5}$ Pa s , mass diffusivity $D_m = 7 \times 10^{-5}$ $\text{m}^2 \text{s}^{-1}$, reduced gravity $g' = 8.41$ m s^{-2} . Compute $Re = \rho\Delta Uh/\mu$, $Sc = \nu/D_m$, $\text{Fr}_d = \Delta U/\sqrt{g'h}$, and the eddy time $t_e \sim h/\Delta U$. Comment on which mechanism dominates initial mixing.
7. **Integral time scale from autocorrelation.** A probe records $u'(t)$ at $\Delta t = 0.1$ s. The normalized autocorrelation at lags $m = 0, 1, 2, 3, 4, 5$ is $\rho = [1, 0.7, 0.45, 0.25, 0.10, 0.00]$. Estimate the Eulerian integral time scale $T_E \approx \Delta t \sum_{m=0}^{m_0} \rho(m)$ (to the first zero crossing m_0). With $u' = 0.3$ m s^{-1} , estimate $\alpha_t \sim u'^2 T_E$ and $l \sim u' T_E$.
8. **Room mixing via covariance.** In a room of height $H = 2.5$ m with measured $w_* = 0.33$ m s^{-1} and $T_0 = 298$ K: (a) estimate $\overline{w'T'} \approx w_*^3/[(g/T_0)H]$; (b) compute $P_b = (g/T_0)\overline{w'T'}$; (c) find $\tau_* = H/w_*$; (d) for a bulk temperature difference $\Delta T = 5$ K, estimate $\tau_{\text{mix}} \sim (gH/T_0) \Delta T/P_b$. Comment on the relation between τ_* and τ_{mix} .

Notation (extended)

ϕ	Generic scalar (temperature T , potential temperature θ , salinity S , concentration c); units problem-dependent.
\mathbf{u}, u_i	Velocity vector and components (m s^{-1}).
κ	Molecular diffusivity of ϕ ($\text{m}^2 \text{s}^{-1}$).
K_ϕ	Eddy (turbulent) diffusivity of ϕ ($\text{m}^2 \text{s}^{-1}$).
K_m	Eddy viscosity ($\text{m}^2 \text{s}^{-1}$); $Pr_t = K_m/K_\phi$.
S_ϕ	Volumetric source/sink of ϕ (units of ϕs^{-1}).
$q_i^{(\phi)}$	Turbulent scalar flux $\overline{u'_i \phi'}$ (units of $\phi \text{ m s}^{-1}$).
b	Buoyancy $= -g\rho'/\rho_0$ (m s^{-2}); $\approx g\theta'/\theta_0$ (dry air).
$\overline{w'b'}$	Buoyancy flux (m s^{-3}); $= \frac{g}{\theta_0} \overline{w'\theta'}$.
B_0	Surface buoyancy flux $\overline{w'b'} _{z=0}$ (m s^{-3}).
Q_H	Surface sensible heat flux $\rho_0 c_p \overline{w'T'} _{z=0}$ (W m^{-2}).
k	Turbulent kinetic energy $\frac{1}{2} \overline{u'_i u'_i}$ ($\text{m}^2 \text{s}^{-2}$).
P_s, ε	Shear production and dissipation of TKE ($\text{m}^2 \text{s}^{-3}$).
L, H	Vertical or characteristic mixing thickness/depth (m).
L_{int}	Turbulent integral length scale (m); u' : rms velocity (m s^{-1}).
α_t	Effective (eddy) diffusivity $\kappa + K_\phi$ ($\text{m}^2 \text{s}^{-1}$).
w_*	Convective velocity scale $(B_0 H)^{1/3}$ (m s^{-1}).
τ_{diff}	Diffusive mixing time L^2/α_t (s).
τ_{flux}	Flux-controlled adjustment time $H \Delta\phi / \overline{w'\phi'} $ (s).
τ_e	Eddy-turnover time L_{int}/u' (s); $\tau_* = H/w_*$ (s).

3.10 Companion Python Notebook

The companion Python notebook *Scalar Mixing* is designed to operationalize the theory in this chapter by constructing a controlled synthetic dataset and applying it across eight focused demonstrations. The notebook mirrors the theoretical order of presentation: after restating learning goals and key equations, it generates a reproducible one-dimensional wall-normal profile that mimics channel-like turbulent scalar transport, and then evaluates standard diagnostic quantities (mean fields, variances, turbulent fluxes, eddy diffusivity, dissipation proxies, and characteristic time scales). Each example is intentionally compact and self-contained so that readers can verify definitions, closure relations, and qualitative trends without relying on external DNS or experimental datasets.

3.10.1 Notebook Architecture and Pedagogical Layout

The notebook is organized into the following sections:

1. **Learning Goals & Roadmap:** A brief outline mapping each theoretical concept to a concrete computation or plot.
2. **Key Equations:** Restatement of the scalar transport relations.
3. **Synthetic Dataset Generation:** Definition of the spatial grid, mean profiles, and fluctuation fields; construction of derived quantities (gradients, fluxes, variances).
4. **Examples 1-8:** Each example is presented with a problem statement, a solution method (analytical/numerical steps referencing the synthetic fields), and expected results (qualitative trends and quantitative signatures to check).
5. **Diagnostics & Consistency Checks:** Sanity checks

(signs, monotonicity, boundary behavior), and internal cross-verification (e.g., flux/gradient consistency in eddy-diffusivity estimates).

6. **Reproducibility Notes:** Notes on parameter seeds and the ordering of computations so outputs are deterministic.

This layout matches the didactic flow of the chapter: theory → definitions → controlled data → targeted demonstrations.

3.10.2 Synthetic Dataset Description

We consider a non-dimensional wall-normal coordinate $y \in [0, 1]$ discretized on a uniform grid. The dataset emulates a channel-like configuration with gently varying thermophysical properties and a passive scalar c . Ensemble (or long-time) means are denoted by $\bar{(\cdot)}$, fluctuations by $(\cdot)'$

Profiles and fields. The following mean profiles are prescribed:

$$\bar{\rho}(y) = \rho_0 + \rho_1 y, \quad \bar{T}(y) = T_0 + \Delta T y, \quad \bar{c}(y) = c_0 + \Delta c y, \quad (3.36)$$

with small-to-moderate density variation and a monotone mean scalar gradient $\partial \bar{c} / \partial y = \Delta c$.

Zero-mean, Gaussian-like synthetic fluctuations are generated for the wall-normal velocity v' and scalar c' with prescribed root-mean-squared (r.m.s.) levels and optional controlled correlation to produce a physically consistent turbulent scalar flux $\bar{v'c'}$. The Reynolds decomposition for a scalar is

$$c = \bar{c} + c', \quad \bar{c}' = 0, \quad (3.37)$$

Derived quantities. The turbulent scalar flux and variance are computed as

$$\bar{v'c'}(y), \quad \bar{c'^2}(y), \quad (3.38)$$

and an eddy-diffusivity estimate K_t is formed via the down-gradient closure

$$\overline{v'c'} = -K_t \frac{\partial \bar{c}}{\partial y} \Rightarrow K_t = -\frac{\overline{v'c'}}{\partial \bar{c}/\partial y}. \quad (3.39)$$

A standard variance budget proxy uses the production P_c and a dissipation-like measure χ ,

$$P_c \equiv -\overline{v'c'} \frac{\partial \bar{c}}{\partial y}, \quad \chi \equiv 2D \overline{\nabla c' \cdot \nabla c'}, \quad (3.40)$$

with D a molecular diffusivity (constant in the synthetic dataset unless otherwise specified). In weakly compressible cases, Favre averages ($\widetilde{\cdot}$) may replace Reynolds averages, but the dataset is constructed so that both are nearly coincident.

3.11 Example Demonstrations Using the Synthetic Dataset

3.11.1 Example 1: Mean Fields, Turbulent Flux, Variance, and Eddy Diffusivity

Problem Statement. Given $\bar{c}(y)$ and synthetic fluctuations $\{v', c'\}$, interpret the signs and magnitudes of $\overline{v'c'}(y)$, $\overline{c'^2}(y)$, and the implied $K_t(y)$ from (3.39).

Solution Method. Compute $\overline{v'c'}$ and $\overline{c'^2}$ directly from fluctuations, estimate K_t via (3.39), and compare its wall-normal variation to the imposed mean gradient $\partial \bar{c}/\partial y$.

Expected Results. For a positive mean gradient ($\partial \bar{c}/\partial y > 0$), physically consistent down-gradient transport yields $\overline{v'c'} < 0$ and $K_t > 0$. Variance $\overline{c'^2}$ peaks away from strictly laminar or highly damped near-wall regions, and K_t typically exhibits a broad interior maximum.

3.11.2 Example 2: Scalar Variance Production and Dissipation Proxy

Problem Statement. Using (3.40), evaluate $P_c(y)$ and $\chi(y)$ and discuss their relative magnitudes and spatial organization.

Solution Method. Form $P_c(y)$ from measured $\overline{v'c'}$ and the known gradient $\partial\bar{c}/\partial y$. Estimate $\chi(y)$ from synthetic scalar gradients $\nabla c'$.

Expected Results. $P_c(y)$ is positive where down-gradient transport operates ($\overline{v'c'} \partial\bar{c}/\partial y < 0$). The dissipation proxy $\chi(y)$ increases where fluctuation gradients intensify, often tracking regions of large K_t and/or sharp mean gradients. A qualitative balance $P_c \sim \chi$ is observed in statistically stationary regions.

3.11.3 Example 3: Shear Mixing, Turbulent Schmidt Number, and Closure Consistency

Problem Statement. Assess the consistency of the eddy diffusivity closure by relating K_t to an eddy viscosity ν_t through a turbulent Schmidt number Sc_t .

Solution Method. Suppose ν_t is modeled from a mixing-length or other shear-based closure. Define

$$Sc_t \equiv \frac{\nu_t}{K_t}. \quad (3.41)$$

Evaluate $Sc_t(y)$ and discuss its wall-normal variability and plausibility.

Expected Results. $Sc_t(y)$ remains $\mathcal{O}(1)$ in most of the interior; near-wall damping of ν_t and K_t can lead to deviations. The synthetic dataset is built so that Sc_t does not exhibit unphysical extremes.

3.11.4 Example 4: One-Dimensional Scalar Diffusion Response

Problem Statement. Given an initial scalar perturbation superposed on $\bar{c}(y)$, analyze the temporal relaxation of $c(y, t)$ under molecular diffusion D (no advection).

Solution Method. Consider

$$\frac{\partial c}{\partial t} = D \frac{\partial^2 c}{\partial y^2}, \quad c(y, 0) = \bar{c}(y) + \delta c(y), \quad (3.42)$$

with homogeneous Neumann or Dirichlet end conditions as appropriate. Track the decay of $c'(y, t)$ and the variance $\overline{c'^2}(t)$.

Expected Results. Exponential-like decay of modal content with rates $\propto Dk^2$; variance decreases monotonically. This establishes a baseline against which turbulent transport effects are contrasted in other examples.

3.11.5 Example 5: Van Driest Damped Mixing-Length and Near-Wall Behavior

Problem Statement. Explore near-wall damping effects on turbulent transport using a Van Driest-type mixing length ℓ_m to infer ν_t and K_t .

Solution Method. Let

$$\ell_m(y^+) = \kappa y^+ \left[1 - \exp\left(-\frac{y^+}{A^+}\right) \right], \quad \nu_t = \ell_m^2 \left| \frac{d\bar{U}}{dy} \right|, \quad K_t = \frac{\nu_t}{Sc_t}, \quad (3.43)$$

where κ is the von Kármán constant and A^+ a damping parameter. Use a synthetic $\bar{U}(y)$ and fixed Sc_t .

Expected Results. K_t vanishes at the wall and grows to an interior maximum; the damping term controls the near-wall growth rate. The resulting $K_t(y)$ is smoother and more physical near boundaries than undamped forms.

3.11.6 Example 6: Buoyancy–Shear Interaction and Gradient Richardson Number

Problem Statement. Investigate the modulation of scalar transport under weak stratification by examining the gradient Richardson number Ri_g .

Solution Method. Define

$$Ri_g = \frac{N^2}{\left(\frac{d\bar{U}}{dy}\right)^2}, \quad N^2 \propto \frac{d\bar{\rho}}{dy}, \quad (3.44)$$

in a Boussinesq-like setting. Discuss how positive (stable) versus negative (unstable) N^2 alters down-gradient flux magnitude and K_t .

Expected Results. Stable stratification ($Ri_g > 0$) suppresses turbulent transport (smaller $|\bar{v}'c'|$, smaller K_t); weak or unstable stratification enhances mixing. The synthetic profiles yield clean trends without secondary complications.

3.11.7 Example 7: Density-Driven (Gravity Current) Motifs in Passive Scalar Traces

Problem Statement. Use the scalar as a proxy for small density excess to reason about the qualitative imprint of gravity-current-like intrusions on \bar{c} and c' statistics.

Solution Method. Consider a localized near-wall enrichment of c and examine its implied buoyancy tendency. Assess qualitative changes in $\bar{c}(y)$ curvature and in $\bar{c'^2}(y)$ and $\bar{v'c'}(y)$.

Expected Results. Enhanced near-wall scalar leads to steeper local gradients and larger variance near the source; if effective buoyancy is present (even weakly), transport is skewed in the direction of the gravity current, visible as asymmetric $\bar{v'c'}$ patterns.

3.11.8 Example 8: Mixing Time Scales from Variance and Dissipation

Problem Statement. Define scalar mixing time scales using variance and dissipation proxies, and compare to eddy-turnover estimates.

Solution Method. Form the scalar time scale

$$\tau_c(y) \equiv \frac{\overline{c'^2}(y)}{\chi(y)}, \quad (3.45)$$

and compare to an eddy time scale $\tau_e \sim \ell/u'$ or its surrogate via $K_t \sim u'\ell$.

Expected Results. τ_c is shortest where χ is large (intense small-scale activity) and longest in quiescent regions. Its wall-normal distribution is broadly consistent with the shape of $K_t(y)$ and the variance production $P_c(y)$, providing an internally consistent picture of mixing intensity across the layer.

3.11.9 Example NB 3.7: Wall-Aware Mixing Length and Closures for Rayleigh–Bénard Convection

Problem Statement. In this example, we analyze turbulent transport in a vertically confined, thermally stratified shear layer bounded by two horizontal plates separated by a height H . The objective is to understand how momentum and heat (or buoyancy) are redistributed by turbulence in a setting where mixing is suppressed near solid boundaries and enhanced in the interior. This case is directly relevant to wall-bounded convection and atmospheric boundary layers.

Model Assumptions. The turbulence is modeled under the *local equilibrium* approximation, where production balances dissipation, i.e. $P_b = \varepsilon$. Buoyancy effects are incorporated via

the Brunt–Väisälä frequency N^2 , defined as

$$N^2 = \frac{g}{\theta_0} \frac{d\bar{\theta}}{dy}, \quad P_b = -\frac{\nu_t}{\text{Pr}_t} N^2, \quad (3.46)$$

where Pr_t is the turbulent Prandtl number, ν_t is the eddy viscosity, and θ denotes potential temperature. The term $P_b > 0$ corresponds to buoyant *production* (unstable stratification, $N^2 < 0$), whereas $P_b < 0$ indicates buoyant *destruction* (stable stratification).

Mixing-Length Formulation. To represent wall effects, we introduce a *wall-aware mixing length* that vanishes at both plates and attains a maximum at mid-height:

$$\ell_m(y) = c_\ell H \sqrt{\frac{y}{H} \left(1 - \frac{y}{H}\right)}, \quad c_\ell \in (0, 1), \quad (3.47)$$

with $c_\ell = 0.25$ used in this example. This functional form ensures that turbulent eddies smoothly reduce to zero at the plates, consistent with DNS and laboratory observations.

Local-Equilibrium Kinetic Energy. Assuming $P_b = \varepsilon$, the turbulent kinetic energy profile follows:

$$k(y) = \frac{C_m}{C_\varepsilon} \frac{\ell_m^2}{\text{Pr}_t} |N^2|, \quad (3.48)$$

where C_m and C_ε are empirical constants. This relationship links the buoyancy frequency directly to the local turbulence intensity through the available mixing length.

Eddy Viscosity and Turbulent Diffusivity. Momentum and scalar transport coefficients are then computed as

$$\nu_t(y) = C_m \ell_m \sqrt{k(y)}, \quad \kappa_t(y) = \frac{\nu_t(y)}{\text{Pr}_t}, \quad (3.49)$$

representing the turbulent analogs of molecular viscosity and diffusivity.

Budget Terms. For diagnostic interpretation, the following local quantities are evaluated:

$$P_b(y) = -\frac{\nu_t N^2}{\text{Pr}_t}, \quad \varepsilon(y) = C_\varepsilon \frac{k^{3/2}}{\ell_m}, \quad \mathcal{P}_\vartheta(y) = \kappa_t \left(\frac{d\bar{T}}{dy} \right)^2, \quad (3.50)$$

where \mathcal{P}_ϑ denotes the scalar-variance (temperature) production term. These quantities describe the balance between buoyant forcing, turbulent dissipation, and scalar transport.

Solution Method. The computational workflow implemented in the companion Python notebook ([Chapter3CompanionPrinciplesofTurbule](#) follows:

1. Define the wall-normal coordinate $y/H \in [0, 1]$ and compute $\ell_m(y)$ from (3.47).
2. Evaluate $k(y)$ using (3.48), assuming known constants C_m , C_ε , and Pr_t .
3. Compute ν_t and κ_t via (3.49).
4. Derive $P_b(y)$, $\varepsilon(y)$, and $\mathcal{P}_\vartheta(y)$ from (3.50).
5. Visualize the wall-normal distributions of ℓ_m , k , and the budget terms.

Expected Results.

- The mixing length ℓ_m exhibits a symmetric parabolic shape with zeros at the plates and a maximum at $y/H = 0.5$ (Figure ??).
- The local-equilibrium kinetic energy $k(y)$ peaks in the interior and diminishes near the walls, mirroring ℓ_m .
- The buoyant production P_b is positive for unstable stratification ($N^2 < 0$) and decreases toward the walls, while $\varepsilon(y)$ balances $P_b(y)$ under local equilibrium (Figure ??).
- The scalar-variance production $\mathcal{P}_\vartheta(y)$ follows the shape of κ_t , highlighting enhanced temperature fluctuation activity away from boundaries (Figure ??).

Physical Interpretation. This wall-aware closure captures the interplay between buoyancy and shear in a vertically confined domain. It provides a compact analytical framework that transitions smoothly between diffusive near-wall behavior and convective interior dynamics, making it suitable for atmospheric mixed layers, Rayleigh–Bénard convection, and other thermally stratified wall-bounded flows.

Chapter 4

Governing Equations of Turbulence: Incompressible Flow

4.1 Introduction

In Chapter 3, we introduced the concepts of mechanical generation of turbulence and buoyant generation of turbulence in the context of scalar mixing. The chapter is organized into four parts. In *Part A: Shear-Driven Flows*. We present formal derivations of the governing equation for turbulence kinetic energy and higher-order correlations, Reynolds stresses, and also for vorticity and enstrophy. *Part B: Buoyancy-Driven Flows* highlights scalar (temperature/density) transport, buoyant production. *Part C: Mixing-Length Theory and Closures* supplies the tools—mixing length, eddy viscosity/diffusivity, and turbulent Prandtl/Schmidt—to close the momentum and scalar fluxes.

Part 1: Shear-Driven Flows

4.2 Reynolds Decomposition

We have introduced the overall concept of Reynold Decomposition in Chapter 3. We will go into more detail here. The idea of separating a turbulent signal into a *mean* part and a *fluctuating* part dates to Osborne Reynolds' landmark 1894-95 paper “*On the dynamical theory of incompressible viscous fluids and the determination of the criterion*” (*Phil. Trans. R. Soc. A*, vol. 186). Reynolds used a long-exposure photographic technique to visualize dye streaks in pipe flow and observed that the instantaneous velocity could be written as the sum of a *steady* component representing the time-average flow, *fluctuation* component associated with the irregular, high-frequency motion. This is the turbulence fluctuation.

4.3 Time-Averaged Navier Stokes Equation (Mean Flow Equation)

Instantaneous governing equations for incompressible flow

Let the instantaneous velocity be given as u_i , instantaneous pressure is p .

Conservation of Mass (Continuity) Equation

$$\frac{\partial u_i}{\partial x_i} = 0. \quad (4.1)$$

Conservation of Momentum Equation

$$\frac{\partial u_i}{\partial t} + u_j \frac{\partial u_i}{\partial x_j} = -\frac{1}{\rho} \frac{\partial p}{\partial x_i} + \nu \frac{\partial^2 u_i}{\partial x_j \partial x_j}. \quad (4.2)$$

Let the strain rate tensor (which is a symmetric tensor) be defined as follows:

$$S_{ij} \equiv \frac{1}{2} \left(\frac{\partial u_i}{\partial x_j} + \frac{\partial u_j}{\partial x_i} \right). \quad (4.3)$$

For a Newtonian fluid, $\tau_{ij} = 2\mu S_{ij}$ and

$$\nu \frac{\partial^2 v_i}{\partial x_j \partial x_j} = \frac{1}{\rho} \frac{\partial \tau_{ij}}{\partial x_j} = 2\nu \frac{\partial S_{ij}}{\partial x_j}. \quad (4.4)$$

Hence Eq.4.2 can be written as

$$\frac{\partial u_i}{\partial t} + u_j \frac{\partial u_i}{\partial x_j} = -\frac{1}{\rho} \frac{\partial p}{\partial x_i} + 2\nu \frac{\partial S_{ij}}{\partial x_j}. \quad (4.5)$$

1. Reynolds decomposition

Decompose the velocity, pressure, and strain rate as follows:

$$u_i = \bar{u}_i + u'_i, \quad p = \bar{p} + p', \quad S_{ij} = \bar{S}_{ij} + S'_{ij}, \quad (4.6)$$

with

$$\bar{S}_{ij} \equiv \frac{1}{2} \left(\frac{\partial \bar{u}_i}{\partial x_j} + \frac{\partial \bar{u}_j}{\partial x_i} \right), \quad S'_{ij} \equiv \frac{1}{2} \left(\frac{\partial u'_i}{\partial x_j} + \frac{\partial u'_j}{\partial x_i} \right), \quad (4.7)$$

and we define the Reynolds stress tensor as

$$R_{ij} \equiv \overline{u'_i u'_j}. \quad (4.8)$$

Note the Averaging rules are: $\overline{u'_i} = 0$, $\overline{p'} = 0$, $\overline{\partial(\cdot)/\partial x_j} = \partial(\overline{\cdot})/\partial x_j$.

4.3.1 Mean flow Continuity equation

Apply the Reynolds average to Eq. (4.1) and use the commutation of averaging with differentiation:

$$\overline{\frac{\partial u_i}{\partial x_i}} = \frac{\partial \bar{u}_i}{\partial x_i} = 0 \iff \nabla \cdot \bar{\mathbf{u}} = 0. \quad (4.9)$$

Fluctuation continuity equation. Subtract Eq.4.9 from Eq.4.1:

$$\overline{\frac{\partial u'_i}{\partial x_i}} = 0 \iff \nabla \cdot \mathbf{u}' = 0, \quad (4.10)$$

and, by averaging (4.10),

$$\overline{\frac{\partial u'_i}{\partial x_i}} = \frac{\partial \bar{u}'_i}{\partial x_i} = 0, \quad (4.11)$$

which is consistent with $\bar{u}'_i = 0$.

2. Use continuity to transform the nonlinear convection term

Start from the identity (product rule):

$$\frac{\partial(u_i u_j)}{\partial x_j} = u_j \frac{\partial u_i}{\partial x_j} + u_i \frac{\partial u_j}{\partial x_j}. \quad (4.12)$$

By incompressibility (4.1), $\partial u_j / \partial x_j = 0$, so

$$u_j \frac{\partial u_i}{\partial x_j} = \frac{\partial(u_i u_j)}{\partial x_j}. \quad (4.13)$$

Average (4.13) and expand $u_i u_j$ via the decomposition:

$$\bar{u}_i \bar{u}_j = \overline{(\bar{u}_i + u'_i)(\bar{u}_j + u'_j)} = \bar{u}_i \bar{u}_j + \overline{u'_i u'_j}. \quad (4.14)$$

Therefore,

$$\overline{u_j \frac{\partial u_i}{\partial x_j}} = \frac{\partial}{\partial x_j} \left(\bar{u}_i \bar{u}_j + R_{ij} \right) = \bar{u}_j \frac{\partial \bar{u}_i}{\partial x_j} + \frac{\partial R_{ij}}{\partial x_j}, \quad (4.15)$$

where we used $\partial \bar{u}_j / \partial x_j = 0$.

3. Time Average the momentum equation

Average Eq.4.5 and use $\overline{\partial u_i / \partial t} = \partial \bar{u}_i / \partial t$, $\overline{\partial p / \partial x_i} = \partial \bar{p} / \partial x_i$, and $\overline{\partial S_{ij} / \partial x_j} = \partial \bar{S}_{ij} / \partial x_j$:

$$\frac{\partial \bar{u}_i}{\partial t} + \bar{u}_j \overline{\frac{\partial u_i}{\partial x_j}} = -\frac{1}{\rho} \frac{\partial \bar{p}}{\partial x_i} + 2\nu \frac{\partial \bar{S}_{ij}}{\partial x_j}. \quad (4.16)$$

Insert Eq.4.15:

$$\frac{\partial \bar{u}_i}{\partial t} + \bar{u}_j \frac{\partial \bar{u}_i}{\partial x_j} + \frac{\partial R_{ij}}{\partial x_j} = -\frac{1}{\rho} \frac{\partial \bar{p}}{\partial x_i} + 2\nu \frac{\partial \bar{S}_{ij}}{\partial x_j}. \quad (4.17)$$

Move the Reynolds-stress term to the right-hand side to obtain the Reynolds-averaged momentum equation (convective form):

$$\frac{\partial \bar{u}_i}{\partial t} + \bar{u}_j \frac{\partial \bar{u}_i}{\partial x_j} = -\frac{1}{\rho} \frac{\partial \bar{p}}{\partial x_i} + 2\nu \frac{\partial \bar{S}_{ij}}{\partial x_j} - \frac{\partial R_{ij}}{\partial x_j}. \quad (4.18)$$

The Conservative (divergence) form using the continuity equation is given as, Using $\partial(\bar{u}_i \bar{u}_j) / \partial x_j = \bar{u}_j \partial \bar{u}_i / \partial x_j$ (since $\partial \bar{u}_j / \partial x_j = 0$), (4.18) is equivalent.

$$\frac{\partial \bar{u}_i}{\partial t} + \frac{\partial}{\partial x_j} (\bar{u}_i \bar{u}_j) = -\frac{\partial}{\partial x_j} \left[\underbrace{\frac{\bar{p}}{\rho} \delta_{ij}}_{\text{pressure}} - \underbrace{2\nu \bar{S}_{ij}}_{\text{viscous}} + \underbrace{R_{ij}}_{\text{Reynolds stress}} \right], \quad (4.19)$$

The viscous diffusion appears compactly through \bar{S}_{ij} , while turbulence enters as the divergence of the Reynolds stresses $-\partial R_{ij} / \partial x_j$, which requires closure modeling.

The physical interpretation of each term is as follows:

$\frac{\partial \bar{u}_i}{\partial t}$ Local (unsteady) acceleration of the mean flow. This component is zero by definition.

CHAPTER 4. GOVERNING EQUATIONS OF TURBULENCE: INCOMPRESSIBLE FLOW

- $\bar{u}_j \frac{\partial \bar{u}_i}{\partial x_j}$ Convective transport of mean momentum.
- $-\frac{1}{\rho} \frac{\partial \bar{p}}{\partial x_i}$ Mean pressure-gradient force.
- $-2\nu S_{ij}$ Molecular viscous diffusion of mean momentum.
- $-\overline{u'_i u'_j}$ Reynolds-stress
- $-\frac{\partial \overline{u'_i u'_j}}{\partial x_j}$ Divergence of Reynolds-stress, which is the turbulent transport of momentum arising from correlated velocity fluctuations.

Equation 4.19 is the momentum equation for the mean flow. The mean momentum equations contain the unknown correlations $\overline{u'_i u'_j}$ between fluctuating velocity components. These are *second-order statistical moments* of the turbulent field. Since the governing equations are now expressed in terms of new unknowns, the system is not closed: there are more unknowns than equations. This is known as the closure problem of turbulence. If one attempts to derive an equation for $\overline{u'_i u'_j}$, it will involve third-order moments such as $\overline{u'_i u'_j u'_k}$. Similarly, the evolution of third-order moments depends on fourth-order moments, and so on. This generates an infinite hierarchy of coupled equations, often called the *momentum hierarchy* or *closure hierarchy*. Without additional assumptions, this hierarchy cannot be solved. The challenge of turbulence modeling lies in closing the system, i.e. relating $\overline{u'_i u'_j}$ to known mean quantities (\bar{u}_i , \bar{p} , etc.). Various turbulence models (e.g. eddy viscosity models, $k-\varepsilon$, $k-\omega$, and Reynolds stress models) propose different strategies to approximate or solve for these correlations.

4.4 Mean Kinetic Energy Equation

The total mean stress tensor is defined as the average stress acting on a material body. It is calculated as the average of the stress tensor over a given volume or area. Mathematically, if \mathbf{T} is the stress tensor, the total mean stress tensor, $\bar{\sigma}$, can be

expressed as:

$$T_{ij} \equiv \frac{\bar{p}}{\rho} \delta_{ij} - 2\nu \bar{S}_{ij} + R_{ij}, \quad (4.20)$$

The Reynolds-averaged momentum equation (in conservative form) is

$$\frac{\partial \bar{u}_i}{\partial t} + \frac{\partial}{\partial x_j} (\bar{u}_i \bar{u}_j) = - \frac{\partial T_{ij}}{\partial x_j}, \quad \frac{\partial \bar{u}_i}{\partial x_i} = 0. \quad (4.21)$$

Let $U_i \equiv \bar{u}_i$ and $K \equiv \frac{1}{2} U_i U_i$. Starting from the RANS momentum in stress form,

$$\frac{\partial U_i}{\partial t} + \frac{\partial}{\partial x_j} (U_i U_j) = - \frac{\partial T_{ij}}{\partial x_j}, \quad (1)$$

multiply by U_i :

$$U_i \frac{\partial U_i}{\partial t} + U_i \frac{\partial}{\partial x_j} (U_i U_j) = - U_i \frac{\partial T_{ij}}{\partial x_j}. \quad (2)$$

Use product/chain rules and incompressibility. For $\partial U_j / \partial x_j = 0$ (incompressible mean flow),

$$U_i \frac{\partial}{\partial x_j} (U_i U_j) = \frac{\partial}{\partial x_j} \left(\frac{1}{2} U_i U_i U_j \right) = \frac{\partial}{\partial x_j} (K U_j), \quad (3)$$

$$U_i \frac{\partial T_{ij}}{\partial x_j} = \frac{\partial}{\partial x_j} (U_i T_{ij}) - T_{ij} \frac{\partial U_i}{\partial x_j}. \quad (4)$$

Eliminate the antisymmetric part of $\partial U_i / \partial x_j$. Write $\partial U_i / \partial x_j = \bar{S}_{ij} + \Omega_{ij}$ with \bar{S}_{ij} symmetric and Ω_{ij} antisymmetric. Since T_{ij} is symmetric, $T_{ij} \Omega_{ij} = 0$, hence

$$T_{ij} \frac{\partial U_i}{\partial x_j} = T_{ij} \bar{S}_{ij}. \quad (5)$$

Collect terms into a conservative form. Using (2)–(??) and $U_i \partial U_i / \partial t = \partial K / \partial t$,

$$\frac{\partial K}{\partial t} + \frac{\partial}{\partial x_j} (K U_j + U_i T_{ij}) = T_{ij} \bar{S}_{ij}. \quad (6)$$

Expand the stress–strain work. With

$$T_{ij} = \frac{\bar{p}}{\rho} \delta_{ij} - 2\nu \bar{S}_{ij} + R_{ij}, \quad (4.22)$$

we get

$$T_{ij} \bar{S}_{ij} = \underbrace{\frac{\bar{p}}{\rho} \delta_{ij} \bar{S}_{ij}}_{\text{pressure-dilatation}} - \underbrace{2\nu \bar{S}_{ij} \bar{S}_{ij}}_{\text{mean viscous dissipation } (\varepsilon_m)} + \underbrace{R_{ij} \bar{S}_{ij}}_{\text{turbulence production } (P_m)} \quad (7)$$

For incompressible mean flow, $\delta_{ij} \bar{S}_{ij} = \partial U_i / \partial x_i = 0$, so the pressure–dilatation term vanishes.

$$\boxed{\frac{\partial K}{\partial t} + \frac{\partial}{\partial x_j} (K U_j + U_i T_{ij}) = -2\nu \bar{S}_{ij} \bar{S}_{ij} + R_{ij} \bar{S}_{ij}.}$$

The left-hand-side term is the temporal change and transport (convection + stress work) of mean kinetic energy K . The right-hand-side is the balance between mean viscous dissipation and transfer from turbulence to the mean (or vice versa) via the production term ($R_{ij} \bar{S}_{ij}$) (positive when Reynolds stresses act with the mean shear).

The following is the significance of the terms:

- **Transport (all as divergence):** $\frac{\partial}{\partial x_j} (\bar{K} U_j + U_i T_{ij}) = \frac{\partial}{\partial x_j} \left(\underbrace{\bar{K} U_j}_{\text{mean advection}} + \underbrace{\frac{\bar{p}}{\rho} U_i \delta_{ij}}_{\text{pressure work}} - \underbrace{2\nu U_i \bar{S}_{ij}}_{\text{viscous work}} + \underbrace{u_i R_{ij}}_{\text{turbulent transport}} \right)$.
- **Mean viscous dissipation:** $\varepsilon_m \equiv 2\nu \bar{S}_{ij} \bar{S}_{ij} \geq 0$ (removes mean kinetic energy).
- **Production/transfer:** $R_{ij} \bar{S}_{ij}$ is the exchange between

mean and turbulent kinetic energy. In canonical shear flows $R_{12} < 0$ and $\bar{S}_{12} > 0$, so $R_{ij}\bar{S}_{ij} < 0$: Mean kinetic energy is *lost* and TKE is *gained*. (In the TKE equation the corresponding term appears with the opposite sign, $-R_{ij}\bar{S}_{ij}$.)

4.5 Governing equation for velocity fluctuation

The component u'_i is the deviation from the instantaneous flow field, and it represents the turbulence. This is a random variable, and by definition, as the mean of a random variable is zero; hence, the fluctuation $u'(t)$ is, by definition,

$$\overline{u'} = 0 \quad (4.23)$$

The magnitude of the turbulence is represented using statistics of the fluctuations, e.g. root-mean-square (r.m.s.) of the velocity fluctuations.

To derive the equations governing the turbulent fluctuations u'_i , one begins with Eq. ??, incompressible Navier–Stokes equations for the instantaneous velocity u_i and pressure p and subtracts the time-averaged Navier-Stokes equation (Eq. ?? from the original instantaneous equations. The result is a set of evolution equations for the velocity fluctuations u'_i :

$$\frac{\partial u'_i}{\partial x_i} = 0 \quad (4.24)$$

$$\frac{\partial u'_i}{\partial t} + U_j \frac{\partial u'_i}{\partial x_j} + u'_j \frac{\partial U_i}{\partial x_j} + u'_j \frac{\partial u'_i}{\partial x_j} = -\frac{1}{\rho} \frac{\partial p'}{\partial x_i} + \nu \frac{\partial^2 u'_i}{\partial x_j \partial x_j}, \quad i = 1, 2, 3 \quad (4.25)$$

These equations for the fluctuations form the foundation for turbulence closure modeling and the statistical analysis of tur-

bulent flows.

4.5.1 Turbulent kinetic energy Equation

We define the mean turbulent kinetic energy (TKE) per unit mass as

$$k = \frac{1}{2} \overline{u'_i u'_i}. \quad (4.26)$$

Notation. fluctuating strain $s'_{ij} = \frac{1}{2}(\partial_i u'_j + \partial_j u'_i)$.

(i) Instantaneous momentum dotted with u_i results in instantaneous Kinetic energy transport).

$$\underbrace{\frac{\partial}{\partial t} \left(\frac{1}{2} u_i u_i \right)}_{\text{local KE}} + \underbrace{\frac{\partial}{\partial x_j} \left(\frac{1}{2} u_i u_i u_j + \frac{p}{\rho} u_j - 2\nu u_i S_{ij} \right)}_{\text{KE + pressure + viscous fluxes}} = - \underbrace{2\nu S_{ij} S_{ij}}_{\text{viscous loss}}. \quad (4.27)$$

(ii) Reynolds-average of 4.27 (total mean of KE: $K + k$).

$$\frac{\partial(\bar{K}+k)}{\partial t} + \frac{\partial}{\partial x_j} (\Phi_j^{\text{tot}}) = -\varepsilon_m - \varepsilon, \quad (4.28)$$

with the total KE flux (all written as a divergence)

$$\Phi_j^{\text{tot}} \equiv \underbrace{\frac{1}{2} \overline{u_i u_i u_j}}_{\text{KE convection}} + \underbrace{\frac{1}{\rho} \overline{p u_j}}_{\text{pressure work / diffusion}} - \underbrace{2\nu \overline{u_i S_{ij}}}_{\text{viscous work / diffusion}}. \quad (4.29)$$

iii. Subtract Mean Kinetic Energy Eq.?? from Eq.???:
TKE equation = (Averaged inst. KE) (Mean KE).

$$[(??)] - [?] \implies \frac{\partial k}{\partial t} + \frac{\partial}{\partial x_j} (\Phi_j^{\text{tke}}) = -R_{ij} \bar{S}_{ij} - \varepsilon, \quad \Phi_j^{\text{tke}} \equiv \Phi_j^{\text{tot}} - \Phi_j^{\text{m}}. \quad (4.30)$$

CHAPTER 4. GOVERNING EQUATIONS OF TURBULENCE: INCOMPRESSIBLE FLOW

Expanding the terms,

$$\text{Let: } P = -\overline{u'_i u'_j} \frac{\partial U_i}{\partial x_j}, \quad \varepsilon = \nu \overline{\partial_j u'_i \partial_j u'_i} \quad (4.31)$$

$$\overline{u'_i \frac{\partial u'_i}{\partial t}} = \frac{\partial}{\partial t} \left(\frac{1}{2} \overline{u'_i u'_i} \right), \quad \overline{u'_i \frac{\partial u'_i}{\partial x_j}} = \frac{\partial}{\partial x_j} \left(\frac{1}{2} \overline{u'_i u'_i} \right) \quad (4.32)$$

Thus, the TKE equation:

$$\frac{\partial k}{\partial t} + U_j \frac{\partial k}{\partial x_j} = P - \frac{\partial}{\partial x_j} \left(\frac{1}{2} \overline{u'_i u'_i u'_j} \right) - \frac{1}{\rho} \frac{\partial}{\partial x_j} \overline{p' u'_j} + \nu \frac{\partial^2 k}{\partial x_j \partial x_j} - \varepsilon$$

(4.33)

In the TKE equation,

- $\frac{\partial k}{\partial t}$: Local, unsteady change of turbulent kinetic energy.
- $U_j \frac{\partial k}{\partial x_j}$: Convection of k by the mean flow.
- $P = -\overline{u'_i u'_j} \frac{\partial U_i}{\partial x_j}$: *Shear turbulence Production* of k by mean-shear (transfer from mean flow to fluctuations).
- $T_t = -\frac{\partial}{\partial x_j} \left(\frac{1}{2} \overline{u'_i u'_i u'_j} \right)$: *Turbulent transport* (self-advection) of k .
- $T_p = -\frac{1}{\rho} \frac{\partial}{\partial x_j} \overline{p' u'_j}$: *Pressure transport* (redistribution of k via pressure–velocity correlations).
- $T_\nu = \nu \frac{\partial^2 k}{\partial x_j \partial x_j}$: *Viscous diffusion* of k .
- $\varepsilon = \nu \frac{\partial u'_i}{\partial x_j} \frac{\partial u'_i}{\partial x_j}$: *Dissipation* of k into heat at the smallest scales.

In the TKE equation for inertial flows, rate of production from shear (P is the only mechanism that generates TKE). This happens at the large scales. Dissipation ε is the only irreversible sink that converts turbulent motion into heat. This happens at the small scales. Transport terms relocate energy in space. Thus the TKE equation maps the full energy pathway of a turbulent cascade—from its extraction out of the mean flow, through

spatial redistribution, to its dissipation at the Kolmogorov scales. Reynolds stress is the key mechanism that transfers energy from the mean flow to turbulence. Just as molecular viscosity smears out mean-velocity gradients, Reynolds stresses represent a much larger, eddy-driven *effective viscosity* that transports momentum from regions of high mean velocity into regions of low mean velocity. The total shear stress is the sum of viscous stress and Reynolds stress. In high-Reynolds-number flows, in most of the regions, the Reynolds stresses dominate over the viscous stresses.

Profiles of k , P , ε are used to validate equilibrium assumptions in boundary layers (where $P \approx \varepsilon$ through the logarithmic region) or to mark the onset of turbulent transition (rapid growth of k).

4.5.2 Reynolds stress Transport Equation

In a Reynolds-averaged momentum balance the divergence of the tensor $R_{ij} = \overline{u'_i u'_j}$ appears as an *additional stress* that may dominate molecular viscosity at high Reynolds numbers. Assigning $R_{ij} = -2\nu_t S_{ij} + \frac{2}{3}k\delta_{ij}$ assumes the turbulence is isotropic and instantly aligned with the local strain-rate tensor S_{ij} . This shortcut fails wherever the turbulence is strongly anisotropic—curved ducts, swirling jets, rotating channels, shock-shear interaction.

To retain the physics, we need to solve the full Reynolds stress equation. In this section, the derivation and the significance of the terms are explained next.

Multiply the equation for the velocity fluctuation (Eq. (4.25)) with u_j and perform the time-averaging will results in the resultant Reynold stress equations :

$$\begin{aligned}
 \frac{\partial R_{ij}}{\partial t} + \bar{u}_k \frac{\partial R_{ij}}{\partial x_k} &= - \underbrace{R_{ik} \frac{\partial \bar{u}_j}{\partial x_k} - R_{jk} \frac{\partial \bar{u}_i}{\partial x_k}}_{\text{production } P_{ij}} \\
 &\quad + \underbrace{\Pi_{ij}}_{\text{pressure-strain}} - \underbrace{\varepsilon_{ij}}_{\text{dissipation}} \\
 &\quad - \frac{\partial}{\partial x_k} \left(\underbrace{T_{ijk}}_{\text{turb. transport}} + \underbrace{D_{ijk}}_{\text{visc. diffusion}} \right), \quad i, j = 1, 2, 3
 \end{aligned} \tag{4.34}$$

where

$$\begin{aligned}
 R_{ij} &= \overline{u'_i u'_j}, \quad \Pi_{ij} = \overline{p' \left(\frac{\partial u'_j}{\partial x_i} + \frac{\partial u'_i}{\partial x_j} \right)}, \quad \varepsilon_{ij} = 2\nu \overline{\frac{\partial u'_i}{\partial x_k} \frac{\partial u'_j}{\partial x_k}}, \\
 T_{ijk} &= \overline{u'_i u'_j u'_k}, \quad D_{ijk} = \nu \frac{\partial R_{ij}}{\partial x_k}.
 \end{aligned}$$

- $\frac{\partial R_{ij}}{\partial t} + \bar{u}_k \frac{\partial R_{ij}}{\partial x_k}$: local storage and mean convection of the stress component.
- $-R_{ik} \frac{\partial \bar{u}_j}{\partial x_k} - R_{jk} \frac{\partial \bar{u}_i}{\partial x_k}$: production by mean-shear gradients.
- Π_{ij} : pressure-strain term that redistributes energy among the stress components.
- ε_{ij} : viscous dissipation of each component.
- $-\frac{\partial}{\partial x_k} (T_{ijk} + D_{ijk})$: transport by turbulence (T_{ijk}) and molecular diffusion (D_{ijk}).

Solving the six Reynolds-stress transport equations transforms a turbulence model from an empirical eddy-viscosity model into a physics-based description of how each component of the turbulent momentum flux evolves. Each Reynolds-stress transport

equation separates the budget into *Production* processes where the individual stress components extract energy from specific mean-shear gradients; *Pressure-strain* which redistributes energy among the three normal and three shear components and drives the tendency toward isotropy; *Dissipation*, draining each component at its own viscous rate and *Turbulent and viscous transport* processes that move the stress energy through space.

An Reynolds stress modeling adds six stress equations plus one for the dissipation rate, increasing the memory and CPU requirements time relative to the eddy viscosity closure model, yet it is still *orders of magnitude cheaper* than Direct numerical simulation.

4.5.3 Vorticity Transport Equations

The vorticity transport equation describes how the rotation of fluid elements evolves under the action of convection, vortex-stretching, and viscous diffusion. By taking the curl of the incompressible Navier–Stokes equations one obtains an exact balance for the instantaneous vorticity field $\omega_i = \varepsilon_{ijk} \partial_j u_k$. Decomposing into mean and fluctuation parts then yields Reynolds-averaged equations for the mean vorticity Ω_i and the fluctuation vorticity ω'_i . Finally, an enstrophy equation—governing $E = \frac{1}{2} \omega_i \omega_i$ —can be derived to track the production, transport, and dissipation of rotational energy in the flow.

Instantaneous Vorticity Transport

We define the vorticity as the curl of the velocity: $\omega_i \equiv \varepsilon_{ijk} \partial_j u_k$. We take the curl of the instantaneous momentum equation One obtains the governing equation for vorticity as follows:

$$\boxed{\frac{\partial \omega_i}{\partial t} + u_j \frac{\partial \omega_i}{\partial x_j} = \underbrace{\omega_j \frac{\partial u_i}{\partial x_j}}_{\text{vortex stretching}} + \underbrace{\nu \frac{\partial^2 \omega_i}{\partial x_j \partial x_j}}_{\text{viscous diffusion}}}. \quad (4.35)$$

- $\frac{\partial \omega_i}{\partial t}$: local unsteady change of vorticity.

- $u_j \partial_j \omega_i$: convection of vorticity by the velocity field.
- $\omega_j \partial_j u_i$: vortex-stretching/tilting—alignment of vorticity with velocity gradients amplifies rotation.
- $\nu \partial_{jj}^2 \omega_i$: viscous diffusion of vorticity.

Time-Averaged Vorticity Equation: Mean Vorticity

Apply Reynolds decomposition Eq.3.6 and average ($\bar{\cdot}$). The mean vorticity $\Omega_i = \varepsilon_{ijk} \partial_j U_k$ simplifies to,

$$\boxed{\frac{\partial \Omega_i}{\partial t} + U_j \frac{\partial \Omega_i}{\partial x_j} = \Omega_j \frac{\partial U_i}{\partial x_j} + \underbrace{\varepsilon_{ijk} \frac{\partial}{\partial x_j} \bar{u'_\ell} \partial_\ell \bar{u'_k}}_{\text{curl of Reynolds-stress}} + \nu \frac{\partial^2 \Omega_i}{\partial x_j \partial x_j}} \quad (4.36)$$

- $\partial_t \Omega_i + U_j \partial_j \Omega_i$: unsteady + mean-flow convection of mean vorticity.
- $\Omega_j \partial_j U_i$: mean vortex stretching by mean-flow gradients.
- $\varepsilon_{ijk} \partial_j \bar{u'_\ell} \partial_\ell \bar{u'_k}$: generation/redistribution of mean vorticity by turbulent Reynolds-stress curl.
- $\nu \partial_{jj}^2 \Omega_i$: viscous diffusion of mean vorticity.

Equation for Vorticity Fluctuations

Subtracting the mean vorticity equation (Eq.4.36) from the instantaneous vorticity (Eq.4.35) gives the equation for vorticity fluctuation ω'_i balance:

$$\boxed{\frac{\partial \omega'_i}{\partial t} + U_j \frac{\partial \omega'_i}{\partial x_j} + u'_j \frac{\partial \Omega_i}{\partial x_j} + u'_j \frac{\partial \omega'_i}{\partial x_j} - \omega'_j \frac{\partial U_i}{\partial x_j} = \dots} \quad (4.37)$$

$$\dots + \underbrace{\varepsilon_{ijk} \frac{\partial}{\partial x_j} (u'_\ell \partial_\ell \bar{u'_k} - \bar{u'_\ell} \partial_\ell \bar{u'_k})}_{\text{turbulent-fluctuation curl}} + \nu \frac{\partial^2 \omega'_i}{\partial x_j \partial x_j}.$$

Terms here represent convection by mean and fluctuating velocities, production/tilting against mean gradients, turbulent-fluctuation interactions, and viscous diffusion.

Enstrophy Transport Equation

Define the instantaneous enstrophy $\xi = \frac{1}{2} \omega_i \omega_i$. Multiply the instantaneous vorticity equation (Eq.4.35) by ω_i :

$$\frac{\partial \xi}{\partial t} + u_j \frac{\partial \xi}{\partial x_j} = \underbrace{\omega_i \omega_j \frac{\partial u_i}{\partial x_j}}_{P_\omega} + \underbrace{\nu \omega_i \frac{\partial^2 \omega_i}{\partial x_j \partial x_j}}_{T_{\omega,\nu}}. \quad (4.38)$$

Using the identity

$$\nu \omega_i \partial_{jj}^2 \omega_i = \nu \partial_j (\omega_i \partial_j \omega_i) - \nu \partial_j \omega_i \partial_j \omega_i, \quad (4.39)$$

yields the enstrophy transport equation:

$$\frac{\partial \xi}{\partial t} + u_j \frac{\partial \xi}{\partial x_j} = P_\omega + \underbrace{\nu \frac{\partial}{\partial x_j} (\omega_i \partial_j \omega_i)}_{T_{\omega,\nu}} - \underbrace{\nu \partial_j \omega_i \partial_j \omega_i}_{\varepsilon_\omega}. \quad (4.40)$$

- $P_\omega = \omega_i \omega_j \partial_j u_i$: enstrophy production by vortex stretching.
- $T_{\omega,\nu} = \nu \partial_j (\omega_i \partial_j \omega_i)$: viscous transport of enstrophy.
- $\varepsilon_\omega = \nu \partial_j \omega_i \partial_j \omega_i$: enstrophy dissipation.

The time-averaged enstrophy equation is given here (the derivation is left to the reader). Let, $\bar{\xi} = \frac{1}{2} \overline{\omega_i \omega_i}$

$$\frac{\partial \bar{\xi}}{\partial t} + \frac{\partial}{\partial x_j} \left(\bar{u}_j \bar{\xi} + \underbrace{\overline{u'_j \xi'}}_{\text{turbulent transport}} - \nu \overline{\omega_i \frac{\partial \omega_i}{\partial x_j}} \right) = \quad (4.41)$$

$$\underbrace{\omega_i \omega_j S_{ij}}_{\text{mean+fluct. production}} - \underbrace{\nu \overline{\left(\frac{\partial \omega_i}{\partial x_j} \right)^2}}_{\text{viscous destruction } (\varepsilon_\Omega)}, \quad (4.42)$$

The flux term contains mean advection $\bar{u}_j \bar{\xi}$, turbulent transport $\overline{u'_j \xi'}$, and viscous diffusion $-\nu \overline{\omega_i \partial_j \omega_i}$. The production $\omega_i \omega_j S_{ij}$ automatically includes contributions from both mean and fluctuating strain/vorticity.

special cases.

- **Homogeneous flow (periodic or far from walls).**

Spatial divergence terms vanish on volume average, giving

$$\frac{d\bar{\xi}}{dt} = \overline{\omega_i \omega_j S_{ij}} - \nu \overline{\left(\frac{\partial \omega_i}{\partial x_j} \right)^2}.$$

- **Statistically steady and homogeneous turbulence.**

$d\bar{\xi}/dt = 0$, so production balances destruction:

$$\overline{\omega_i \omega_j S_{ij}} = \nu \overline{\left(\frac{\partial \omega_i}{\partial x_j} \right)^2}.$$

- **Relation to TKE dissipation (isotropic, incompressible, homogeneous).** Under standard assumptions, $\varepsilon = 2\nu \overline{S'_{ij} S'_{ij}} = \nu \overline{\omega'_i \omega'_i}$. Thus enstrophy (of the fluctuations) directly measures the dissipation rate.

Part II: Mixing Length Closure Models

4.6 Mixing Length Model

Assuming a local mixing length ℓ_m and mean strain rate magnitude

$$S = \sqrt{2S_{ij}S_{ij}}, \quad S_{ij} = \frac{1}{2} \left(\frac{\partial \bar{u}_i}{\partial x_j} + \frac{\partial \bar{u}_j}{\partial x_i} \right), \quad (4.43)$$

the eddy viscosity is modeled as

$$\nu_t = \ell_m^2 |S|. \quad (4.44)$$

4.6.1 Reynolds Stress Closure

R_{ij} is a symmetric tensor with trace $R_{kk} = 2k$.

We can separate the R_{ij} into isotropic (k) and deviatoric parts (a_{ij}) as follows:

$$R_{ij} = a_{ij} + \frac{2}{3} k \delta_{ij}, \quad a_{ij} \equiv R_{ij} - \frac{2}{3} k \delta_{ij}, \quad a_{kk} = 0. \quad (4.45)$$

We assume the following: (i) *linearity in weak mean gradients*, (ii) *Galilean invariance and material frame indifference* (iii) *local isotropy* of the small scales, so that any tensor relation must be built from δ_{ij} and the mean-velocity gradient $\partial \bar{u}_i / \partial x_j$. The only symmetric, traceless, second-order tensor that is linear in $\partial \bar{u}_i / \partial x_j$ and objective is the mean strain-rate deviator,

$$S_{ij}^\circ \equiv S_{ij} - \frac{1}{3} S_{kk} \delta_{ij}, \quad S_{ij} \equiv \frac{1}{2} \left(\frac{\partial \bar{u}_i}{\partial x_j} + \frac{\partial \bar{u}_j}{\partial x_i} \right). \quad (4.46)$$

By the representation theorem for isotropic tensor functions, the most general *linear* form is

$$a_{ij} = -2\nu_t S_{ij}^\circ, \quad (4.47)$$

Combining Eqs.4.45-4.47 gives the eddy-viscosity closure for

the Reynolds stress:

$$R_{ij} = -2\nu_t \left(S_{ij} - \frac{1}{3} S_{kk} \delta_{ij} \right) + \frac{2}{3} k \delta_{ij} \quad (4.48)$$

For incompressible mean flow ($S_{kk} = \partial \bar{u}_k / \partial x_k = 0$), this reduces to

$$R_{ij} = -2\nu_t S_{ij} + \frac{2}{3} k \delta_{ij} \quad (4.49)$$

which mirrors the laminar viscous stress $\tau_{ij}^{(\mu)} = 2\mu S_{ij}$ and motivates the name *eddy viscosity*

4.6.2 Production Term (Mixing-Length Form)

The production of turbulent kinetic energy (Eq.4.33) is

$$P_k = -R_{ij} \frac{\partial \bar{u}_i}{\partial x_j}. \quad (4.50)$$

Substituting Eq. (??) gives

$$P_k = 2\nu_t S_{ij} S_{ij} = \nu_t |S|^2 = \ell_m^2 |S|^3. \quad (4.51)$$

For homogeneous one-dimensional shear flow $\bar{U} = \bar{U}(y)$, $S_{12} = S_{21} = \frac{1}{2} d\bar{U} / dy$ and $|S| = \left| \frac{d\bar{U}}{dy} \right|$, hence

$$P_k = \ell_m^2 \left| \frac{d\bar{U}}{dy} \right|^3. \quad (4.52)$$

4.6.3 Empirical Closure for Dissipation

The dissipation rate ε represents the rate at which turbulent kinetic energy is converted into internal energy. Following Kolmogorov's dimensional reasoning, the dissipation rate must scale as

$$[\varepsilon] = \frac{[\text{velocity}]^3}{[\text{length}]} \Rightarrow \varepsilon \sim \frac{k^{3/2}}{L}. \quad (4.53)$$

Introducing an empirical proportionality constant C_ε ,

$$\boxed{\varepsilon = C_\varepsilon \frac{k^{3/2}}{L}}, \quad (4.54)$$

where L is the characteristic large-eddy length scale. For most shear flows C_ε ranges from 0.09 to 1.0, depending on the flow and definition of L .

The corresponding turbulent (eddy turnover) time scale is

$$\tau = \frac{k}{\varepsilon} = \frac{L}{C_\varepsilon k^{1/2}},$$

showing that ε represents the energy decay rate per unit time.

4.6.4 Mixing-Length Expression for Dissipation

In equilibrium shear flows, turbulent production and dissipation are approximately balanced ($P_k \simeq \varepsilon$). Using the mixing-length hypothesis for the turbulent shear stress:

$$-\overline{u'v'} = \ell_m^2 \left| \frac{d\bar{U}}{dy} \right| \frac{d\bar{U}}{dy}, \quad (4.55)$$

the TKE production becomes

$$P_k = -\overline{u'v'} \frac{d\bar{U}}{dy} = \ell_m^2 \left| \frac{d\bar{U}}{dy} \right|^3. \quad (4.56)$$

Under local equilibrium ($P_k = \varepsilon$),

$$\boxed{\varepsilon = \ell_m^2 \left| \frac{d\bar{U}}{dy} \right|^3}. \quad (4.57)$$

Link Between Empirical and Mixing-Length Forms.
Combining Eqs. (4.54) and (4.57) gives an algebraic relationship

among k , ε , and the mean shear:

$$\ell_m^2 \left| \frac{d\bar{U}}{dy} \right|^3 = C_\varepsilon \frac{k^{3/2}}{L}. \quad (4.58)$$

This expression shows how the energy-containing eddies (through k and L) interact with the mean shear field (through ℓ_m and $d\bar{U}/dy$). It bridges classical mixing-length models and modern two-equation (k - ε) models, where both k and ε are obtained from transport equations.

4.6.5 Modeled TKE Equation (Mixing-Length Form)

Using the modeled closures:

$$P_k = \ell_m^2 |S|^3, \quad \varepsilon = C_\varepsilon \frac{k^{3/2}}{\ell_m}, \quad T_j \approx -(\nu + \nu_t) \frac{\partial k}{\partial x_j}, \quad \nu_t = \ell_m^2 |S|, \quad (4.59)$$

the TKE equation becomes

$$\frac{\partial k}{\partial t} + \bar{u}_j \frac{\partial k}{\partial x_j} = \ell_m^2 |S|^3 - C_\varepsilon \frac{k^{3/2}}{\ell_m} + \frac{\partial}{\partial x_j} \left[(\nu + \nu_t) \frac{\partial k}{\partial x_j} \right]. \quad (4.60)$$

4.6.6 Final Simplified 1-D Steady Shear Form

For a statistically steady, one-dimensional shear flow ($\bar{U} = \bar{U}(y)$):

$$0 = \ell_m^2 \left| \frac{d\bar{U}}{dy} \right|^3 - C_\varepsilon \frac{k^{3/2}}{\ell_m} + \frac{d}{dy} \left[(\nu + \nu_t) \frac{dk}{dy} \right], \quad \nu_t = \ell_m^2 \left| \frac{d\bar{U}}{dy} \right|. \quad (4.61)$$

- The first term represents local production of turbulence by mean shear.
- The second term represents dissipation at small scales.
- The third term accounts for diffusion of k due to viscous and turbulent transport.

At local equilibrium (negligible diffusion), $P_k \simeq \varepsilon$, giving $\ell_m^2 |d\bar{U}/dy|^3 = C_\varepsilon k^{3/2}/\ell_m$.

How do we choose the mixing length ℓ_m ?

Example 4.0 Homogeneous simple shear (no walls).
With imposed constant shear and no geometric length, take

$$\ell_m = \text{const}, \quad \text{or} \quad \ell_m = c_L L,$$

where L is the integral scale from two-point correlations or spectra; c_L is calibrated ($\sim 0.2-0.5$).

Data-driven estimate from measured stresses. If R_{12} and fracdUdy are known,

$$\nu_t = -\frac{R_{12}}{U_y} \implies \ell_m = \sqrt{\frac{\nu_t}{|S|}} = \sqrt{\frac{-R_{12}}{|U_y|^3}} |U_y|. \quad (4.62)$$

4.6.7 Example 4.1: Homogeneous, incompressible steady, shear flow:

We consider homogeneous, incompressible turbulence subject to a constant mean shear $\bar{U}_1 = S x_2$ (so $\partial\bar{U}_1/\partial x_2 = S$, all other mean gradients zero). Statistical steadiness and homogeneity imply that unsteadiness and transport vanish at one point, so the TKE balance(Eq.4.33)reduces to

$$0 = P_k - \varepsilon, \quad (4.63)$$

For simple shear, only $\partial\bar{u}_1/\partial x_2$ is nonzero, hence using Eq.??, Eq. 4.63 simplifies to,

$$P_k = -R_{12} S = \varepsilon. \quad (4.64)$$

Using Eq.4.54, Eq.4.64 simplifies to an algebraic equation,

$$k = \left(\frac{\ell_m^2 |S|^3 L}{C_\varepsilon} \right)^{2/3}, \quad \varepsilon = \ell_m^2 |S|^3, \quad \nu_t = \ell_m^2 |S| \quad (4.65)$$

4.6.8 Example 4.2: Decaying Homogeneous–Isotropic Turbulence in a Periodic Box

Consider homogeneous, isotropic turbulence in a periodic box with no mean flow and no external forcing for $t \geq t_0$. It can be shown that production and transport vanish by symmetry, so the turbulent kinetic energy (TKE) obeys the unsteady balance

$$\frac{dk}{dt} = -\varepsilon, \quad t \geq t_0, \quad (4.66)$$

Given $k(t_0) = k_0 > 0$:

The TKE balance simplifies as,

$$\frac{dk}{dt} = -\varepsilon. \quad (4.67)$$

Assuming a self-preserving decay with a single evolving large scale $L(t)$ and closure from Eq.4.54 gives

$$\frac{dk}{dt} = -C_\varepsilon \frac{k^{3/2}}{L(t)}. \quad (4.68)$$

With $L(t)$ slowly varying or following a power law, this ODE yields the classic power-law decays $k \propto t^{-n}$.

Separate variables and integrate from t_0 to t :

$$\int_{k_0}^{k(t)} k^{-3/2} dk = -\frac{C_\varepsilon}{L_0} \int_{t_0}^t ds \quad (4.69)$$

$$\implies -2k(t)^{-1/2} + 2k_0^{-1/2} = -\frac{C_\varepsilon}{L_0} (t - t_0). \quad (4.70)$$

Hence

$$k(t) = \left[k_0^{-1/2} + \frac{C_\varepsilon}{2L_0} (t - t_0) \right]^{-2}, \quad (4.71)$$

$$\varepsilon(t) = C_\varepsilon \frac{k(t)^{3/2}}{L_0} = C_\varepsilon \frac{1}{L_0} \left[k_0^{-1/2} + \frac{C_\varepsilon}{2L_0} (t - t_0) \right]^{-3} \quad (4.72)$$

The box turbulence setting (no mean flow, no production, periodic boundaries) is the canonical case where $dk/dt = -\varepsilon$ holds exactly at one-point level. The closure for ε and the choice/evolution of $L(t)$ determine the precise decay law.

4.7 Example 4.3: Grid-Generated Turbulence and Homogeneous Isotropic Decay

Regular grids in wind tunnels have been central to experimental turbulence research since the classical works of Simmons (1934), Taylor (1935), Batchelor (1947) and Townsend (1948) followed by many careful studies (e.g., ComteBellot (1966), Hinze (1975)). Downstream of a suitably designed grid and beyond the developing region, the turbulence is approximately homogeneous and (locally) isotropic, making it an ideal canonical flow for studying decaying turbulence.

4.7.1 Homogeneity and Isotropy:

Homogeneity. Statistics are invariant under translations in the homogeneous directions. In the decay region downstream of grids, the streamwise evolution is slow while cross-stream planes are approximately homogeneous.

Isotropy. Statistics are invariant under rotations; all directions are statistically equivalent. A consequence is the vanishing

of shear correlations

$$\overline{u'v'} = \overline{v'w'} = \overline{u'w'} = 0,$$

and equality of component variances (in the ideal limit). The one-point PDF of velocity components tends toward Gaussian, with skewness $S_u = 0$ and flatness $F_u = 3$ for well-resolved small scales (Batchelor (1953), Hinze (1975)). In practice, isotropy is approximate (local isotropy), particularly at small scales far from the grid.

Isotropic relations. In strictly isotropic turbulence,

$$q^2 \equiv \overline{u'^2} + \overline{v'^2} + \overline{w'^2} = 3\overline{u'^2}. \quad (4.73)$$

Grid measurements often show small departures, e.g.

$$q^2 \approx 2.5\overline{u'^2}, \quad \overline{v'^2} \approx \overline{w'^2} \approx 0.75\overline{u'^2}, \quad (4.74)$$

indicating near-, but not perfect, isotropy.

4.7.2 TKE Balance in the Decay Region

Far enough downstream of the grid, production and mean-shear effects are negligible and the Reynolds averaged turbulent kinetic energy (TKE) budget (Eq.4.33) reduces to a decay balance

$$\frac{dk}{dt} = -\varepsilon, \quad t \equiv \frac{x - x_0}{U_\infty}, \quad (4.75)$$

where U_∞ is the mean tunnel velocity, and x_0 is the virtual origin.

4.7.3 Power-Law Decay and Empirical Ranges

A large body of experiments (e.g., ComteBellot (1966), Hinze (1975), Batchelor (1953)) supports the self-similar power-law form

$$k(x) = A \left(\frac{x - x_0}{M} \right)^{-n}, \quad t = \frac{x - x_0}{U_\infty}, \quad (4.76)$$

where M is the grid mesh size and A is set by initial conditions. Typical measured decay exponents lie in

$$1.2 \lesssim n \lesssim 1.4.$$

4.7.4 Large-Scale Invariants and Length-Scale Growth

The downstream decay links k and the integral scale L through infrared (small-wavenumber) behavior of the energy spectrum $E(k)$,

$$E(k) \sim k^{m_0}, \quad k \rightarrow 0, \quad (4.77)$$

which implies the classical invariant (Batchelor, 1953; Frisch, 1995)

$$k L^{m_0+1} = \text{const.} \quad (4.78)$$

Hence,

$$L \propto k^{-1/(m_0+1)}. \quad (4.79)$$

Two canonical infrared families are:

- **Saffman turbulence** ($m_0 = 2$): $E(k) \sim k^2$ with finite linear-momentum integral (Saffman, 1967).
- **Loitsyansky turbulence** ($m_0 = 4$): $E(k) \sim k^4$ with finite angular-momentum integral (Loitsyansky, 1939 and Batchelor, 1953).

4.7.5 Decay Exponent from $\varepsilon \sim k^{3/2}/L$

Using the empirical/dimensional dissipation closure

$$\varepsilon = C_\varepsilon \frac{k^{3/2}}{L}, \quad C_\varepsilon = \mathcal{O}(1), \quad (4.80)$$

together with (4.79) and the balance (4.75),

$$\frac{dk}{dt} = -C_\varepsilon \frac{k^{3/2}}{L} \sim -k^{3/2+1/(m_0+1)}. \quad (4.81)$$

A self-similar solution $k \sim t^{-n}$ then gives

$$n = \frac{2(m_0 + 1)}{m_0 + 3}. \quad (4.82)$$

Therefore,

$$n = \frac{6}{5} = 1.2, \quad \text{Saffman } (m_0 = 2), \quad (4.83)$$

$$n = \frac{10}{7} \approx 1.43, \quad \text{Loitsyansky } (m_0 = 4). \quad (4.84)$$

These bracket the commonly observed range $n \approx 1.2\text{-}1.4$.

4.7.6 Dissipation Decay

From (4.75) and (4.76), the dissipation decays one power faster:

$$\varepsilon(x) = \frac{U_\infty A n}{M} \left(\frac{x - x_0}{M} \right)^{-(n+1)}. \quad (4.85)$$

Equivalently,

$$\boxed{\varepsilon \sim \beta ((x - x_0)/M)^{-m}, \quad m = n + 1, \quad \beta = \frac{U_\infty A n}{M}}. \quad (4.86)$$

4.7.7 Flow Regions of Grid turbulence

The downstream evolution can be sketched as:

1. *Developing region*: jet-wake interactions behind the grid.
2. *Power-law decay region*: approximately homogeneous/isotropic; $k \sim (x - x_0)^{-n}$.
3. *Dominating large-scale region*: energy shifts to larger eddies as small scales dissipate.
4. *Final decay*: low-Re turbulence with only large eddies remaining.
 - Grid turbulence offers a near-homogeneous, near-isotropic testbed for *decaying* turbulence.
 - The reduced TKE balance is $dk/dt = -\varepsilon$ with $t = (x - x_0)/M$

$x_0)/U_\infty.$

- Combining $\varepsilon \sim k^{3/2}/L$ with infrared invariants $k L^{m_0+1} = \text{const}$ yields $k \sim t^{-n}$ with $n = 2(m_0 + 1)/(m_0 + 3)$.
- Saffman ($n = 6/5$) and Loitsyansky ($n = 10/7$) exponents bound typical experimental decay ($n \approx 1.2\text{-}1.4$).
- Dissipation decays as $\varepsilon \sim t^{-(n+1)}$ (or $\sim (x - x_0)^{-(n+1)}$).

Part III:

Buoyancy-Driven Flows

4.8 Turbulent Kinetic Energy Equation with Buoyancy generation

The derivation of the turbulent kinetic energy (TKE) equation for buoyancy-generated flows is *identical in structure* to the mechanical (shear-only) case presented earlier: we Reynolds-decompose, form the fluctuation momentum equation, dot with u'_i , and time-average to obtain a balance for $k = \frac{1}{2}\overline{u'_i u'_i}$. We do not repeat those algebraic steps here. The only substantive change under the Boussinesq approximation is the presence of a buoyancy force in the fluctuation momentum equation, whose work on the velocity fluctuations appears as an *additional production (or sink) term* in the TKE budget,

$$P_b = \overline{u'_i b' \hat{g}_i} = \overline{u'_3 b'}. \quad (4.87)$$

For thermal stratification $b' = g \alpha_T \theta'$ (or $b' = -g \rho'/\rho_0$ in density form), so $P_b = g \alpha_T \overline{u'_3 \theta'}$. This term is *sign-indefinite*: $P_b > 0$ in unstable/convective conditions (adds TKE) and $P_b < 0$ in stable stratification (removes TKE). Importantly, the same turbulent scalar flux $\overline{u'_3 \theta'}$ that produces scalar variance also drives P_b , linking the TKE and scalar-variance budgets. Thus the mechanical equilibrium statement $P_s \simeq \varepsilon$ generalizes to $P_s + P_b \simeq \varepsilon$ in buoyancy-affected flows, while the transport term retains the same form as before (triple correlations, pressure diffusion, viscous diffusion).

The time-averaged TKE equation of incompressible flows with the Boussinesq approximation is,

$$\frac{\partial k}{\partial t} + \bar{u}_j \frac{\partial k}{\partial x_j} = \underbrace{-\overline{u'_i u'_j} \frac{\partial \bar{u}_i}{\partial x_j}}_{P_{\text{shear}}} + \underbrace{\overline{u'_3 b'}}_{P_b} - \varepsilon - \frac{\partial T_j}{\partial x_j} \quad (4.88)$$

where $P_b = \overline{u'_3 b'}$ is the *buoyancy production* (positive in unstable convection, negative in stable stratification), $\varepsilon = \nu \overline{\partial_j u'_i \partial_j u'_i}$, and transport terms are,

$$T_j = \frac{1}{2} \overline{u'_i u'_i u'_j} + \frac{\overline{p' u'_j}}{\rho_0} - \nu \frac{\partial k}{\partial x_j}. \quad (4.89)$$

The three terms represent: transport of TKE by turbulent fluctuations, transport by pressure fluctuations, and transport by molecular viscosity.

4.9 Scalar-variance equation (temperature or density).

The derivation of the scalar-variance equation is *parallel in structure* to the TKE derivation and is not repeated here. Starting from the advection-diffusion equation for the scalar (temperature or density), we subtract the mean equation to obtain a fluctuation equation for θ' , multiply by θ' , and time-average.

This yields a balance for the variance $\vartheta \equiv \frac{1}{2} \overline{\theta'^2}$ with the same four term types as in TKE: (i) *production* by the mean scalar gradient through the turbulent scalar flux, $\overline{u'_j \theta'} \frac{\partial \bar{\theta}}{\partial x_j}$, (ii) a positive-definite *dissipation* $\chi = \kappa \overline{\frac{\partial \theta'}{\partial x_j} \frac{\partial \theta'}{\partial x_j}}$ that destroys small-scale variance, (iii) *transport* written as a divergence of turbulent triple correlations plus molecular diffusion, and (iv) mean advection/unsteadiness. Under Boussinesq, the scalar can be *active*: the same flux $\overline{u'_3 \theta'}$ that appears in the variance production also enters the TKE equation as buoyancy work $P_b = g\alpha_T \overline{u'_3 \theta'}$, directly coupling the two budgets.

The variance budget is:

$$\frac{\partial \vartheta}{\partial t} + \overline{u}_j \frac{\partial \vartheta}{\partial x_j} = - \underbrace{\overline{u'_j \theta'} \frac{\partial \bar{\theta}}{\partial x_j}}_{\text{production by mean gradient}} - \underbrace{\chi}_{\text{scalar dissipation}} - \frac{\partial \Phi_j}{\partial x_j} \quad (4.90)$$

with $\chi = \kappa \overline{\partial_j \theta' \partial_j \theta'}$ and $\Phi_j = \frac{1}{2} \overline{\theta'^2 u'_j} - \kappa \partial_j \vartheta$.

Part IV: Mixing Length Closure Models for Buoyancy-driven

Turbulence

4.10 Buoyancy Closures with Gradient Diffusion

We model the turbulent scalar flux with a gradient-diffusion closure and use mixing-length/ k -based forms for the eddy diffusivity. Throughout, Boussinesq approximation is assumed.

4.10.1 Scalar flux (eddy diffusivity).

$$\overline{u'_j \theta'} = -\kappa_t \frac{\partial \bar{\theta}}{\partial x_j}, \quad \kappa_t = \frac{\nu_t}{\text{Pr}_t}, \quad (4.92)$$

with turbulent Prandtl number Pr_t and eddy viscosity ν_t supplied by the shear section (e.g. mixing length).

4.10.2 Closure for the Dissipation rate

$$\varepsilon = C_\varepsilon \frac{k^{3/2}}{\ell_m}, \quad \chi \equiv 2\kappa \overline{\nabla \theta' \cdot \nabla \theta'} \approx C_\theta \frac{\vartheta \sqrt{k}}{\ell_m}, \quad (4.93)$$

where $\vartheta \equiv \frac{1}{2} \overline{\theta'^2}$ is the scalar variance.

4.10.3 Brunt–Väisälä frequency.

$$N^2 \equiv g \alpha_T \frac{\partial \bar{\theta}}{\partial y}, \quad (4.94)$$

with g gravity and α_T the thermal expansion coefficient.

4.10.4 Turbulent Buoyant Production

The buoyancy term in the TKE budget is

$$P_b \equiv \overline{u'_3 b'} = g \alpha_T \overline{u'_3 \theta'}. \quad (4.95)$$

Using (4.92) in the vertical ($j = 3$) direction,

$P_b = -g \alpha_T \kappa_t \frac{\partial \bar{\theta}}{\partial y} = -\frac{\nu_t}{\text{Pr}_t} N^2.$

(4.96)

Hence $P_b > 0$ for unstable stratification ($N^2 < 0$) and $P_b < 0$ for stable stratification ($N^2 > 0$).

4.10.5 Production of Scalar Variance

The scalar-variance production term is

$$\mathcal{P}_\vartheta \equiv -\overline{u'_j \theta'} \frac{\partial \bar{\theta}}{\partial x_j}. \quad (4.97)$$

With (4.92),

$$\mathcal{P}_\vartheta = \kappa_t |\nabla \bar{\theta}|^2, \quad (\text{1-D vertical}) : \mathcal{P}_\vartheta = \kappa_t \left(\frac{d \bar{\theta}}{dy} \right)^2.$$

(4.98)

Both P_b (in TKE) and \mathcal{P}_ϑ (in scalar-variance) depend on the same $\overline{u'_3 \theta'}$:

$$P_b = g \alpha_T \overline{u'_3 \theta'}, \quad \mathcal{P}_\vartheta = -\overline{u'_3 \theta'} \frac{\partial \bar{\theta}}{\partial y}. \quad (4.99)$$

Stability (N^2) and \Pr_t thus govern conversion between available potential energy (via P_b) and scalar-variance growth (via \mathcal{P}_ϑ).

4.10.6 Example 4.4: 1-D Vertical, Steady Flow

Assume steady, 1-D variation in y ; use ν_t and $\kappa_t = \nu_t/\Pr_t$ from the shear section.

For the 1-D steady flow, the TKE equation is:

$$0 = \underbrace{P_s}_{\text{shear (from shear section)}} + \underbrace{\left(-\frac{\nu_t}{\Pr_t} N^2 \right)}_{P_b} - \underbrace{C_\varepsilon \frac{k^{3/2}}{\ell_m}}_{\varepsilon} + \frac{d}{dy} \left[\left(\nu + \frac{\nu_t}{\sigma_k} \right) \frac{dk}{dy} \right]. \quad (4.100)$$

Scalar variance.

$$0 = \underbrace{\kappa_t \left(\frac{d\bar{\theta}}{dy} \right)^2}_{\mathcal{P}_\vartheta} - \underbrace{C_\theta \frac{\vartheta \sqrt{k}}{\ell_m}}_{\chi} + \frac{d}{dy} \left[\left(\kappa + \frac{\kappa_t}{\sigma_\vartheta} \right) \frac{d\vartheta}{dy} \right], \quad \kappa_t = \frac{\nu_t}{\text{Pr}_t}. \quad (4.101)$$

- Use a chosen ν_t model from the shear section (e.g. $\nu_t = \ell_m^2 |\bar{U}'/dy|$ or $C_\varepsilon^{1/3} \ell_m \sqrt{k}$); buoyancy enters only through P_b and κ_t .
- Local equilibria in homogeneous regions: $P_s + P_b \simeq \varepsilon$ and $\mathcal{P}_\vartheta \simeq \chi$.

In buoyancy-affected turbulence, the scalar-variance production and the TKE buoyant production are two manifestations of the same turbulent scalar flux. The variance budget gains energy through $\mathcal{P}_\vartheta = -\overline{u'_j \theta' \frac{\partial \bar{\theta}}{\partial x_j}}$ (in 1D: $\kappa_t (\frac{\partial \bar{\theta}}{\partial x_j})^2$ under $\overline{u'_j \theta'} = -\kappa_t \frac{\partial \bar{\theta}}{\partial x_j}$), while the TKE budget gains or loses energy through $P_b = \overline{u'_3 b'} = g\alpha_T \overline{u'_3 \theta'} = -(\nu_t/\text{Pr}_t) N^2$. Because both terms depend on $\overline{u'_3 \theta'}$, stability (N^2) and the turbulent Prandtl number (Pr_t) jointly control how scalar gradients are converted into kinetic energy versus scalar variance: in unstable flow ($N^2 < 0$), $P_b > 0$ converts available potential energy into TKE while \mathcal{P}_ϑ grows variance until gradients are eroded; in stable flow ($N^2 > 0$), $P_b < 0$ extracts TKE even as variance production persists but is countered by dissipation. In homogeneous, steady regions, the local equilibria $P_s + P_b = \varepsilon$ and $\mathcal{P}_\vartheta = \chi$ emphasize that shear and buoyancy together sustain the dissipation rates, while transport mainly redistributes energy without net production. Practically, closures link the two budgets via ν_t and $\kappa_t = \nu_t/\text{Pr}_t$, so choosing Pr_t and the mixing length ℓ_m determines the partitioning between momentum mixing, scalar mixing, and buoyancy conversion.

4.10.7 Example 4.5: Purely Buoyancy-generated turbulence: Rayleigh–Bernard Turbulence

Consider a Rayleigh–Benard convection cell where there is no mean shear ($P_s = 0$) and the mean flow is negligible. The TKE balance reduces to

$$\frac{dk}{dt} = P_b - \varepsilon. \quad (4.102)$$

Assume that the turbulent heat flux can be modeled as

$$\overline{u'_3 T'} = -\alpha_t \frac{\partial \bar{T}}{\partial z}, \quad (4.103)$$

where α_t is the turbulent thermal diffusivity. Then

$$P_b = -g \beta_T \alpha_t \frac{\partial \bar{T}}{\partial z}. \quad (4.104)$$

For unstable stratification ($\partial \bar{T} / \partial z < 0$), this term is positive and supplies energy to the turbulence.

4.10.8 Self-similar solution.

A simplified closure assumes equilibrium between buoyant production and dissipation,

$$P_b \approx \varepsilon. \quad (4.105)$$

Using the standard dissipation scaling

$$\varepsilon \sim C_\varepsilon \frac{k^{3/2}}{L}, \quad (4.106)$$

with L the integral length scale, gives

$$g \beta_T \alpha_t \left| \frac{\partial \bar{T}}{\partial z} \right| \sim C_\varepsilon \frac{k^{3/2}}{L}. \quad (4.107)$$

Solving for k ,

$$k \sim \left(\frac{g \beta_T \alpha_t |\partial \bar{T} / \partial z| L}{C_\varepsilon} \right)^{2/3}. \quad (4.108)$$

Equation (4.108) shows that, in buoyancy-generated turbulence:

- The TKE grows with increasing buoyancy flux ($g\beta_T \overline{w' T'}$).
- Larger integral scales L support higher levels of k .
- The solution has the same 2/3 scaling exponent found in shear-dominated turbulence (mixing-length arguments), but the production term is now thermal.

Thus, buoyant turbulence provides a canonical example in which the energy source comes directly from conversion of potential energy to kinetic energy, rather than from mechanical shear.

4.11 Exercises

Problem 1 (Classic grid decay with growing integral scale). A wind tunnel with uniform mean speed $U_\infty = 10 \text{ m s}^{-1}$ produces shear-free turbulence downstream of a grid. Assume the integral (energy-containing) length

$$\ell(x) = a(x - x_0), \quad a = 0.06, \quad x_0 = 0.15 \text{ m},$$

and the dissipation closure

$$\varepsilon = C_\varepsilon \frac{k^{3/2}}{\ell}, \quad C_\varepsilon = 0.09.$$

The shear production is negligible ($P_s = 0$), so the TKE convects and decays as

$$U_\infty \frac{dk}{dx} = -\varepsilon.$$

1. Solve for $k(x)$ in the form $k(x) = \frac{A}{(x - x_0)^n}$ and report (A, n) .

2. If $k(0.50 \text{ m}) = 0.20 \text{ m}^2/\text{s}^2$, predict $k(1.00 \text{ m})$.
3. With $\nu = 1.5 \times 10^{-5} \text{ m}^2/\text{s}$, estimate the Kolmogorov scale $\eta = (\nu^3/\varepsilon)^{1/4}$ at $x = 1.00 \text{ m}$ and comment on whether $\eta \ll \ell$ holds.
4. *Grid-turbulence modification (alternate ℓ -law)*. Repeat part (b) if instead

$$\ell(x) = \ell_0 [1 + \beta(x - x_0)], \quad \ell_0 = 0.02 \text{ m}, \quad \beta = 0.12 \text{ m}^{-1},$$

with the same U_∞ and C_ε . Report the ratio $k_{\text{alt}}(1.00 \text{ m})/k_{\text{linear}}(1.00 \text{ m})$ and state which ℓ -model gives faster decay.

Problem 2 (Passive scalar co-decay behind the grid). A scalar (dye or temperature) is injected upstream so that downstream there is *no mean scalar gradient*; only the variance $\vartheta = \frac{1}{2}\overline{\theta'^2}$ decays. Assume

$$U_\infty \frac{d\vartheta}{dx} = -\chi, \quad \chi = C_\theta \frac{\vartheta \sqrt{k}}{\ell}, \quad C_\theta = 2.0,$$

with $k(x)$ and $\ell(x)$ from Problem 1.

1. Solve for $\vartheta(x)$ in closed form (give a power law in $x - x_0$).
2. If $\vartheta(0.50 \text{ m}) = 0.08 \text{ (units)}^2$, predict $\vartheta(1.00 \text{ m})$ using your $k(x)$ from Problem 1.

Problem 3 (Minimal data fusion: recover x_0 and check ε). Assume the grid-decay model $k(x) = \frac{A}{(x - x_0)^2}$ and $\ell(x) = a(x - x_0)$ with $a = 0.06$. You measured

$$(x_1, k_1, \lambda_1) = (0.60 \text{ m}, 0.18 \text{ m}^2/\text{s}^2, 6.5 \text{ mm}), \quad (x_2, k_2, \lambda_2) = (0.90 \text{ m}, 0.11 \text{ m}^2/\text{s}^2, 7.5 \text{ mm}),$$

and $\nu = 1.5 \times 10^{-5} \text{ m}^2/\text{s}$.

1. Eliminate A to solve directly for the virtual origin x_0 using the two k -measurements. Then compute A .

2. Using $\varepsilon = C_\varepsilon k^{3/2}/\ell$ (with $C_\varepsilon = 0.09$), evaluate the modeled ε at x_1 and x_2 .
3. Independently estimate $\varepsilon_{\text{iso}} = 15 \nu u'^2/\lambda^2$ at each location with $u' = \sqrt{2k/3}$. Compare ε vs ε_{iso} and comment on which point is less consistent with the grid-decay assumptions.

Problem 4 (Intermittency knob in grid decay). Suppose small-scale intermittency enhances dissipation so that

$$\varepsilon = C_\varepsilon(1 + \beta) \frac{k^{3/2}}{\ell}, \quad \beta \in [0, 0.3].$$

1. Re-solve the decay ODE $U_\infty dk/dx = -\varepsilon$ with $\ell = a(x - x_0)$ and show how the *decay exponent* of k changes with β .
2. For $\beta = 0.20$, by what % does the downstream distance required for k to drop by a factor of two decrease compared with $\beta = 0$? Express your answer in terms of $(x - x_0)$.

Problem 5 (Almost shear-free: small imposed mean shear). Far downstream, a weak uniform shear $S = |d\bar{U}/dy| = 0.15 \text{ s}^{-1}$ is imposed so that

$$U_\infty \frac{dk}{dx} = P_s - \varepsilon, \quad P_s = \nu_t S^2, \quad \nu_t \approx C_\varepsilon^{1/3} \ell \sqrt{k},$$

with $\ell = a(x - x_0)$ and $C_\varepsilon = 0.09$.

1. Show that the ratio P_s/ε scales as

$$\frac{P_s}{\varepsilon} = \frac{C_\varepsilon^{1/3}}{C_\varepsilon} \frac{S^2 \ell^2}{k} = C_\varepsilon^{-2/3} S^2 \frac{\ell^2}{k},$$

and express its x -dependence using $k(x)$ from the shear-free decay.

2. Determine the downstream distance x^* (in terms of parameters) at which $P_s/\varepsilon = 0.20$. Briefly interpret the

physical meaning: beyond x^* , mean shear non-negligibly feeds TKE compared with inertial decay.

4.12 Companion Notebook: Chapter 4

The companion Jupyter notebook ([Chapter4CompanionPrinciplesofTurbulence.ipynb](#)) provides a computational supplement to Chapter 4, bridging the theoretical derivations of the Reynolds-averaged equations, turbulent kinetic energy budgets, and mixing-length approximations with practical numerical examples. Each section is designed to allow readers to interact with the fundamental equations, visualize turbulent transport terms, and develop an intuitive understanding of model assumptions and closures.

Organization of the Notebook

The notebook is organized to follow the same sequence as the textbook:

- 1. Reynolds Decomposition and Averaging.** Demonstrates how instantaneous velocity and scalar fields are decomposed into mean and fluctuating components, and how ensemble averages are computed numerically.
- 2. RANS Momentum Equation.** Illustrates the term-by-term contributions in the Reynolds-averaged momentum equation for a steady, one-dimensional wall-normal channel. Numerical differentiation of synthetic mean fields is used to identify viscous, pressure, and Reynolds stress gradients.
- 3. Turbulent Kinetic Energy (TKE) Equation.** Evaluates the single-point form of the TKE equation, emphasizing the balance among production, dissipation, and transport. Students compute production terms using modeled Reynolds stresses and mean velocity gradients.
- 4. Mixing-Length Model (Van Driest Damping).** Im-

plements Prandtl's mixing-length hypothesis and the Van Driest damping function to evaluate near-wall eddy viscosity and production terms, with visual comparisons against undamped models.

5. **Datasets and Utility Files.** Introduces the datasets and external utility modules used in the computations, including synthetic, grid-based, and isotropic turbulent fields.
6. **Worked Examples.** A series of guided numerical exercises (NB 4.1–4.5) reinforce the theoretical development by computing mean gradients, stresses, and fluxes using the provided data.
7. **Buoyancy-Generated Turbulence.** Applies the mixing-length framework to temperature-driven flows under unstable, neutral, and stable stratification using the Boussinesq approximation. The section concludes with comparisons of heat flux and buoyancy production across regimes.

Description of Datasets

Three compact datasets are used for demonstration and validation:

Synthetic Channel Dataset. A parameterized dataset containing analytic mean velocity and scalar profiles with prescribed gradients. It provides a noise-free environment to verify sign conventions and the relative magnitude of modeled terms.

Grid (HIT-style) Dataset. A spatially sampled set of fluctuating velocity and scalar components representing homogeneous isotropic turbulence. This dataset enables estimation of Reynolds stresses, TKE, and scalar fluxes over an idealized uniform domain.

Isotropic Snapshot. A reduced dataset used to test isotropy

and sampling effects. It serves as a compact example for computing normal-stress ratios and assessing statistical convergence in small ensembles.

All datasets are accessed programmatically through short utility scripts. The utility modules (e.g., `chapter4_util.py` and `ch4_buoyancy_examples.py`) handle data loading, computation of mean gradients, eddy viscosity, turbulent heat fluxes, and plotting routines.

Structure of Worked Examples

Each example in the notebook corresponds to a subtopic introduced in the main text:

Example NB 4.1 — RANS Momentum Terms. Evaluates the momentum balance for a one-dimensional synthetic channel and verifies the equivalence between pressure gradients, viscous diffusion, and Reynolds stress divergence.

Example NB 4.2 — Mixing-Length and Production. Compares standard and Van Driest-damped mixing-length models, quantifying their effect on eddy viscosity and local TKE production.

Example NB 4.3 — Grid (HIT-style) Dataset. Computes Reynolds stresses and TKE from the grid dataset, verifies isotropy in the core region, and relates the results to theoretical scaling laws.

Example NB 4.4 — HIT Dataset: Isotropy Check. Repeats the stress and TKE computation on a smaller isotropic snapshot to explore the impact of sample size on isotropy ratios and uncertainty.

Example NB 4.5 — Buoyancy-Generated Turbulence. Constructs unstable, neutral, and stable stratified profiles, evaluates thermal eddy diffusivity (K_h), turbulent heat flux ($\overline{w'\theta'}$), and the buoyancy term in the TKE equation (G_b). The section emphasizes the physical interpretation

of sign changes across stability regimes.

Student Activities and Interpretation

Each worked example concludes with reflection prompts encouraging interpretation of numerical trends. Students are asked to:

- Relate the magnitude and sign of modeled fluxes to the mean gradients.
- Assess where simplified models (e.g., constant Pr_t) deviate from physical expectations.
- Compare isotropy ratios with theoretical limits.
- Interpret buoyancy effects on the balance between production and dissipation.

This structure ensures that the notebook reinforces conceptual understanding rather than reproducing formulaic computations.

Homework and Extensions

The final section provides short computational exercises aligned with the textbook's homework problems:

1. Evaluate the eddy diffusivity and buoyancy term for prescribed mean gradients and discuss sign consistency.
2. Perform a parametric sweep on Pr_t to examine sensitivity of K_h and G_b .
3. Implement a capped mixing length (l_{\max}) and quantify its influence on near-wall and outer-layer behavior.
4. Estimate TKE and isotropy ratios from the reduced dataset and discuss statistical convergence.

Chapter 5

Favre averaging of

Navier Stokes

Equations

5.1 Introduction

In high Mach number flows, flows with shock waves, compressibility effects become very significant; the turbulence is referred to as Compressible turbulence. In such flows, there are significant changes in the thermodynamic and state variables. Compressible turbulence is the coupling of the density/temperature fluctuations with the velocity fluctuations. Compressible turbulence shares key similarities with active scalar mixing in incompressible flows, such as temperature fluctuations driving buoyant motions in wildland fires. In both cases, the scalar field is *active*, meaning it directly modifies the momentum field and turbulent kinetic energy (TKE), rather than simply being transported passively. Reynolds averaging fails to decouple velocity and density fluctuations in compressible turbulence and incompressible flows with active scalar mixing. In this chapter, we introduce the concept of Favre-averaging, and show the derivation for the governing equations of turbulence for compressible Turbulence.

5.2 Favre Averaging and Favre Decomposition

We define a density-weighted averaging procedure, known as *Favre averaging*.

Favre average. For any flow variable $\phi(x_i, t)$, the Favre average is defined as

$$\tilde{\phi} \equiv \frac{\overline{\rho\phi}}{\overline{\rho}}, \quad (5.1)$$

where $\overline{(\cdot)}$ denotes the Reynolds (ensemble or time) average.

Favre decomposition. The instantaneous variable is then written as

$$\phi = \tilde{\phi} + \phi'', \quad (5.2)$$

where ϕ'' is the Favre fluctuation.

Favre fluctuation property. By construction,

$$\overline{\rho\phi''} = 0. \quad (5.3)$$

That is, Favre fluctuations always vanish when weighted by density.

Comparison with Reynolds decomposition. For incompressible flows, $\rho = \text{constant}$ and $\tilde{\phi} = \overline{\phi}$, so the Favre average reduces to the Reynolds average. In compressible flows, however, the two differ because density fluctuations couple with velocity and scalar fields. The Favre decomposition ensures that fluxes take a simplified form. For example,

$$\overline{\rho u_i \phi} = \overline{\rho} \tilde{u}_i \tilde{\phi} + \overline{\rho} \widetilde{u''_i \phi''}. \quad (5.4)$$

This closely parallels the Reynolds-averaged flux form in incompressible turbulence, but now accounts correctly for density variations.

5.3 Favre-Averaged Conservation Equations

5.3.1 Favre Decomposition for Velocity and Pressure

The instantaneous velocity, pressure, and density fields are decomposed as follows:

Velocity decomposition. The Favre average of velocity is

$$\tilde{u}_i \equiv \frac{\rho u_i}{\bar{\rho}}, \quad (5.5)$$

and the instantaneous velocity is decomposed as

$$u_i = \tilde{u}_i + u''_i, \quad (5.6)$$

where u''_i is the Favre velocity fluctuation. By definition,

$$\overline{\rho u''_i} = 0. \quad (5.7)$$

Pressure and Density decomposition. The standard Reynolds decomposition is used to decompose the pressure and density as follows,

$$p = \bar{p} + p', \rho = \bar{\rho} + \rho' \quad (5.8)$$

since pressure is not conveniently expressed in density-weighted form. Thus p' is the Reynolds pressure fluctuation with $\bar{p}' = 0$.

and taking the time average of the equation gives the resultant equations for the mean flow. The mass conservation equation is:

5.3.2 Favre averaged continuity Equation)

$$\frac{\partial \bar{\rho}}{\partial t} + \frac{\partial (\bar{\rho} \tilde{u}_j)}{\partial x_j} = 0. \quad (5.9)$$

5.3.3 Favre-averaged Conservation of Momentum Equation

The Favre-averaged mean momentum equation is derived as follows: In the instantaneous momentum equation, replace the velocity with the Favre-decomposition, pressure and density with the Reynolds-decomposition, take the Reynolds averaging of the equation and subtract the instantaneous momentum equation. The resultant equation is,

$$\frac{\partial(\bar{\rho}\tilde{u}_i)}{\partial t} + \frac{\partial(\bar{\rho}\tilde{u}_i\tilde{u}_j)}{\partial x_j} = -\frac{\partial\bar{p}}{\partial x_i} + \frac{\partial}{\partial x_j}\left(\bar{\tau}_{ij}\right) - \underbrace{\frac{\partial}{\partial x_j}\left(\bar{\rho}\overline{u''_i u''_j}\right)}_{\text{Turbulent stress}} \quad (5.10)$$

where the significant terms are:

- $\frac{\partial(\bar{\rho}\tilde{u}_i)}{\partial t}$: *Unsteady acceleration* of the mean momentum.
- $\frac{\partial(\bar{\rho}\tilde{u}_i\tilde{u}_j)}{\partial x_j}$: *Mean-flow convection* of momentum.
- $-\frac{\partial\bar{p}}{\partial x_i}$: *Mean pressure gradient* force driving or resisting the flow.
- $\frac{\partial\bar{\tau}_{ij}}{\partial x_j}$: *Viscous diffusion* (molecular momentum transport).
- $-\frac{\partial}{\partial x_j}\left(\bar{\rho}\overline{u''_i u''_j}\right)$: *Turbulent (Favre-Reynolds) stress*, representing momentum transfer by velocity fluctuations; this term must be modeled (e.g. via an eddy-viscosity hypothesis) to close the equations.

5.3.4 Favre-Averaged Conservation of Energy Equation

The Favre-averaged total-energy equation is given as,

$$\frac{\partial(\bar{\rho}\tilde{E})}{\partial t} + \frac{\partial(\bar{\rho}\tilde{E}\tilde{u}_j)}{\partial x_j} = -\frac{\partial(\tilde{u}_j\bar{p})}{\partial x_j} + \frac{\partial}{\partial x_j}\left(\tilde{u}_i\bar{\tau}_{ij}\right) \quad (5.11)$$

$$-\frac{\partial q_j}{\partial x_j} - \frac{\partial}{\partial x_j}\left(\bar{\rho}\overline{u''_j h''}\right), \quad (5.12)$$

where \tilde{E} is the Favre-averaged total energy per unit mass, q_j the mean heat flux, and $\bar{\rho} \bar{u}_j'' h''$ the turbulent enthalpy flux.

- $\frac{\partial(\bar{\rho} \tilde{E})}{\partial t}$: *Local change* of mean total energy per unit volume.
- $\frac{\partial(\bar{\rho} \tilde{E} \tilde{u}_j)}{\partial x_j}$: *Mean flow convection* transporting energy with the bulk motion.
- $-\frac{\partial(\tilde{u}_j \bar{p})}{\partial x_j}$: *Pressure work* term, representing work done by mean pressure forces.
- $\frac{\partial(\tilde{u}_i \bar{\tau}_{ij})}{\partial x_j}$: *Viscous work*, the transfer of energy between mean flow and viscous stresses.
- $-\frac{\partial q_j}{\partial x_j}$: *Molecular heat conduction*, divergence of the Fourier heat-flux vector.
- $-\frac{\partial}{\partial x_j} (\bar{\rho} \bar{u}_j'' h'')$: *Turbulent enthalpy flux*, representing energy transport by correlations of velocity and enthalpy fluctuations; this term must be modeled (e.g. via gradient-diffusion) to close the equation.

5.4 Additional Transport Equations

The Favre-averaged Navier–Stokes framework not only yields the turbulent kinetic energy (TKE) equation, but also generates additional equations for higher-order correlations. These include turbulent mass flux, temperature variance, density variance, and mixed correlation terms. Together, they describe the coupling between velocity, scalar, and thermodynamic fluctuations in compressible turbulence.

5.4.1 Transport Equation for the density variance

We define the density-variance as:

$$\Phi = \overline{\rho' \rho'} \quad (5.13)$$

The budget terms of $\overline{\rho'^2}$ is computed:

$$\tilde{u}_j \frac{\partial \Phi}{\partial x_j} = \mathcal{P}_\rho + P_\rho + \mathcal{T}_\rho + \Pi_\rho + \pi_\rho. \quad (5.14)$$

Similar to equation (5.22), the term on the left hand side of the equation is the convection. On the right hand side of the equation, \mathcal{P}_ρ and P_ρ are the production by the mean flows and density gradient, respectively. \mathcal{T}_ρ is the transport, Π_ρ and π_ρ are the density-dilatation connected with the mean flows and fluctuations, respectively. The explicit form of each term is provided as follows:

$$\mathcal{P}_\rho = -2\overline{\rho'^2} \frac{\partial \tilde{u}_j}{\partial x_j} \quad (5.15a)$$

$$P_\rho = -2\overline{\rho' u''_j} \frac{\partial \overline{\rho}}{\partial x_j} \quad (5.15b)$$

$$\mathcal{T}_\rho = -\frac{\partial \overline{\rho' \rho' u''_j}}{\partial x_j} \quad (5.15c)$$

$$\Pi_\rho = -2\overline{\rho} \overline{\rho'} \frac{\partial \overline{u''_j}}{\partial x_j} \quad (5.15d)$$

$$\pi_\rho = -\overline{\rho'^2} \frac{\partial \overline{u''_j}}{\partial x_j}. \quad (5.15e)$$

5.4.2 Transport equation for Temperature variance

We define the Favre temperature variance as:

$$\Theta''^2 = \overline{T'' T''}.$$

The budget analysis of $\widetilde{T''^2}$ is computed:

$$\widetilde{\rho} \widetilde{u}_j \frac{\partial \Theta''^2}{\partial x_j} = \mathcal{P}_T + P_T + \Pi_T + \epsilon_T + \mathcal{T}_T. \quad (5.16)$$

Besides the convection terms on the left side of the equation,

\mathcal{P}_T and P_T , on the right side of the equation, are the production from the mean flows and temperature gradient, respectively. Π_T is the temperature-dilatation connected with the pressure. \mathcal{T}_T is the summation of all the transport terms and ϵ_T is the dissipation. The explicit form of those budget terms is given as

$$\mathcal{P}_T = -\frac{2}{C_v} \overline{p T''} \frac{\partial \tilde{u}_j}{\partial x_j} + \frac{2}{C_v} \overline{T'' \sigma_{ij}} \frac{\partial \tilde{u}_i}{\partial x_j} \quad (5.17a)$$

$$P_T = -2\bar{\rho} \widetilde{T'' u_j''} \frac{\partial \tilde{T}}{\partial x_j} \quad (5.17b)$$

$$\Pi_T = -\frac{2}{C_v} \overline{p T''} \frac{\partial \tilde{u}_j''}{\partial x_j} \quad (5.17c)$$

$$\epsilon_T = \frac{2}{C_v} \overline{T'' \sigma_{ij}} \frac{\partial \tilde{u}_i''}{\partial x_j} - \frac{2}{C_v} \overline{k_T} \frac{\partial T''}{\partial x_j} \frac{\partial T}{\partial x_j} \quad (5.17d)$$

$$\mathcal{T}_T = -\frac{\partial \overline{\rho T''^2 u_j''}}{\partial x_j} + \frac{2}{C_v} \frac{\partial}{\partial x_j} \overline{k_T T''} \frac{\partial T}{\partial x_j} \quad (5.17e)$$

where, C_v is the specific heat capacity at constant volume. \mathcal{T}_T contains both turbulent and thermal transport, and ϵ_T includes viscous and thermal dissipation.

5.4.3 Equation for Turbulent Mass Flux

The turbulent mass flux vector,

$$m_i \equiv \frac{\overline{\rho u_i''}}{\overline{\rho}},$$

obeys its own transport equation. It represents the correlation between density fluctuations and velocity fluctuations. This term couples the momentum and continuity equations, and is absent in incompressible flows because $\rho' = 0$. Physically, m_i controls the relative drift between light and heavy fluid parcels in variable-density turbulence, and plays a central role in buoyancy-driven mixing.

The budget terms of turbulent mass fluxes are computed as

follows,

$$\frac{\partial \tilde{u}_j M_i}{\partial x_j} = B_\rho + \mathcal{P}_{\rho u} + P_{\rho u} + \Pi_{\rho u} + \Phi_\rho + \epsilon_{\rho u} + \mathcal{T}_{\rho u}. \quad (5.18)$$

The turbulent mass flux equation is governed by similar processes as the Reynolds stress equation. The term on the left hand side is the convection term and it represents the spatial variation of the density and velocity correlation. The convection term is balanced by the terms on the right hand side. These terms include the buoyancy B_ρ , production $\mathcal{P}_{\rho u}$ and $P_{\rho u}$, dilatation $\Pi_{\rho u}$, pressure-distribution $\Phi_{\rho u}$, dissipation $\epsilon_{\rho u}$, and transport $\mathcal{T}_{\rho u}$. The mathematical form of those terms is given as

$$B_\rho = -\frac{\overline{\rho'^2}}{\bar{\rho}} g_i \quad (5.19a)$$

$$\mathcal{P}_{\rho u} = \overline{\rho' u''_j} \frac{\partial \tilde{u}_i}{\partial x_j} + \frac{\overline{\rho'^2}}{\bar{\rho}} \frac{\partial \overline{\sigma_{ij}}}{\partial x_j} \quad (5.19b)$$

$$P_{\rho u} = -R_{ij} \frac{\partial \bar{\rho}}{\partial x_j} \quad (5.19c)$$

$$\Pi_{\rho u} = -\bar{\rho} \overline{u''_i} \frac{\partial \overline{u''_j}}{\partial x_j} \quad (5.19d)$$

$$\Phi_\rho = \frac{1}{\bar{\rho}} \overline{p' \frac{\partial \rho'}{\partial x_i}} \quad (5.19e)$$

$$\epsilon_{\rho u} = -\frac{1}{\bar{\rho}} \overline{\sigma'_{ij} \frac{\partial \rho'}{\partial x_j}} \quad (5.19f)$$

$$\mathcal{T}_{\rho u} = -\frac{1}{\bar{\rho}} \overline{\frac{\partial \rho' p'}{\partial x_i}} + \frac{1}{\bar{\rho}} \overline{\frac{\partial \rho' \sigma'_{ij}}{\partial x_j}} - \frac{1}{\bar{\rho}} \frac{\partial}{\partial x_j} \overline{\frac{\rho' u''_i u''_j}{\bar{\rho}}}. \quad (5.19g)$$

5.4.4 Equation for Reynolds stresses transport

The transport equation for the Favre-averaged Reynolds stress tensor $R_{ij} = \bar{\rho} \overline{u''_i u''_j}$ is derived as follows:

In the instantaneous N-S equations, the velocity is decomposed

using Favre-averaged decomposition(Eq. 5.2 and the pressure is decomposed using the Reynolds averaging. From this equation, the Reynolds-averaged N-S equation is subtracted (Eq.(??) resulting in the following:

$$\begin{aligned} \rho \frac{\partial u_i''}{\partial t} + \rho \tilde{u}_j \frac{\partial u_i''}{\partial x_j} + \rho u_j'' \frac{\partial \tilde{u}_i}{\partial x_j} + \rho u_j'' \frac{\partial u_i''}{\partial x_j} &= - \frac{\partial p'}{\partial x_i} + \frac{\partial \sigma'_{ij}}{\partial x_j} + \frac{\partial \bar{\rho} R_{ij}}{\partial x_j} \\ &+ \frac{\rho'}{\bar{\rho}} \left[\frac{\partial \bar{p}}{\partial x_i} - \frac{\partial \sigma_{ij}}{\partial x_j} + \frac{\partial \bar{\rho} R_{ij}}{\partial x_j} \right] - \bar{\rho} g_i. \end{aligned} \quad (5.20)$$

The equation of Reynolds stresses is, therefore, generated by averaging the product of u_j'' with the equation of $\rho u_i''$, and summing with the average of the product of u_i'' with the equation of $\rho u_j''$. Finally, equation (5.22) is formed by implementing the hydrostatic condition ($\partial_\alpha \bar{p} = -\bar{\rho} g_\alpha$)

$$\begin{aligned} \bar{\rho} \frac{\partial R_{\alpha\alpha}}{\partial t} + \bar{\rho} \tilde{u}_k \frac{\partial R_{\alpha\alpha}}{\partial x_k} &= - 2 \bar{\rho}' u_\alpha'' g_\alpha - 2 \bar{\rho} R_{\alpha k} \frac{\partial \tilde{u}_\alpha}{\partial x_k} + 2 \bar{p}' \frac{\partial u_\alpha''}{\partial x_\alpha} - 2 \bar{\sigma}'_{\alpha k} \frac{\partial u_\alpha''}{\partial x_k} \\ &+ 2 \bar{u}_\alpha'' \frac{\partial \bar{\sigma}_{\alpha k}}{\partial x_k} - \frac{\partial \bar{\rho} u_\alpha'' u_\alpha'' u_k''}{\partial x_k} - 2 \frac{\partial \bar{p}' u_\alpha''}{\partial x_\alpha} + 2 \frac{\partial \bar{\sigma}'_{\alpha k} u_\alpha''}{\partial x_k}. \end{aligned} \quad (5.21)$$

For stationary turbulent flows, the transient term can be dropped. Similar methods can also be applied to obtain the equations of $\bar{\rho}^2$, \bar{T}''^2 , $\bar{\rho}' u_i''$ and $\bar{T}'' u_i''$.

The budget equation for Reynolds stresses is given as:

$$\bar{\rho} \tilde{u}_k \frac{\partial R_{\alpha\alpha}}{\partial x_k} = P_B + P_S + \Pi + \epsilon + M + \mathcal{T}. \quad (5.22)$$

In equation (5.22), the left hand term is the mean convection equation On the right hand side, P_B and P_S are the production terms. Π is the pressure-dilatation, ϵ is the dissipation, M is the mass-flux contribution, and \mathcal{T} is the summation of all transport terms. The explicit form of each term is given as

follows:

$$P_B = -2\bar{\rho}'\bar{u}_{\alpha}''g_{\alpha} \quad (5.23a)$$

$$P_S = -2\bar{\rho}R_{\alpha k}\frac{\partial\tilde{u}_{\alpha}}{\partial x_k} \quad (5.23b)$$

$$\Pi = 2p'\overline{\frac{\partial u''_{\alpha}}{\partial x_{\alpha}}} \quad (5.23c)$$

$$\epsilon = -2\sigma'_{\alpha k}\overline{\frac{\partial u''_{\alpha}}{\partial x_k}} \quad (5.23d)$$

$$M = 2\bar{u}_{\alpha}''\overline{\frac{\partial\sigma_{\alpha k}}{\partial x_k}} \quad (5.23e)$$

$$\mathcal{T} = -\frac{\partial\bar{\rho}\bar{u}_{\alpha}''\bar{u}_{\alpha}''\bar{u}_k''}{\partial x_k} - 2\frac{\partial p'\bar{u}_{\alpha}''}{\partial x_{\alpha}} + 2\frac{\partial\bar{\sigma}'_{\alpha k}\bar{u}_{\alpha}''}{\partial x_k}. \quad (5.23f)$$

The three terms in \mathcal{T} are turbulent, pressure and viscous transport. In summary, the derivation of the Favre-averaged compressible turbulence equations highlights the central role of density fluctuations in modifying the structure of the governing equations. Unlike incompressible turbulence, where Reynolds averaging suffices, compressible flows require density-weighted Favre averaging to obtain a clean separation between mean and fluctuating contributions. The resulting equations reveal new terms absent in incompressible turbulence, such as pressure-dilatation and compressible transport, which act analogously to the buoyant production term in active scalar incompressible flows. Together, these additional mechanisms highlight the complexity of compressible turbulence and its close connection to active scalar mixing processes. The framework established here provides the foundation for modeling high-speed turbulent flows, including shock-turbulence interactions, supersonic mixing layers, and buoyancy-driven combustion phenomena such as wildland fires.

- **Mass flux** $m_i = \bar{\rho}'\bar{u}'_i$: appears in the *density-variance production* $-m_j\partial_j\ln\bar{\rho}$ (??) and is produced by mean density gradients $-R_{ij}\partial_j\bar{\rho}$ (??).

- **Turbulent heat/scalar flux** $q_i^{(T)} = \overline{\rho u''_i T''}$: drives temperature-variance production via $-\overline{q_j^{(T)} \partial_j \tilde{T}}$ (??), and couples back to m_i through EOS terms $\overline{\rho' T'}$ inside $C_i^{(\text{th})}$ (??).
- **Pressure–dilatation and pressure gradients** ($\overline{p' \Theta'}$, $\overline{\rho' \partial_i p'}$, $\overline{p' \partial_i \rho'}$): enter m_i (??) and the variance couplings $C_{\text{comp/thermo}}^{(T)}$, $C_{\text{comp/thermo}}^{(\rho)}$ (??)–(??); they mediate compressibility effects.
- **Transport terms (triple correlations, pressure transport, viscous diffusion)**: structurally present in all three budgets (last divergence terms), ensuring interscale and inter-region redistribution.
- **Relaxation/dissipation analogs** ($\varepsilon_i^{(m)}$, χ_T , ε_ρ): provide small-scale sinks, typically modeled with time-scale arguments $\sim k^{1/2}/\ell$.

The three budgets form a *tightly coupled system*: mean density and temperature gradients feed the mass and scalar fluxes, which in turn set the production of density and temperature variances; pressure–dilatation terms transmit compressible effects across all equations; transport terms redistribute these quantities; and modeled relaxation closes the cascade to small scales.

E. Symbol Table for Second-Moment Budgets

Symbol	Definition / Meaning
$\overline{(\cdot)}$	Reynolds average (ensemble or time).
$\tilde{(\cdot)}$	Favre (density-weighted) average, $\tilde{\phi} = \bar{\rho}\phi/\bar{\rho}$.
$(\cdot)'$	Reynolds fluctuation, $\phi' = \phi - \bar{\phi}$.
$(\cdot)''$	Favre fluctuation, $\phi'' = \phi - \tilde{\phi}$, with $\overline{\rho\phi''} = 0$.
$\bar{\rho}$	Mean density, $\bar{\rho} = \bar{\rho}$.
\tilde{u}_i	Favre mean velocity, $\tilde{u}_i = \overline{\rho u_i}/\bar{\rho}$.
u_i''	Favre velocity fluctuation, $u_i'' = u_i - \tilde{u}_i$, with $\overline{\rho u_i''} = 0$.
R_{ij}	Reynolds stress tensor, $R_{ij} = \overline{u'_i u'_j}$.
m_i	Turbulent mass flux, $m_i = \overline{\rho' u'_i}$.
a_i	Normalized mass flux, $a_i = m_i/\bar{\rho}$.
$q_i^{(T)}$	Turbulent scalar/heat flux, $q_i^{(T)} = \overline{\rho u_i'' T''}$.
$\overline{T''^2}$	Favre temperature variance, $\overline{(T - \tilde{T})^2}$.
$\overline{\rho'^2}$	Density variance, $\overline{(\rho - \bar{\rho})^2}$.
Θ'	Dilatation fluctuation, $\Theta' = \partial_j u'_j$.
χ_T	Scalar-dissipation rate, $\chi_T = \alpha \overline{\partial_j T'' \partial_j T''}$, with $\alpha = \lambda$.
$\varepsilon_i^{(m)}$	Viscous relaxation (modeled dissipation) of mass flux r .
ε_ρ	Relaxation/dissipation of density variance.
λ	Thermal conductivity.
D_ρ	Effective diffusivity for density variance.
$T_{ij}^{(m)}$	Transport of mass flux ($\rho' u'_i u'_j$, pressure transport, viscous).
$C_i^{(p)}$	Pressure-gradient and pressure-dilatation coupling in r .
$C_i^{(\text{th})}$	Thermodynamic/EOS coupling in m_i (e.g. $\overline{\rho' T'}$, $\overline{\rho' Y_\alpha'}$).
$C_{\text{comp/thermo}}^{(T)}$	Compressibility/thermodynamic coupling in T''^2 equation.
$C_{\text{comp/thermo}}^{(\rho)}$	Compressibility/thermodynamic coupling in ρ'^2 equation.
Y_α	Species mass fraction of component α .
c_p	Specific heat at constant pressure.
a_s	Speed of sound (appears in some closure models).
k	Turbulent kinetic energy (TKE).

Note: This table collects all variables and correlations used in the turbulent mass flux (??), temperature variance (??), and density variance (??) equations. The common correlations across the three budgets are:

- m_i links mass flux to density-variance production.
- $q_i^{(T)}$ links scalar/heat flux to temperature-variance production and couples into m_i via EOS terms.
- $\overline{\rho' T'}$ couples density variance and temperature variance.
- Pressure correlations ($\overline{p'\Theta'}$, $\overline{p'\partial_i p'}$, etc.) transmit compressibility effects into all three budgets.

5.5 Companion Notebook: Chapter 5 (Favre Averaging)

The companion Jupyter notebook (Chapter5CompanionPrinciplesofTurbulen... provides a computational supplement to Chapter 5. It links the concepts of Favre (density-weighted) averaging and compressible turbulence with reproducible numerical demonstrations. The notebook is designed to let readers inspect definitions, compute statistics from synthetic and small research-style datasets, and compare Favre quantities with their Reynolds counterparts in controlled settings.

Organization and Flow

The notebook follows the chapter sequence:

1. **Favre Decomposition and Averages.** Practical demonstration of density-weighted means and fluctuations, with contrasts against Reynolds averages on controlled synthetic data.
2. **Compressible RANS (Continuity, Momentum, Energy).** Term-by-term interpretation pointers (no derivations repeated) and how the notebook computes the relevant averaged quantities from data.

3. **Favre Stresses, Heat Fluxes, and Scalar Transport.** How the notebook estimates these quantities from provided fields and compares them with Reynolds-based estimates where meaningful.
4. **Datasets and Utility Modules.** Description of datasets and the helper code used to load and process them.
5. **Worked Examples (NB 5.x).** Guided activities that compute and interpret density-weighted statistics, TKE, and fluxes under variable-density conditions.
6. **Homework and Extensions.** Short computational prompts aligning with the chapter's end-of-section problems.

5.6 Datasets and Utilities

The following compact datasets are used. Each is intentionally small enough for rapid experimentation while capturing the essential behaviors needed for comparison studies.

Compressible Synthetic Field. A parameterized, low-noise dataset with prescribed density and velocity fluctuations to highlight how Favre means differ from Reynolds means as density variance and correlation with velocity energy are varied.

Variable-Density (Small) Dataset. A sampled set with modest density fluctuations and co-located velocity/scalar components; suitable for computing Favre stresses and heat fluxes, and for contrasting with Reynolds-based analogues.

Isotropic Compressible Simulation (Monte Carlo). A generated ensemble of velocity components with controllable density variance and tunable correlation between density and instantaneous velocity energy; used to compare Reynolds vs Favre TKE.

Utility Modules. Short helper scripts provide functions for density-weighted means, fluctuations, Favre stresses/fluxes, basic plotting, and export of tables/figures. Typical usage includes: loading a dataset; computing means and fluctuations; forming Favre statistics; visualizing distributions and comparing to Reynolds-based quantities.

5.7 Worked Examples (Notebook-Aligned)

Each example is designed to be self-contained, with brief prompts that connect the computation to the concepts in the main text.

NB 5.1 Synthetic Compressible Field — Favre vs Reynolds Means.

Compute \tilde{u} (density-weighted mean) and \bar{u} (Reynolds mean) as density variance and density–velocity correlation are dialed up or down. Visualize the difference and discuss when they coincide approximately.

NB 5.2 Reynolds vs Favre TKE — Isotropic Compressible Simulation

Generate an isotropic ensemble with adjustable density fluctuations and correlation to instantaneous kinetic energy. Compare the two TKE measures and report the ratio across settings, with comments on sensitivity.

NB 5.3 Variable-Density Jet/Plume — Fluxes and TKE Balance.

For a synthetic or small sampled jet/plume, compute Favre heat/scalar fluxes, production terms, and diagnostic TKE balance components along a centerline or selected sections. Summarize observed trends with height or radius.

5.8 Student Activities and Interpretation

Each worked example includes short prompts to guide interpretation:

- Identify conditions under which density-weighted means

approximate Reynolds means.

- Explain how density variance and $\rho-q^2$ correlation influence Favre stresses, fluxes, and TKE.
- Assess the sensitivity of modeled transport to choices of Pr_t and any length-scale caps.
- Describe sampling effects (ensemble size, noise) on the robustness of Favre vs Reynolds comparisons.

5.9 Homework and Extensions

1. Using the synthetic compressible field, tabulate \tilde{u} and \bar{u} as density variance increases for fixed $\rho-q^2$ correlation. Comment on when the two means become practically indistinguishable.
2. On the variable-density dataset, compute Favre and Reynolds TKE, report their ratio for several regions, and discuss which features of the data most strongly affect the difference.
3. Repeat a flux calculation with constant and variable Pr_t ; summarize how the choice alters the inferred heat/scalar transport and any downstream diagnostic terms.
4. For the isotropic simulation, sweep both density variance and $\rho-q^2$ correlation; plot the ratio of Favre to Reynolds TKE and briefly interpret the observed trends.

Chapter 6

Statistical Description of Turbulent Flows

6.1 Deterministic vs. Stochastic Processes

Turbulent flows cannot be predicted with complete certainty due to the inherently random nature of the dynamics, limitations in measurements, and the influence of unresolved scales of motion. A *stochastic process* provides a mathematical framework for describing such systems by explicitly incorporating randomness into the representation of time- or space-dependent variables.

A *deterministic process* is one where the future state is fully determined by the initial conditions and the governing equations. For example, the solution of:

$$\frac{dx}{dt} = ax, \quad x(0) = x_0 \quad (6.1)$$

is $x(t) = x_0 e^{at}$, which is entirely predictable for given x_0 and a .

6.1.1 Stochastic Process.

A stochastic quantity is one whose value is not fixed but is described by a probability distribution. A *stochastic process* is

a family of random variables.

$$\{X(t) : t \in T\}, \quad (6.2)$$

defined on a common probability space $(\Omega, \mathcal{F}, \mathbb{P})$, where $t \in T$ is the index parameter (e.g., time, spatial coordinate, or wavenumber). For each fixed $t \in T$, $X(t)$ is a random variable; for each fixed $\omega \in \Omega$, the mapping $t \mapsto X(t, \omega)$ is called a *realization* or *sample path*.

6.1.2 Expected Value $\mathbb{E}[X]$

The *expected value* (mean) of a random variable X is the probability-weighted average of its outcomes:

$$\mathbb{E}[X] = \int_{\Omega} X(\omega) d\mathbb{P}(\omega) = \begin{cases} \sum_k x_k p_k, & \text{(discrete),} \\ \int_{-\infty}^{\infty} x f_X(x) dx, & \text{(continuous).} \end{cases}$$

the symbol ω denotes an *elementary outcome*—a single point in the sample space Ω . Each outcome ω specifies a complete “scenario” of the random experiment (for instance, one particular coin flip, or one particular realization of a turbulent velocity field).

The notation $d\mathbb{P}(\omega)$ is the differential of the probability measure \mathbb{P} ; it tells us how much probability weight is assigned to an infinitesimal neighborhood of the outcome ω . Integrating $X(\omega)$ against this measure therefore computes the probability-weighted average of all possible values that the random variable X can take on the space Ω . In discrete settings $d\mathbb{P}(\omega)$ reduces to the probability mass p_k at each outcome, while in continuous settings it plays the role analogous to $f_X(x) dx$, where f_X is the probability density function of X . For a stochastic process $X(t)$ one may define a *mean function* $\mu(t) = \mathbb{E}[X(t)]$ and a *covariance function* $C(t, s) = \mathbb{E}[(X(t) - \mu(t))(X(s) - \mu(s))]$.

6.1.3 Ensemble vs. time average.

The *ensemble mean* is obtained by averaging over many independent realizations of the process:

$$\mathbb{E}[X(t)] = \lim_{N \rightarrow \infty} \frac{1}{N} \sum_{n=1}^N X^{(n)}(t), \quad (6.3)$$

where $X^{(n)}(t)$ denotes the n th realization.

For *stationary and ergodic* processes, the ensemble mean equals the *time mean* along a single realization:

$$\mathbb{E}[X(t)] = \lim_{T \rightarrow \infty} \frac{1}{T} \int_0^T X(t') dt'. \quad (6.4)$$

6.1.4 Mean Function.

The *mean function* of a stochastic process is the expected value of $X(t)$:

$$m_X(t) = \mathbb{E}[X(t)]. \quad (6.5)$$

For a *stationary* process, the mean is constant in time:

$$m_X(t) = \mu, \quad \forall t \in T. \quad (6.6)$$

For an *ergodic* process, the ensemble mean equals the time mean:

$$\mathbb{E}[X(t)] = \lim_{T \rightarrow \infty} \frac{1}{T} \int_0^T X(t') dt'. \quad (6.7)$$

6.1.5 Variance Function.

The *variance* of $X(t)$ is defined as:

$$\sigma_X^2(t) = \mathbb{E}\left[(X(t) - m_X(t))^2\right]. \quad (6.8)$$

For a stationary process, $\sigma_X^2(t)$ is constant in time.

In turbulent flow analysis, $\mathbb{E}[\cdot]$ is often denoted by an overbar ($\bar{\cdot}$)

for time averages or angle brackets $\langle \cdot \rangle$ for ensemble averages. For a velocity field decomposed as $u(t) = \bar{u} + u'(t)$, the fluctuation $u'(t)$ satisfies

$$\mathbb{E}[u'(t)] = 0, \quad (6.9)$$

meaning that the random fluctuations have zero mean by construction.

The expected operator $\mathbb{E}[\cdot]$ is a *linear functional* that returns the mean value of a random quantity. It is the central concept in defining higher-order moments, variances, correlations, and spectra in stochastic process theory.

6.1.6 Autocorrelation function.

For a real-valued, zero-mean, wide-sense stationary random process $\{X(t)\}$, the *autocorrelation function* $R_{XX}(\tau)$ quantifies the statistical dependence between the process values at times t and $t + \tau$:

$$R_{XX}(\tau) = \mathbb{E}[X(t) X(t + \tau)], \quad (6.10)$$

where τ is the time lag, and the expectation is taken over the ensemble of realizations of $X(t)$. If the process has a nonzero mean μ_X , the general form is

$$R_{XX}(\tau) = \mathbb{E}[(X(t) - \mu_X)(X(t + \tau) - \mu_X)]. \quad (6.11)$$

The autocorrelation satisfies the symmetry property $R_{XX}(\tau) = R_{XX}(-\tau)$, and $R_{XX}(0)$ equals the variance σ_X^2 . Turbulent velocity fluctuations $u'(t)$ are modeled as stochastic processes because exact pointwise predictions are impossible, but statistical properties can be described.

6.2 Central Limit Theorem (CLT): Connection to PDFs and Moments

Let $\{X_i\}_{i=1}^\infty$ be independent and identically distributed random variables with finite mean $\mu = \mathbb{E}[X_1]$ and variance $\sigma^2 =$

$\text{Var}(X_1) \in (0, \infty)$. Define the normalized sum

$$Z_n = \frac{\sum_{i=1}^n X_i - n\mu}{\sigma\sqrt{n}}. \quad (6.12)$$

Then, as $n \rightarrow \infty$,

$$Z_n \xrightarrow{d} \mathcal{N}(0, 1), \quad (6.13)$$

i.e. Z_n converges in distribution to a standard normal random variable.

PDF viewpoint (convolutions). Let f_X be the pdf of X_1 . The pdf of the sum $S_n = \sum_{i=1}^n X_i$ is the n -fold convolution $f_X * f_X * \dots * f_X$. The CLT states that, after centering and scaling by $\sigma\sqrt{n}$, this convolved pdf tends to the *Gaussian* pdf $\phi(z) = (2\pi)^{-1/2} \exp(-z^2/2)$:

$$f_{Z_n}(z) \longrightarrow \phi(z), \quad n \rightarrow \infty. \quad (6.14)$$

Thus, Gaussian pdfs arise *universally* as the large- n limit of (properly normalized) sums, regardless of the shape of f_X , provided the variance is finite.

Moment viewpoint (standardized moments). Let $m_k = \mathbb{E}[X_1^k]$ be raw moments and $\mu_k = \mathbb{E}[(X_1 - \mu)^k]$ central moments. The standardized moments of Z_n are

$$\mathbb{V}\mathcal{D}\backslash(Z_n) = 1, \quad S_n = \frac{\mathbb{E}[Z_n^3]}{1^{3/2}}, \quad F_n = \frac{\mathbb{E}[Z_n^4]}{1^2}.$$

As $n \rightarrow \infty$, higher standardized moments approach those of the normal law:

$$S_n \rightarrow 0, \quad F_n \rightarrow 3, \quad (6.15)$$

so the limiting pdf is fully characterized by mean 0 and variance 1, with vanishing skewness and Gaussian kurtosis. More refined approximations (e.g., Edgeworth expansions) express the finite- n deviations of f_{Z_n} from ϕ in terms of the standardized cumulants (skewness, excess kurtosis, etc.).

Limitations and exceptions. If X_i lack a finite variance (e.g. heavy-tailed with power-law index < 2), then the normalized sum may converge to a non-Gaussian *stable* law rather than a normal distribution. Likewise, strong long-range dependence can slow or prevent Gaussianization.

Many turbulent observables at large scales (or coarse-grained over many eddies) can be modeled as sums of many weakly dependent contributions. The CLT then explains why such aggregated quantities often have nearly Gaussian pdfs with $S \approx 0$ and $F \approx 3$. Departures from Gaussianity (e.g. nonzero skewness, $F > 3$) signal intermittency, strong correlations, or scale-localized events that violate the effective independence assumptions underlying the CLT.

6.2.1 Examples of Stochastic Processes

Stochastic processes vary in their statistical structure, continuity, and memory properties. They serve as both idealized mathematical constructs and physically motivated models for turbulence and other random phenomena. Below are important examples,

1. White Noise. An idealized process with zero mean and delta-correlated variance:

$$\mathbb{E}[X(t)] = 0, \quad (6.16)$$

$$R_X(\tau) = \sigma^2 \delta(\tau), \quad (6.17)$$

where $\delta(\tau)$ is the Dirac delta function.

The *Dirac delta function* $\delta(t)$ is a generalized function (or distribution) defined by its *shifting property*:

$$\int_{-\infty}^{\infty} f(t) \delta(t - t_0) dt = f(t_0), \quad (6.18)$$

for any continuous function $f(t)$. It is often described as being zero everywhere except at $t = t_0$, where it is “infinite,” in such

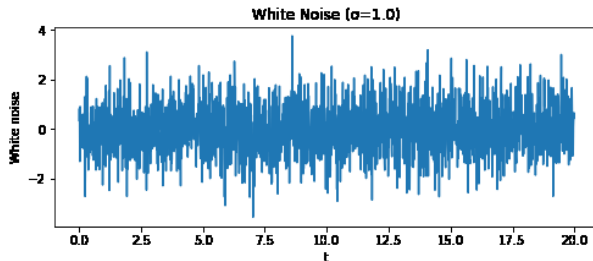
a way that its total integral equals one:

$$\delta(t - t_0) = 0, \quad t \neq t_0, \quad (6.19)$$

$$\int_{-\infty}^{\infty} \delta(t - t_0) dt = 1. \quad (6.20)$$

The delta function is not a classical function but a distribution in the sense of generalized functions, and it is rigorously defined through its action under an integral.

The white noise represents the small-scale, rapidly varying component of turbulent velocity or scalar fields when modeled as random forcing in numerical simulations (e.g., in Large Eddy Simulation (LES) subgrid forcing). Generally, thermal noise in velocity measurements, electronic noise in hot-wire anemometers, or artificially generated forcing in turbulence experiments is represented as white noise.



2. Ornstein–Uhlenbeck (OU) Process. A continuous-time, Gaussian, Markov process with exponential autocorrelation:

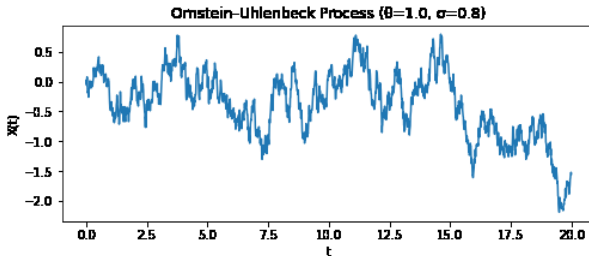
$$dX(t) = -\theta X(t) dt + \sigma dW(t), \quad (6.21)$$

where $W(t)$ is a Wiener process. The autocorrelation decays as:

$$R_X(\tau) = \sigma_X^2 e^{-\theta|\tau|}. \quad (6.22)$$

OU processes are widely used as Lagrangian velocity models in particle dispersion simulations because they mimic turbulent

eddies with finite lifetimes. Tracking of dye markers in river flows, atmospheric balloon drift in the planetary boundary layer are examples of OU processes.

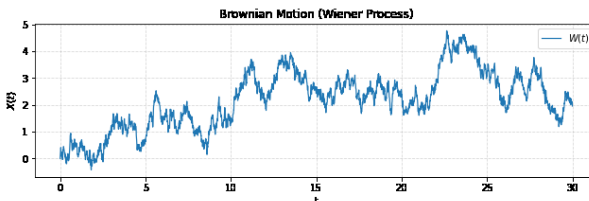


3. Brownian Motion (Wiener Process). A continuous-time process with stationary, independent increments:

$$W(0) = 0, \quad (6.23)$$

$$W(t) - W(s) \sim \mathcal{N}(0, t - s), \quad t > s. \quad (6.24)$$

The Brownian motion models pure diffusion due to turbulent mixing at small scales, and serves as the foundation of stochastic Lagrangian particle tracking. Pollen grain motion in water (Einstein's 1905 analysis), passive tracer dispersion in turbulent jets are examples of Brownian motion.



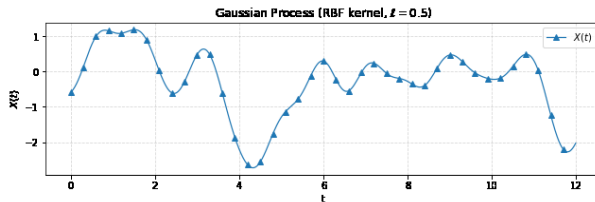
4. Random Walk. The discrete-time analog of Brownian motion:

$$X_n = X_{n-1} + \xi_n, \quad \xi_n \text{ i.i.d. random steps.} \quad (6.25)$$

The random walk process is useful in simplified Monte Carlo models for turbulent diffusion, where discrete jumps represent eddy displacement over fixed time steps. Pedestrian movement in crowds, pollutant plume spreading are approximated as successive random steps.



5. Gaussian Process. A process where every finite set $\{X(t_1), \dots, X(t_n)\}$ has a joint Gaussian distribution, fully described by its mean $m_X(t)$ and covariance $C_X(t_1, t_2)$. Many turbulence theories (e.g., Kraichnan's passive scalar model) assume Gaussian velocity fields for mathematical tractability. Surface elevation in wind waves is modeled as a Gaussian process when wave phases are random.



6. Markov Process. A process satisfying the *Markov property*:

$$\mathbb{P}[X(t_{n+1})|X(t_n), \dots, X(t_0)] = \mathbb{P}[X(t_{n+1})|X(t_n)]. \quad (6.26)$$

Markov models capture turbulence as a memory-less process in scale space, as in the stochastic modeling of velocity increments. Weather prediction models for short time horizons, wind speed transitions for wind energy estimation are modeled as Markov

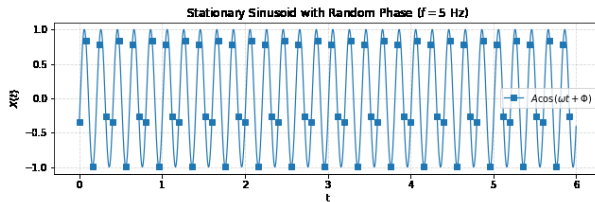
process.

7. Stationary Sinusoid with Random Phase. It is represented as follows:

$$X(t) = A \cos(\omega t + \Phi), \quad \Phi \sim U[0, 2\pi]. \quad (6.27)$$

This forms the basis for synthetic turbulence generation using superpositions of random-phase modes.

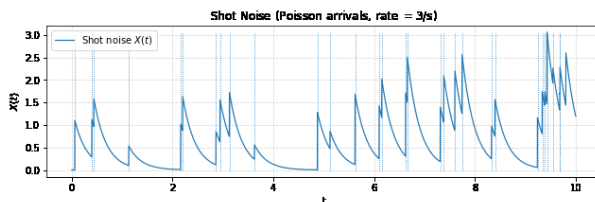
Ocean swell with random wave phases, components in machinery noise with uncertain initial phase are approximated in this form.



8. Poisson Process. A counting process with rate λ :

$$\mathbb{P}[N(t + \tau) - N(t) = k] = \frac{(\lambda\tau)^k e^{-\lambda\tau}}{k!}. \quad (6.28)$$

It models the occurrence of intermittent, discrete turbulent events such as vortex shedding or bursting in boundary layers. The arrival of vehicles at an intersection, raindrop impacts on a surface are examples.



9. Shot Noise Process.

$$X(t) = \sum_n A_n h(t - t_n), \quad (6.29)$$

with pulse arrivals $\{t_n\}$, amplitudes A_n , and pulse shape $h(t)$. It is used to model intermittent turbulent structures such as coherent packets of vortices. Examples are Electrical shot noise in vacuum tubes, acoustic signals from intermittent jet turbulence.

6.3 Probability Density Function and Moments

When X is continuous, its statistics can be described by the probability density $f_X(x)$. For every instant t the random variable $X(t)$ possesses a probability-density function defined as:

$$\Pr\{x \leq X(t) \leq x+dx\} = f_{X(t)}(x) dx, \quad \int_{-\infty}^{\infty} f_{X(t)}(x) dx = 1. \quad (6.30)$$

More generally, finite-dimensional statistics requires the joint pdf

$$f_{t_1, \dots, t_n}(x_1, \dots, x_n) = \frac{\partial^n}{\partial x_1 \cdots \partial x_n} \Pr\{X(t_1) \leq x_1, \dots, X(t_n) \leq x_n\}.$$

Knowing all such functions completely characterizes the process.

satisfying $\int_{-\infty}^{\infty} f_X(x) dx = 1$ and $F_X(x) = \int_{-\infty}^x f_X(s) ds$ for the cumulative distribution function F_X .

Define the raw (non-central) moments

$$\mu'_n = \mathbb{E}[X^n] = \int_{-\infty}^{\infty} x^n f(x) dx, \quad n = 0, 1, 2, \dots \quad (6.31)$$

In particular, the mean is $\mu = \mu'_1 = \int x f(x) dx$.

The central moments are

$$\mu_n = \mathbb{E}[(X - \mu)^n] = \int_{-\infty}^{\infty} (x - \mu)^n f(x) dx, \quad (6.32)$$

so that the variance is $\sigma^2 = \mu_2$.

Central moments in terms of raw moments. Using the binomial expansion $(X - \mu)^n = \sum_{k=0}^n \binom{n}{k} X^k (-\mu)^{n-k}$ and linearity of expectation,

$$\mu_n = \sum_{k=0}^n \binom{n}{k} (-\mu)^{n-k} \mu'_k. \quad (6.33)$$

Central moments in terms of raw moments (for the first five):

$$\mu_0 = 1 \quad (6.34)$$

$$\mu_1 = 0 \quad (6.35)$$

$$\mu_2 = \mu'_2 - \mu^2, \quad (6.36)$$

$$\mu_3 = \mu'_3 - 3\mu \mu'_2 + 2\mu^3, \quad (6.37)$$

$$\mu_4 = \mu'_4 + 4\mu \mu'_3 + 6\mu^2 \mu'_2 - 3\mu^4. \quad (6.38)$$

Skewness and kurtosis (from the PDF). Provided the relevant integrals exist (i.e., $\int |x|^k f(x) dx < \infty$ for needed k),

$$\text{Skewness: } \gamma_1 = \frac{\mu_3}{\sigma^3} = \frac{\int_{-\infty}^{\infty} (x - \mu)^3 f(x) dx}{\left(\int_{-\infty}^{\infty} (x - \mu)^2 f(x) dx \right)^{3/2}}, \quad (6.39)$$

$$\text{Kurtosis: } \beta_2 = \frac{\mu_4}{\sigma^4} = \frac{\int_{-\infty}^{\infty} (x - \mu)^4 f(x) dx}{\left(\int_{-\infty}^{\infty} (x - \mu)^2 f(x) dx \right)^2}, \quad (6.40)$$

$$\kappa = \beta_2 - 3 \text{ (excess kurtosis).} \quad (6.41)$$

Equivalent expressions via raw moments. Using the relations above with $\sigma^2 = \mu'_2 - \mu^2$,

$$\gamma_1 = \frac{\mu'_3 - 3\mu\mu'_2 + 2\mu^3}{(\mu'_2 - \mu^2)^{3/2}}, \quad (6.42)$$

$$\beta_2 = \frac{\mu'_4 - 4\mu\mu'_3 + 6\mu^2\mu'_2 - 3\mu^4}{(\mu'_2 - \mu^2)^2}, \quad \kappa = \beta_2 - 3. \quad (6.43)$$

Summary of computation of moments for a given pdf $f(x)$.

1. Compute $\mu = \int xf(x) dx$.
2. Compute $\sigma^2 = \int(x - \mu)^2 f(x) dx$.
3. Compute $\mu_3 = \int(x - \mu)^3 f(x) dx$ and $\mu_4 = \int(x - \mu)^4 f(x) dx$.
4. Form $\gamma_1 = \mu_3/\sigma^3$, $\beta_2 = \mu_4/\sigma^4$, $\kappa = \beta_2 - 3$.

Example 2.1: Moments of Gaussian Distribution

We say that a random variable X is *normally distributed* with mean μ and variance σ^2 if its probability density function is

$$f_X(x) = \frac{1}{\sqrt{2\pi}\sigma} \exp\left[-\frac{(x - \mu)^2}{2\sigma^2}\right], \quad x \in \mathbb{R}, \quad (6.44)$$

where $\mu \in \mathbb{R}$ is the *location parameter* and $\sigma > 0$ is the *scale parameter*. We write this concisely as

$$X \sim \mathcal{N}(\mu, \sigma^2).$$

The normal distribution specified as $X \sim \mathcal{N}(\mu, \sigma^2)$, serves as the fundamental model for many stochastic processes due to the central limit theorem. The PDF is symmetric about the mean μ and characterized by zero skewness and zero excess kurtosis.

Gaussian PDF (standard normal). For $X \sim \mathcal{N}(0, 1)$,

$$f(x) = \frac{1}{\sqrt{2\pi}} \exp\left(-\frac{x^2}{2}\right), \quad x \in \mathbb{R}.$$

Moments Let $\mu = \mathbb{E}[X]$, $\sigma^2 = \text{Var}(X)$, $\mu'_n = \mathbb{E}[X^n]$ (raw), and $\mu_n = \mathbb{E}[(X - \mu)^n]$ (central). For a Gaussian,

$$\mu = 0, \quad \sigma^2 = 1, \quad \mu_{2m+1} = 0, \quad \mu_{2m} = (2m - 1)!,$$

where $(2m - 1)! = 1 \cdot 3 \cdot 5 \cdots (2m - 1)$ and $\mu_4 = 3$, $\mu_6 = 15$, etc. Skewness and kurtosis are

$$\gamma_1 = \frac{\mu_3}{\sigma^3} = 0, \quad \beta_2 = \frac{\mu_4}{\sigma^4} = 3, \quad \kappa = \beta_2 - 3 = 0.$$

Computed values for $\mu = 0$, $\sigma = 1$.

$$\mu'_1 = \mu = 0, \quad \mu'_2 = \sigma^2 + \mu^2 = 1, \quad \mu'_3 = 0, \quad \mu'_4 = 3.$$

$$\mu_2 = 1, \quad \mu_3 = 0, \quad \mu_4 = 3, \quad \gamma_1 = 0, \quad \beta_2 = 3, \quad \kappa = 0.$$

Table 6.1: Numerical moments for $X \sim \mathcal{N}(0, 1)$.

Quantity	Value
Mean μ	0
Variance σ^2	1
Std. deviation σ	1
Third central moment μ_3	0
Fourth central moment μ_4	3
Skewness γ_1	0
Kurtosis β_2	3
Excess kurtosis κ	0

The figure 6.1 shows the probability density function of a Gaussian (Normal) random variable $X \sim \mathcal{N}(0, 1.5^2)$, characterized by mean $\mu = 0$ and standard deviation $\sigma = 1.5$. The solid dark

blue curve represents the PDF, the vertical dashed dark red line marks the mean, and the dotted dark green and dark orange lines denote one standard deviation below and above the mean, respectively. The symmetry of the Gaussian distribution about the mean is evident, with the area under the curve equal to unity. The spread of the curve is determined by σ , controlling the dispersion and tail decay rate, while the peak height reflects the normalization required for a valid probability density.

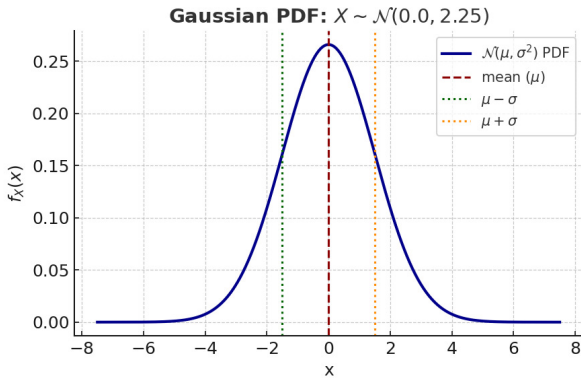


Figure 6.1: Gaussian Probability Density Function with Zero Mean

Example 2.2: skew-normal distribution

Skew-normal probability density function. Let $X \sim \text{SN}(\mu, \sigma, \lambda)$, where $\mu \in \mathbb{R}$ is the location parameter, $\sigma > 0$ the scale parameter, and $\lambda \in \mathbb{R}$ the shape (skewness) parameter. Define the standardized variable

$$z = \frac{x - \mu}{\sigma}, \quad (6.45)$$

the standard normal pdf

$$\phi(z) = \frac{1}{\sqrt{2\pi}} \exp\left(-\frac{z^2}{2}\right), \quad (6.46)$$

and the standard normal cumulative density function

$$\Phi(a) = \int_{-\infty}^a \phi(t) dt.$$

The skew–normal pdf is then (??)

$$f_X(x; \mu, \sigma, \lambda) = \frac{2}{\sigma} \phi\left(\frac{x - \mu}{\sigma}\right) \Phi\left(\lambda \frac{x - \mu}{\sigma}\right), \quad x \in \mathbb{R}. \quad (6.47)$$

For $\lambda = 0$, the distribution reduces to the Gaussian $\mathcal{N}(\mu, \sigma^2)$.

Moment generating function. For $X \sim \text{SN}(\mu, \sigma, \lambda)$, let

$$\delta = \frac{\lambda}{\sqrt{1 + \lambda^2}}.$$

The moment generating function (MGF) of X is given by Azzalini1985, Azzalini2014

$$M_X(t) = \mathbb{E}[e^{tX}] = 2 \exp\left(\mu t + \frac{\sigma^2 t^2}{2}\right) \Phi(\delta \sigma t), \quad t \in \mathbb{R}. \quad (6.48)$$

Derivation of moments. The n -th raw moment is obtained from

$$\mathbb{E}[X^n] = M_X^{(n)}(0),$$

where $M_X^{(n)}(t)$ denotes the n -th derivative of $M_X(t)$ with respect to t .

First moment (mean). From (6.48),

$$M'_X(t) = 2 \exp\left(\mu t + \frac{\sigma^2 t^2}{2}\right) [(\mu + \sigma^2 t) \Phi(\delta \sigma t) + \phi(\delta \sigma t) \delta \sigma].$$

Evaluating at $t = 0$ and using $\Phi(0) = 1/2$, $\phi(0) = 1/\sqrt{2\pi}$:

$$\mathbb{E}[X] = \mu + \sigma \delta \sqrt{\frac{2}{\pi}}.$$

Second moment and variance. The second derivative $M''_X(t)$ evaluated at $t = 0$ yields

$$\mathbb{E}[X^2] = \mu^2 + \sigma^2 + \frac{2\mu\sigma\delta}{\sqrt{\pi/2}}.$$

From $\text{Var}(X) = \mathbb{E}[X^2] - (\mathbb{E}[X])^2$, one finds:

$$\text{Var}(X) = \sigma^2 \left(1 - \frac{2\delta^2}{\pi}\right).$$

Third moment and skewness. Differentiating $M_X(t)$ three times, evaluating at $t = 0$, and using the definition of the standardized skewness

$$S = \frac{\mathbb{E}[(X - \mu_X)^3]}{\text{Var}(X)^{3/2}},$$

one obtains

$$S = \frac{(4 - \pi)}{2} \cdot \frac{\left(\delta \sqrt{\frac{2}{\pi}}\right)^3}{\left(1 - \frac{2\delta^2}{\pi}\right)^{3/2}}.$$

Fourth moment and kurtosis. Similarly, the fourth derivative yields $\mathbb{E}[X^4]$, from which the Pearson kurtosis

$$F = \frac{\mathbb{E}[(X - \mu_X)^4]}{\text{Var}(X)^2}$$

can be expressed in closed form as

$$F = 3 + \frac{2(\pi - 3)\delta^4}{\left(1 - \frac{2\delta^2}{\pi}\right)^2}.$$

The excess kurtosis is $\gamma_2 = F - 3$.

Summary. Thus, the moments of $\text{SN}(\mu, \sigma, \lambda)$ are:

$$\mathbb{E}[X] = \mu + \sigma \delta \sqrt{\frac{2}{\pi}}, \quad (6.49)$$

$$\text{Var}(X) = \sigma^2 \left(1 - \frac{2\delta^2}{\pi} \right), \quad (6.50)$$

$$S = \frac{(4 - \pi)}{2} \cdot \frac{\left(\delta \sqrt{\frac{2}{\pi}} \right)^3}{\left(1 - \frac{2\delta^2}{\pi} \right)^{3/2}}, \quad (6.51)$$

$$F = 3 + \frac{2(\pi - 3)\delta^4}{\left(1 - \frac{2\delta^2}{\pi} \right)^2}. \quad (6.52)$$

Figure ?? shows the analytical probability density functions of the skew-normal distribution for $\mu = 0$, $\sigma = 1$, and selected shape parameters $\lambda \in \{-4, -2, 0, 2, 4\}$. As $|\lambda|$ increases, the distribution departs from symmetry: positive λ values generate right skew (longer right tail, mode shifted left of the mean), whereas negative λ values generate left skew (longer left tail, mode shifted right of the mean). The skewness coefficient S increases in magnitude with $|\lambda|$, while the kurtosis F also rises above the Gaussian value $F = 3$, indicating heavier tails and greater intermittency. Table 6.2 lists the theoretical mean, variance, skewness, and kurtosis for each λ , computed from the closed-form moment expressions.

Table 6.2: Theoretical moments of the skew-normal distribution for $\mu = 0$, $\sigma = 1$, and selected λ values.

λ	Mean m	Variance v	Skewness S	Kurtosis F
-4	-0.774	0.401	-0.784	4.561
-2	-0.714	0.491	-0.454	3.753
0	0.000	1.000	0.000	3.000
2	0.714	0.491	0.454	3.753
4	0.774	0.401	0.784	4.561

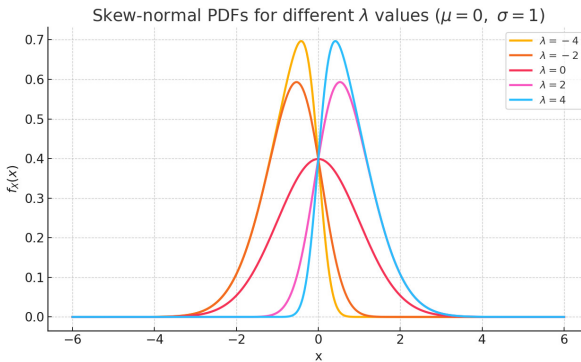


Figure 6.2: Analytical probability density functions of the skew-normal distribution for $\mu = 0$, $\sigma = 1$, and shape parameters $\lambda \in \{-4, -2, 0, 2, 4\}$.

Example 2.3: Moments from a Gamma Distribution PDF

PDF. Let $X \sim \text{Gamma}(k, \theta)$ with shape parameter $k > 0$ and scale parameter $\theta > 0$. Its probability density function (PDF) is

$$f(x) = \frac{1}{\Gamma(k) \theta^k} x^{k-1} e^{-x/\theta}, \quad x > 0, \quad (6.53)$$

and $f(x) = 0$ for $x \leq 0$. The Gamma function is

$$\Gamma(z) = \int_0^\infty t^{z-1} e^{-t} dt \quad (6.54)$$

Here: k is the shape parameter ($k > 0$) that controls skewness and kurtosis; θ is the scale parameter ($\theta > 0$), stretches the distribution; $\Gamma(\cdot)$ is the Gamma function,

With the change of variable $y = x/\theta$, $x = \theta y$, $dx = \theta dy$:

$$\begin{aligned} \int_0^\infty f(x) dx &= \frac{1}{\Gamma(k) \theta^k} \int_0^\infty (\theta y)^{k-1} e^{-y} \theta dy \\ &= \frac{\theta^k}{\Gamma(k) \theta^k} \int_0^\infty y^{k-1} e^{-y} dy = 1, \end{aligned} \quad (6.55)$$

since $\int_0^\infty y^{k-1} e^{-y} dy = \Gamma(k)$.

Raw (non-central) moments. The n -th raw moment is

$$\begin{aligned}\mu'_n &= \mathbb{E}[X^n] = \int_0^\infty x^n f(x) dx \\ &= \frac{1}{\Gamma(k)\theta^k} \int_0^\infty (\theta y)^{n+k-1} e^{-y} \theta dy \\ &= \theta^n \frac{\Gamma(k+n)}{\Gamma(k)}.\end{aligned}\quad (6.56)$$

Thus:

$$\begin{aligned}\mu'_1 &= k\theta, \\ \mu'_2 &= \theta^2 k(k+1), \\ \mu'_3 &= \theta^3 k(k+1)(k+2), \\ \mu'_4 &= \theta^4 k(k+1)(k+2)(k+3).\end{aligned}\quad (6.57)$$

Mean and variance.

$$\mu = \mu'_1 = k\theta, \quad (6.58)$$

$$\sigma^2 = \mu'_2 - \mu^2 = k\theta^2, \quad (6.59)$$

where σ is the standard deviation.

Central moments. The third and fourth central moments are obtained via:

$$\mu_3 = \mu'_3 - 3\mu\mu'_2 + 2\mu^3 = 2k\theta^3, \quad (6.60)$$

$$\mu_4 = \mu'_4 - 4\mu\mu'_3 + 6\mu^2\mu'_2 - 3\mu^4 = 3k(k+2)\theta^4. \quad (6.61)$$

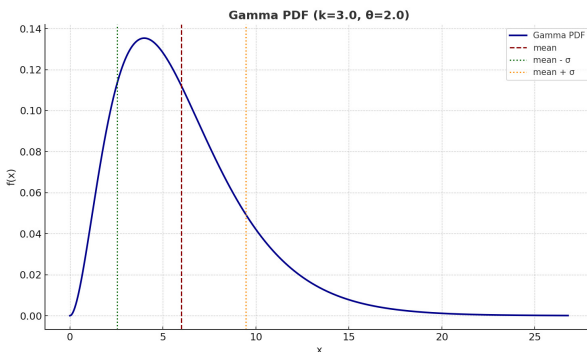
Skewness and kurtosis.

$$\gamma_1 = \frac{\mu_3}{\sigma^3} = \frac{2}{\sqrt{k}}, \quad (6.62)$$

$$\beta_2 = \frac{\mu_4}{\sigma^4} = 3 \left(1 + \frac{2}{k} \right), \quad (6.63)$$

$$\kappa = \beta_2 - 3 = \frac{6}{k}. \quad (6.64)$$

Here: y : change of variable $y = x/\theta$



The probability density function of a Gamma-distributed random variable with shape parameter $k = 3.0$ and scale parameter $\theta = 2.0$ is illustrated in Figure ???. The solid dark blue curve represents the continuous PDF, while the vertical dashed dark red line marks the mean value $\mu = k\theta = 6.0$. The dotted dark green and dark orange lines indicate one standard deviation below and above the mean, respectively, with the standard deviation given by $\sigma = \sqrt{k}\theta \approx 3.464$. This representation highlights the positively skewed nature of the Gamma distribution, which occurs for finite k and diminishes in skewness as k increases. The area under the PDF equals unity, consistent with the fundamental property of probability densities, and the extended right-hand tail reflects the influence of the shape parameter on the dispersion and tail heaviness of the distribution.

Table 6.3: Summary of parameters and moments for the Gamma distribution with $k = 3.0$, $\theta = 2.0$.

Quantity	Value
Shape parameter k	3.0
Scale parameter θ	2.0
Mean $\mu = k\theta$	6.0
Variance $\sigma^2 = k\theta^2$	12.0
Standard deviation σ	3.464
Third central moment μ_3	48.0
Fourth central moment μ_4	576.0
Skewness γ_1	1.1547
Excess kurtosis κ	2.0

6.4 Stationarity and Ergodicity

Joint probability density function. Let (X, Y) be a pair of continuous random variables defined on \mathbb{R}^2 . The *joint probability density function* (joint pdf) $f_{X,Y}(x, y)$ is a non-negative function satisfying

$$P((X, Y) \in A) = \iint_A f_{X,Y}(x, y) dx dy \quad (6.65)$$

for every region $A \subseteq \mathbb{R}^2$. The joint pdf must satisfy the normalization condition.

$$\iint_{-\infty}^{\infty} f_{X,Y}(x, y) dx dy = 1. \quad (6.66)$$

If $f_{X,Y}(x,y)$ is known, the *marginal* pdfs are obtained by integrating over the other variable:

$$f_X(x) = \int_{-\infty}^{\infty} f_{X,Y}(x,y) dy, \quad (6.67)$$

$$f_Y(y) = \int_{-\infty}^{\infty} f_{X,Y}(x,y) dx. \quad (6.68)$$

When $f_{X,Y}(x,y) = f_X(x) f_Y(y)$ for all (x,y) , X and Y are said to be *independent*.

Two core qualifiers—**stationary** and **ergodic**—tell us when a single, sufficiently long record can stand in for an entire ensemble of independently repeated experiments.

1. Stationarity

A process is said to be *strictly (strongly) stationary* if the joint probability-density function of any finite set $\{X(t_1), \dots, X(t_n)\}$ is invariant under a common shift of the time origin; that is,

$$f_{t_1, \dots, t_n}(x_1, \dots, x_n) = f_{t_1 + \Delta, \dots, t_n + \Delta}(x_1, \dots, x_n) \quad \text{for all } \Delta \in \mathbb{R}.$$

This requirement locks down *every* statistical feature, however high its order.

In practice, we often settle for *wide-sense* (or weak) stationarity because many engineering quantities involve only first and second moments. A process $X(t)$ is wide-sense stationary when the mean μ and the auto-correlation (R_{XX}) satisfy,

$$\langle X(t) \rangle = \mu = \text{const}, \quad R_{XX}(t, s) = R_{XX}(t - s) = R_{XX}(\tau).$$

The mean no longer changes with time and the auto-covariance depends only on the time lag τ . Velocity signals in statistically steady DNS or in an equilibrium channel experiment are commonly assumed to satisfy this weaker form.

2. Ergodicity

Stationarity describes invariance under time translation; **ergodicity** describes equivalence between two ways of averaging:

$$\text{ensemble average } \mathbb{E}[X] \iff \text{time average } \lim_{T \rightarrow \infty} \frac{1}{T} \int_0^T X(t) dt.$$

If this limit equals the ensemble mean almost surely, the process is *mean-ergodic*. Higher-order ergodicity (for autocovariance, full PDF, etc.) generalises the idea to other statistical objects. A classic sufficient condition is that the process be strongly stationary *and* its autocorrelation decay to zero for large $|\tau|$ (Birkhoff's pointwise ergodic theorem).

For turbulence the gain is enormous: one hot-wire probe operated over a period much longer than the integral time scale supplies the same first and second moments as an infinite collection of simultaneous probes. DNS databases exploit the same principle to turn a time series of snapshots into an ensemble of realizations.

In summary, *stationarity* assures us that the statistics do not wander in time, while *ergodicity* allows us to harvest those statistics from a single, sufficiently long measurement—an assumption so pervasive that most turbulence experiments and simulations build it into their very design.

A stochastic process $Q(t)$ is *weakly stationary* if $\langle Q(t) \rangle = \text{const}$ and its autocorrelation $R_{QQ}(\tau)$ depends only on the time lag τ . The *ergodic hypothesis* asserts that, for such processes, time averages equal ensemble averages:

$$\langle Q \rangle = \lim_{T \rightarrow \infty} \frac{1}{T} \int_0^T Q(t) dt. \quad (6.69)$$

Ergodicity allows replacing costly ensemble averages by single,

long time series in many laboratory and DNS studies.

6.4.1 Homogenous Turbulence

A turbulent flow is said to be *homogeneous* if its statistical properties are invariant under spatial translations. Formally, for a velocity field $\mathbf{u}(\mathbf{x}, t)$, the n -point joint statistics depend only on the relative separations between points, not on their absolute positions:

$$\langle u_{i_1}(\mathbf{x}_1, t) u_{i_2}(\mathbf{x}_2, t) \cdots u_{i_n}(\mathbf{x}_n, t) \rangle = F_{i_1 i_2 \dots i_n}(\mathbf{x}_2 - \mathbf{x}_1, \dots, \mathbf{x}_n - \mathbf{x}_1; t), \quad (6.70)$$

where $\langle \cdot \rangle$ denotes an ensemble average. In homogeneous turbulence:

- The mean velocity and the variance of fluctuations are the same everywhere in the flow domain.
- Correlation functions depend only on the distance between points, not their coordinates.
- Statistical invariance under translation simplifies the analysis of turbulence, allowing spectral methods and Fourier transforms to be used naturally.

An idealized example of homogeneous turbulence is found in the central region of a wind tunnel far from boundaries, or in large-scale atmospheric turbulence away from obstacles, where the turbulent field appears statistically the same in all locations.

Relation to isotropy. If, in addition to being homogeneous, the turbulence statistics are also invariant under rotations and reflections, the flow is said to be *isotropic*. Isotropy is a stronger condition than homogeneity. Figures 6.3 illustrate a synthetic realization of a statistically homogeneous, approximately isotropic turbulence field generated via spectral synthesis on a periodic domain. No systematic spatial variation in the statistical appearance of the field is visible, consistent with the definition of homogeneity—its statistical properties are invariant under translations in x or y .

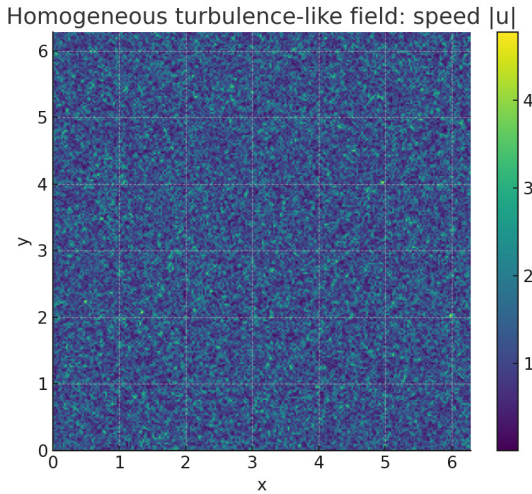


Figure 6.3: Homogenous Turbulence representation

Nomenclature

Random Variables & Statistics

X	Continuous random variable.
$f_X(x)$	Probability density function (PDF) of X .
$\mathbb{P}(\cdot)$	Probability of an event.
$\mathbb{E}[\cdot]$	Expectation (mean) operator.
μ'_n	n -th raw (non-central) moment: $\mu'_n = \mathbb{E}[X^n]$.
μ_n	n -th central moment: $\mu_n = \mathbb{E}[(X - \mu)^n]$.
μ	Mean of the distribution: $\mu = \mu'_1$.
σ^2	Variance: $\sigma^2 = \mu_2$.
σ	Standard deviation: $\sigma = \sqrt{\sigma^2}$.
γ_1	Skewness: $\gamma_1 = \mu_3/\sigma^3$.
β_2	Kurtosis: $\beta_2 = \mu_4/\sigma^4$.
κ	Excess kurtosis: $\kappa = \beta_2 - 3$.
m_k, μ_k	Raw and central moments of X_1 .
S, F	Skewness and (Pearson) kurtosis (standardized moments).
$\phi(z)$	Standard normal PDF: $\phi(z) = (2\pi)^{-1/2} e^{-z^2/2}$.
$\Gamma(z)$	Gamma function: $\Gamma(z) = \int_0^\infty t^{z-1} e^{-t} dt$.
$\Gamma_{\alpha, \beta}$	Generalized gamma function: $\Gamma_{\alpha, \beta}(z) = \int_0^\infty t^{z-1} e^{-\beta t} \alpha^{-1} e^{-\alpha/t} dt$.

Problems

1. Conceptual: Gaussian Limit from the CLT

Explain why the Central Limit Theorem predicts that, for a velocity signal composed of the sum of many weakly dependent eddy contributions, the pdf should approach a Gaussian. Identify the assumptions that may fail in real turbulence, leading to nonzero skewness and excess kurtosis.

2. Derivation of Moment Convergence

Let $\{X_i\}$ be i.i.d. random variables with $\mathbb{E}[X_i] = \mu$, $\text{Var}(X_i) = \sigma^2 < \infty$, and skewness S_X and kurtosis F_X .

Show that the standardized skewness S_n and kurtosis F_n of $Z_n = \frac{\sum_{i=1}^n X_i - n\mu}{\sigma\sqrt{n}}$ satisfy

$$S_n = \frac{S_X}{\sqrt{n}}, \quad F_n = 3 + \frac{F_X - 3}{n}.$$

Interpret these formulas in terms of the CLT.

3. PDF Evolution Under Convolution

Let X_1 have pdf $f_X(x) = \frac{1}{2}e^{-|x|}$ (Laplace distribution). Using the fact that convolution in physical space corresponds to multiplication in Fourier space, derive the pdf of $S_n = \sum_{i=1}^n X_i$ for $n = 1, 2, 3$, and plot them. Discuss how the pdf shape changes as n increases and compare to the Gaussian limit.

4. Application to Turbulence Statistics

A turbulent velocity increment δu_ℓ at large separation ℓ is modeled as the sum of N uncorrelated small-scale contributions, each with variance σ_0^2 and skewness S_0 . Use the CLT to estimate the skewness S_ℓ of δu_ℓ as a function of N . For what value of N would $|S_\ell| < 0.05 |S_0|$?

5. Monte Carlo Verification of the CLT

Write a Python script that:

- (a) Generates N_{samples} realizations of Z_n for different n using a chosen non-Gaussian parent distribution (e.g. exponential).
- (b) Estimates the pdf from the samples and compares it with the standard normal pdf.
- (c) Computes skewness and kurtosis for each n and verifies their convergence to $(0, 3)$ as n increases.

6. Beyond the CLT: Heavy-Tailed Example

Consider a symmetric α -stable distribution with stability index $\alpha = 1.5$ as the parent distribution for the X_i . Explain why the classical CLT does not apply, and describe the expected limit distribution for normalized sums. Compare this to the Gaussian case.

6.5 Python Notebook Companion: Statistical Theory of Turbulence

The accompanying Jupyter notebook (`Chapter6_Companion_Principles.ipynb`) serves as an interactive extension of the material developed in this chapter. It provides computational demonstrations that mirror the theoretical flow of the text: from random processes and probability distributions to the concepts of stationarity, ergodicity, and moment-based characterization of turbulence.

The notebook begins by contrasting deterministic and stochastic representations of motion, illustrating the transition from purely predictive systems to those governed by probabilistic variability. Canonical stochastic processes—including white noise, the Ornstein–Uhlenbeck (OU) process, Gaussian and Poisson signals, and random walks—are simulated to visualize memory, correlation, and statistical equilibrium. Each process is linked to the theoretical framework presented in Section 6.1–6.2: the OU model embodies a stationary Markov process with

exponential decay of correlation, while the Poisson and random walk realizations illustrate discrete and cumulative randomness.

Subsequent sections compute empirical probability density functions (PDFs) from synthetic or measured data. These exercises operationalize the theoretical definition of $p(x)$ from Section 6.3, showing how normalization and histogram discretization approximate continuous distributions. The statistical moments—mean, variance, skewness, and kurtosis—introduced analytically in Section 6.4 are estimated numerically from sample data to demonstrate their sensitivity to asymmetry and intermittency, both key features of turbulent fluctuations.

An interactive comparison of normal, gamma, and skew-normal distributions (Example NB 6.4) enables students to explore the deformation of the PDF and its corresponding moments as parameters vary. This computational activity directly reinforces the discussion of distributional modeling of turbulence statistics. Similarly, the gamma-fit procedure (Example NB 6.7) connects the method of moments to empirical modeling of dissipation-like variables, illustrating how observed positive-valued turbulence quantities often deviate from Gaussian behavior.

Sections 6.6–6.7 provide interactive demonstrations of *stationarity* and *ergodicity*. Here, the temporal evolution of the mean and variance is visualized for stationary and non-stationary processes, emphasizing the physical meaning of these assumptions in statistical turbulence theory. The ergodicity demonstration compares ensemble-averaged and time-averaged quantities, showing numerically that, for stationary ergodic systems, both approaches yield equivalent statistics. These exercises connect the theoretical framework of Section 6.6 to tangible data behavior.

Finally, the notebook concludes with a set of structured **homework exercises** designed to reinforce computational intuition. Students are encouraged to reproduce the core analyses—varying parameters, testing stationarity, fitting PDFs—and to interpret the physical meaning of statistical parameters within the context of turbulent flows.

This pedagogical sequence—*theory → definition → controlled simulation → interactive exploration → interpretation*—parallels the didactic flow of the printed text. The notebook thus functions as a self-contained laboratory for statistical turbulence, transforming abstract definitions into quantitative, reproducible analyses.

Chapter 7

Two point correlations

7.1 Introduction

In Chapter 2 we emphasized the *physical interpretation* of the hierarchy of turbulence scales: the integral scale, Taylor microscale, and Kolmogorov scales, and how they govern mixing and characteristic time-scales. Our treatment was deliberately heuristic, designed to give intuition for how eddies stir, stretch, and dissipate scalars. To move beyond intuition, we now require *quantitative, statistical definitions* of turbulence scales.

A central tool for this purpose is the **two-point correlation function**, which measures how velocity fluctuations at one point in space (or time) are related to those at another. Correlation functions provide a rigorous way to quantify the size of coherent eddies, the rate at which velocity fluctuations lose their coherence, and the pathway by which energy is transferred from large scales to small. From these correlations, the canonical scales of turbulence: *Integral scale*, *Taylor microscale*, *Kolmogorov scale* are formally defined.

Two-point statistics also form the bridge between physical space and spectral representations. Through Fourier transforms, the correlation functions are connected to the turbulence energy spectrum $E(k)$.

Scope of this Chapter

In this chapter we will:

- (a) Define autocovariance and autocorrelation functions for turbulent velocity fields.
- (b) Derive formal expressions for the integral scale and Taylor microscale from these functions.
- (c) Connect two-point correlations to spectral densities and the energy spectrum via Fourier transforms.
- (d) Show how these statistical measures provide the rigorous foundation for the heuristic scale hierarchy introduced earlier.

This progression allows us to unify physical intuition with statistical definitions, preparing us to analyze turbulence in both laboratory measurements and numerical simulations.

7.2 Two-Point Correlation

Single-point statistics tell us how energetic and intermittent a turbulent flow is *at one location*, yet they contain no information about how eddies extend through space or how long fluctuations persist. That spatial (or temporal) *coherence* is captured by the two-point velocity-correlation tensor.

Definition Given a velocity field $u_i(\mathbf{x}, t)$ we introduce its fluctuation $u'_i(\mathbf{x}, t) = u_i - \langle u_i \rangle$. The **two-point correlation tensor**

$$R_{ij}(\mathbf{x}, \mathbf{r}, t, \tau) = \left\langle u'_i(\mathbf{x}, t) u'_j(\mathbf{x} + \mathbf{r}, t + \tau) \right\rangle \quad (7.1)$$

measures how strongly velocity components at two different space-time points co-fluctuate. Here \mathbf{r} is the separation vector and τ the time lag; angular brackets denote the ensemble (or, under ergodicity, long-time) average.

Matrix form (Cartesian components). Writing the tensor explicitly,

$$\mathbf{R}(\mathbf{r}) = \begin{pmatrix} R_{11}(\mathbf{r}) & R_{12}(\mathbf{r}) & R_{13}(\mathbf{r}) \\ R_{21}(\mathbf{r}) & R_{22}(\mathbf{r}) & R_{23}(\mathbf{r}) \\ R_{31}(\mathbf{r}) & R_{32}(\mathbf{r}) & R_{33}(\mathbf{r}) \end{pmatrix}, \quad R_{ij}(\mathbf{r}) = \langle u_i(\mathbf{x}) u_j(\mathbf{x}+\mathbf{r}) \rangle.$$

$R_{11} = \langle u_1(\mathbf{x}) u_2(\mathbf{x} + \mathbf{r}) \rangle,$ $R_{12} = \langle u_1(\mathbf{x}) u_2(\mathbf{x} + \mathbf{r}) \rangle,$ \vdots
--

(The remaining entries follow cyclically)

7.2.1 Correlation coefficient

In many canonical flows the statistics depend only on \mathbf{r} and τ :

$$R_{ij}(\mathbf{x}, \mathbf{r}, t, \tau) \xrightarrow{\text{homog., stat.}} R_{ij}(\mathbf{r}, \tau). \quad (7.2)$$

Normalizing (7.1) by the local variance gives the **correlation coefficient**

$$\rho_{ij}(\mathbf{r}, \tau) = \frac{R_{ij}(\mathbf{r}, \tau)}{\sqrt{R_{ii}(\mathbf{0}, 0) R_{jj}(\mathbf{0}, 0)}}, \quad |\rho_{ij}| \leq 1. \quad (7.3)$$

7.3 Taylor's Statistical Framework for Turbulence

In Taylor's statistical approach, the velocity field $\mathbf{u}(\mathbf{x}, t)$ is a random function of space and time.

Denote the ensemble by $\langle \cdot \rangle$. Decompose $u_i = \langle u_i \rangle + u'_i$ with $\langle u'_i \rangle = 0$.

Assuming the turbulent flow is homogeneous and stationary: For a homogeneous turbulent flow the *two-point correlation tensor* is defined by

$$R_{ij}(\mathbf{r}) = \langle u'_i(\mathbf{x}, t) u'_j(\mathbf{x} + \mathbf{r}, t) \rangle, \quad \mathbf{r} \in \mathbb{R}^3, \quad (7.4)$$

At zero separation $R_{ij}(0) = \langle u'_i u'_j \rangle$ reproduces the Reynolds-stress tensor. *Homogeneous* turbulence has statistics invariant under translations; hence the two-point second-order moment depends only on separation \mathbf{r}

If, in addition, statistics are invariant under rotations and reflections, the flow is *isotropic*. In that case, R_{ij} admits the classical isotropic tensor form

$$R_{ij}(\mathbf{r}) = [f(r) - g(r)] \frac{r_i r_j}{r^2} + g(r) \delta_{ij}, \quad r = \|\mathbf{r}\|. \quad (7.5)$$

Here $f(r)$ and $g(r)$ are, respectively, the *longitudinal* and *transverse* correlation functions:

$$R_L(r) = f(r) = \langle u'_L(x) u'_L(x + r) \rangle, \quad (7.6)$$

$$R_T(r) = g(r) = \langle u'_N(x) u'_N(x + r) \rangle, \quad (7.7)$$

where u'_L is the velocity fluctuation along \mathbf{r} and u'_N is the velocity fluctuation normal to \mathbf{r} .

The two-point tensor can be written

$$R_{ij}(\mathbf{r}) = [R_T(r) - R_L(r)] \frac{r_i r_j}{r^2} + R_L(r) \delta_{ij}, \quad r = \|\mathbf{r}\|,$$

with

$$R_L(r) = \langle u'_L(\mathbf{x}) u'_L(\mathbf{x}+\mathbf{r}) \rangle, \quad R_T(r) = \langle u'_T(\mathbf{x}) u'_T(\mathbf{x}+\mathbf{r}) \rangle.$$

The divergence-free condition $\partial_{x_i} u'_i = 0$ implies

$$\partial_{r_j} R_{ij}(\mathbf{r}) = 0 \implies \boxed{R_T(r) = R_L(r) + \frac{r}{2} \frac{dR_L}{dr}}. \quad (\text{A})$$

As fluid elements cannot accumulate or dilate volume, a longitudinal stretch ($\partial u'_L / \partial x_L$) must be balanced by transverse motions; relation (A) encodes that balance.

Expressing R_L via the trace. The trace of the tensor is

$$R_{kk}(r) = R_{11}(r) + R_{22}(r) + R_{33}(r) = R_L(r) + 2R_T(r).$$

Insert (A):

$$R_{kk}(r) = 3R_L(r) + r \frac{dR_L}{dr}. \quad (\text{B})$$

Equation (B) is a first-order linear ODE for $R_L(r)$. Multiplying by the integrating factor r^3 and integrating gives

$$\boxed{R_L(r) = \frac{1}{r^3} \int_0^r s^2 R_{kk}(s) ds}. \quad (\text{C})$$

Hence the longitudinal correlation at separation r is the

cumulative average of the trace up to that distance.

2. Relation between R_L and R_{kk}

Because $R_{kk} = R_{11} + R_{22} + R_{33} = R_L + 2R_T$, substituting the above gives the ordinary differential equation

$$R_{kk}(r) = 3R_L(r) + r \frac{dR_L}{dr}.$$

Solving for R_L with the integrating-factor method (or by direct inspection) yields the compact integral form

$$R_L(r) = \frac{1}{r^3} \int_0^r s^2 R_{kk}(s) ds.$$

(1)

7.3.1 Integral length scale.

The *integral length scale* L is a measure of the size of the largest energy-containing eddies in a turbulent flow. It characterizes the spatial extent over which velocity fluctuations remain significantly correlated. For a stationary, homogeneous turbulence with longitudinal velocity fluctuation $u'(t)$, the integral length scale (L) is

$$L_{u_k} = \int_0^\infty \frac{R_{kk}(r\mathbf{e}_k, 0)}{R_{kk}(\mathbf{0}, 0)} dr,$$
(7.8)

Because $R_L(0) = \frac{1}{3}R_{kk}(0) = \frac{1}{3}\langle u_i^2 \rangle$, the standard definition

$$L = \int_0^\infty \frac{R_L(r)}{R_L(0)} dr$$

Physically, L represents the average size of the energy-containing structures that dominate the turbulent kinetic energy.

Frozen–turbulence (Taylor) hypothesis For steady flows with mean speed U much greater than fluctuation velocities, turbulence is “frozen” as it is convected past a point:

$$r \approx U\tau, \quad E(k) \approx \frac{U}{2\pi} S(f), \quad f = \frac{Uk}{2\pi}, \quad (7.9)$$

where $S(f)$ is the temporal spectrum and τ the time lag.

Using the Taylor’s frozen turbulence hypothesis, in practice, L can be estimated from velocity measurements in space to convert time lags to spatial separations):

$$L \approx U \int_0^\infty \frac{R_L(\tau)}{R_L(0)} d\tau, \quad (7.10)$$

where U is the mean flow speed and τ is the time lag.

The integral length scale is important in turbulence modeling, as it sets the scale for energy input in the energy cascade, influences mixing and dispersion rates, and often appears in closure models (e.g., $k-\varepsilon$ turbulence models) as a key parameter.

L is computable once either $R_L(r)$ or the easier to measure $R_{kk}(r)$ is known. In practice, experimentalists often estimate R_{kk} from three simultaneous hot-wire probes or from DNS data and then recover R_L through (C), avoiding the numerical derivative required by (A).

L is a measure of the size of the energy-containing eddies. In laboratory grid flows L_{u_1} extracted from (7.8) grows monotonically as the turbulence decays downstream. Figure ?? presents the normalized radial autocorrelation function $R_{uu}(r)$ for a synthetic homogeneous, approximately isotropic turbulence field generated with a low-pass spectral envelope that emphasizes low wavenumbers. This spectral shaping produces larger energy-containing eddies.

The shaded region under the curve, integrated from $r = 0$ to the first zero crossing, represents the *integral length scale* L_{int} , which quantifies the average size of the dominant energy-containing structures in the flow. For this realization, $L_{\text{int}} \approx 0.265$ (in domain units) is the correlation length. The vertical dashed line marks the location of the first zero crossing, beyond which the correlation becomes negative, reflecting oscillatory spatial structure at scales larger than L_{int} .

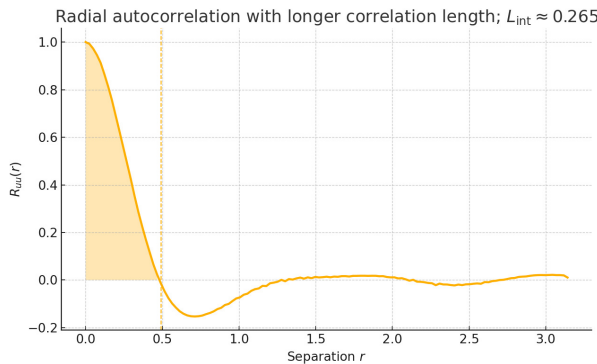


Figure 7.1: Homogenous Turbulence with correlation length of $L_{\text{int}} \approx 0.265$

The *integral length scale* $L = \int_0^\infty R_L(r)/R_L(0) dr$ quantifies the diameter of the largest, energy-containing eddies—roughly the distance over which a fluctuation “knows” about itself.

At the opposite end of the inertial range, the curvature of the correlation at the origin, $\lambda^2 = -R_L(0)/R_L''(0)$, defines the *Taylor micro-scale*, a key intermediate length that enters the Taylor-scale Reynolds number R_λ . Fourier transforming $R_{ii}(r)$ yields the energy spectrum $E(k)$, allowing real-space measurements to be compared with Kolmogorov’s $E(k) \sim k^{-5/3}$ law.

Relevance in direct numerical simulation (DNS).

In DNS every velocity component is available on a three-dimensional grid, so $R_{ij}(\mathbf{r})$ can be computed directly, averaged over directions, and checked for isotropy. The resulting correlation functions are used to validate the simulation resolution (e.g. ensuring the domain is large enough so that R_{ij} decays to zero) and to extract integral quantities such as L , λ , and $E(k)$ without ambiguity from sampling noise.

Relevance in experiments. Hot-wire anemometry and particle-image velocimetry cannot measure the full field instantaneously, but they do record long time-series at one or several points. Using Taylor's frozen-turbulence hypothesis ($r = U\tau$, where U is the mean convection speed), temporal two-point correlations $\langle u(t) u(t + \tau) \rangle$ are converted into spatial correlations $R_L(r)$. From these, experimentalists infer integral scales, compare with DNS and theory, and detect departures from homogeneity or isotropy (e.g. near walls). Because two-point statistics are second-order quantities, they converge faster than high-order moments, making them a practical workhorse for diagnosing flow quality in both laboratory and atmospheric settings.

7.3.2 Taylor's Microscale

Taylor's microscale λ_T is an intermediate length scale in turbulence, lying between the *integral length scale* L (associated with the largest energy-containing eddies) and the *Kolmogorov length scale* η (associated with the smallest dissipative eddies).

For homogeneous isotropic turbulence, the longitudinal velocity autocorrelation $R_{LL}(r)$ can be expanded near $r = 0$ as

$$R_{LL}(r) \approx 1 - \frac{r^2}{2\lambda_T^2} + \mathcal{O}(r^4), \quad (7.11)$$

where λ_T is *Taylor's microscale*. It characterizes the curvature of the correlation function at zero separation, and thus the scale of eddies dominating the rate of strain and dissipation.

Equivalently, for isotropic turbulence,

$$\lambda_T = \sqrt{\frac{\langle u'^2 \rangle}{\langle (\frac{\partial u'}{\partial x})^2 \rangle}}, \quad (7.12)$$

where $\langle u'^2 \rangle$ is the variance of the velocity fluctuations, and $\langle (\partial u'/\partial x)^2 \rangle$ is the mean square of the longitudinal velocity gradient.

For incompressible, homogeneous, isotropic turbulence, the mean dissipation rate ε and kinematic viscosity ν satisfy

$$\lambda_T = \sqrt{\frac{15 \nu \langle u'^2 \rangle}{\varepsilon}}. \quad (7.13)$$

This relation follows from the isotropic form of the dissipation rate: $\varepsilon = 15\nu \langle (\partial u'/\partial x)^2 \rangle$.

λ_T represents the characteristic scale at which viscous effects start to become important, but are not yet dominant as in the Kolmogorov scale η . It is much smaller than L but much larger than η . It is frequently used in experimental turbulence studies to estimate ε from measured velocity gradients and provides a bridge between large-scale turbulence statistics and small-scale dissipative dynamics.

Example 2.3 Figure ?? illustrates the estimation of Taylor's microscale λ_T from a synthetic one-dimensional homogeneous velocity fluctuation field generated via spectral synthesis. Panel (a) shows the time-series $u'(x)$ normalized to zero mean and unit variance. Panel (b) presents the normalized spatial autocorrelation $\rho_{uu}(r)$ along with a quadratic fit in the vicinity of $r = 0$. Two in-

dependent estimates of λ_T are obtained: (i) from the gradient definition $\lambda_T = \sqrt{\langle u'^2 \rangle / \langle (\partial u' / \partial x)^2 \rangle}$, and (ii) from the curvature of $\rho_{uu}(r)$ at $r = 0$ using $\rho_{uu}(r) \approx 1 - r^2 / (2\lambda_T^2)$. The close agreement between these estimates validates both approaches. The gradient-based definition directly relates λ_T to the velocity gradient variance, which is also linked to the dissipation rate via $\varepsilon = 15\nu \langle (\partial u' / \partial x)^2 \rangle$ for isotropic turbulence.

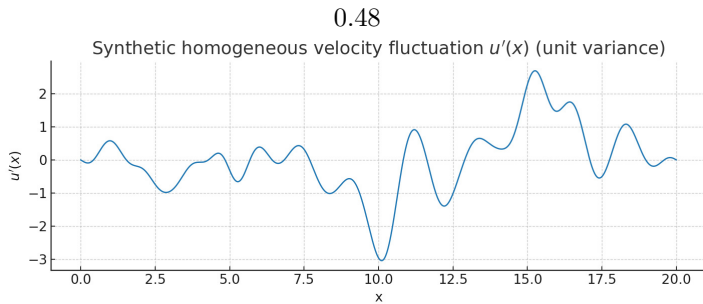


Figure 7.2: Synthetic homogeneous fluctuation $u'(x)$ (zero mean, unit variance).

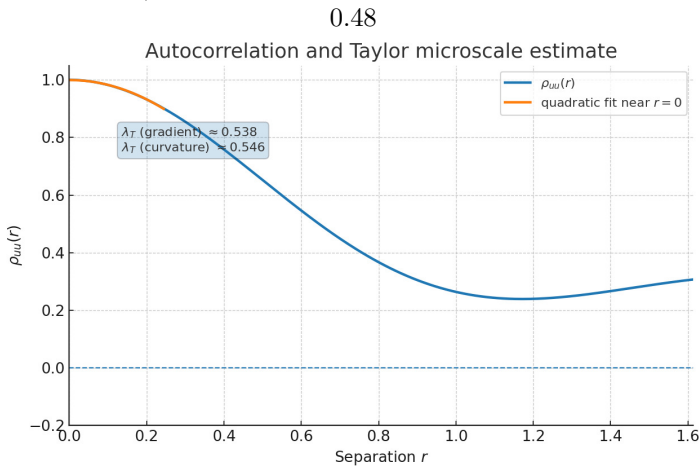


Figure 7.3: Normalized autocorrelation $\rho_{uu}(r)$ with quadratic fit near $r = 0$.

7.4 Energy Spectrum

Taylor connects spatial correlations to wavenumber spectra via Fourier analysis.

Definition The *spectral (energy) tensor* of a homogeneous flow is the Fourier transform of the two-point correlation tensor:

$$\Phi_{ij}(\mathbf{k}) = \int_{\mathbb{R}^3} R_{ij}(\mathbf{r}) e^{-i\mathbf{k}\cdot\mathbf{r}} d^3\mathbf{r}, \quad R_{ij}(\mathbf{r}) = \langle u_i(\mathbf{x}) u_j(\mathbf{x} + \mathbf{r}) \rangle. \quad (7.14)$$

The inverse transform is

$$R_{ij}(\mathbf{r}) = \frac{1}{(2\pi)^3} \int_{\mathbb{R}^3} \Phi_{ij}(\mathbf{k}) e^{i\mathbf{k}\cdot\mathbf{r}} d^3\mathbf{k}. \quad (7.15)$$

Parseval's theorem at $\mathbf{r} = 0$ gives the energy per unit mass

$$\frac{1}{2} \langle u_i u_i \rangle = \frac{1}{2} R_{ii}(0) = \frac{1}{2} (2\pi)^{-3} \int_{\mathbb{R}^3} \Phi_{ii}(\mathbf{k}) d^3\mathbf{k}. \quad (7.16)$$

Assuming *Isotropic, Incompressible conditions*, the spectral tensor Eq. (7.14) reduces to

$$\Phi_{ij}(\mathbf{k}) = \frac{E(k)}{4\pi k^2} \left(\delta_{ij} - \frac{k_i k_j}{k^2} \right), \quad k = \|\mathbf{k}\|, \quad (7.17)$$

where $E(k)$ is the *isotropic energy spectrum*. Consequently

$$\int_0^\infty E(k) dk = \frac{1}{2} R_{ii}(0) = \frac{1}{2} \langle u_i u_i \rangle. \quad (7.18)$$

Substituting the isotropic form (7.17) into the inverse transform (7.15) and tracing gives the Hankel transform

pair

$$E(k) = \frac{k^2}{2\pi^2} \int_0^\infty R_{ii}(r) \frac{\sin kr}{kr} 4\pi r^2 dr, \quad R_{ii}(r) = \int_0^\infty E(k) \frac{\sin kr}{kr} 4\pi k^2 dr. \quad (7.19)$$

Using the incompressible relation $R_{ii} = R_L + 2R_T$, one may write the spectrum solely in terms of the longitudinal correlation:

$$E(k) = \frac{2}{\pi} \int_0^\infty r^2 R_L(r) \frac{\sin kr}{kr} dr. \quad (7.20)$$

7.4.1 Example 2.4. Analytic example: exponential correlation model

Let us assume the following,

$$R_{11}(r) = u'^2 \exp\left(-\frac{r}{L}\right), \quad u'^2 = R_{11}(0). \quad (7.21)$$

7.5 Structure Functions

Scope and Role

Structure functions quantify how turbulent fluctuations change with separation. By focusing on *differences* rather than absolute values, they provide a real-space measure of multiscale variability that connects directly to the cascade, the exact 4/5-law, and inertial-range similarity. This section organizes the topic from definitions → exact result (4/5-law) → K41 predictions → refined similarity and intermittency models → practical diagnostics.

7.5.1 Definitions: Increments and Structure Functions

Let $\mathbf{u}(\mathbf{x}, t)$ be an incompressible velocity field and ℓ a separation vector with $\ell = |\ell|$ and $\hat{\ell} = \ell/\ell$. The *longitudinal velocity increment* is

$$\delta_\ell u = [\mathbf{u}(\mathbf{x} + \ell, t) - \mathbf{u}(\mathbf{x}, t)] \cdot \hat{\ell}, \quad (7.22)$$

and the p -th order *longitudinal structure function* is

$$S_p(\ell) = \langle |\delta_\ell u|^p \rangle, \quad (7.23)$$

where $\langle \cdot \rangle$ denotes an ensemble (or ergodic space/time) average. Transverse structure functions $S_p^\perp(\ell)$ are defined by projecting the increment perpendicular to $\hat{\ell}$.

Low orders and diagnostics.

- $p = 2$: $S_2(\ell)$ provides a scale-wise measure of fluctuation energy associated with eddies of size ℓ (more precisely, with wavenumbers $k \sim 1/\ell$).
- $p = 3$: $S_3(\ell)$ enters the exact inertial-range relation $S_3(\ell) = -\frac{4}{5}\varepsilon\ell$ (the 4/5-law).
- Ratios such as S_4/S_2^2 , S_6/S_2^3 quantify non-Gaussianity and *intermittency* (spatial heterogeneity of intense small-scale activity).

7.5.2 Connection to Two-Point Correlation

In homogeneous turbulence, the second-order longitudinal structure function and the longitudinal correlation $R_{LL}(\ell)$ are related by

$$S_2^\parallel(\ell) = 2[R_{LL}(0) - R_{LL}(\ell)], \quad R_{LL}(\ell) \equiv \langle u_\parallel(\mathbf{x}) u_\parallel(\mathbf{x} + \ell) \rangle. \quad (7.24)$$

Thus S_2 is an alternative (often more revealing) representation of the same physics, emphasizing differences across scales and exposing power laws.

7.5.3 Transverse structure functions and PDF connection

Longitudinal (S_p^{\parallel}) and transverse (S_p^{\perp}) increments share the same exponents ζ_p but different prefactors. Taking the trace of the invariant measure yields a *generalised hyperbolic / NIG* probability density for velocity increments; each order p has its own NIG with parameters linked to τ_p . This gives the correct heavy tails and asymmetric features seen in experiments.

For a velocity field $u_i(\mathbf{x}, t)$, the n -th-order structure function is the ensemble average of the n -th power of velocity increments across a spatial separation \mathbf{r} :

$$S_n^{(i_1 \dots i_n)}(\mathbf{r}) = \langle [u_{i_1}(\mathbf{x} + \mathbf{r}) - u_{i_1}(\mathbf{x})] \cdots [u_{i_n}(\mathbf{x} + \mathbf{r}) - u_{i_n}(\mathbf{x})] \rangle. \quad (7.25)$$

The most frequently used objects are the second-order ($n = 2$) structure functions, distinguishing longitudinal and transversal orientations:

$$\text{longitudinal: } S_2^{\parallel}(r) = \langle [u_{\parallel}(\mathbf{x} + \mathbf{r}) - u_{\parallel}(\mathbf{x})]^2 \rangle, \quad (7.26)$$

$$\text{transversal: } S_2^{\perp}(r) = \langle [u_{\perp}(\mathbf{x} + \mathbf{r}) - u_{\perp}(\mathbf{x})]^2 \rangle. \quad (7.27)$$

Here u_{\parallel} is the component of the velocity increment parallel to \mathbf{r} ; u_{\perp} lies in a plane normal to \mathbf{r} .

Relation to two-point correlation

In homogeneous turbulence, the second-order structure function is related to the two-point correlation by

$$S_2^{\parallel}(r) = 2[R_{LL}(0) - R_{LL}(r)], \quad R_{LL}(r) \equiv \langle u_{\parallel}(\mathbf{x}) u_{\parallel}(\mathbf{x+r}) \rangle. \quad (7.28)$$

Thus $S_2(r)$ is essentially another representation of the same information; its advantage is that it emphasizes *differences* across scales, making power-law behavior easier to detect.

Canonical experimental illustration

In grid-generated turbulence the longitudinal second-order structure function can be obtained from a single hot-wire trace $u(t)$ by invoking Taylor's frozen-flow hypothesis, $r = U_{\infty}\tau$. Plotting $S_2^{\parallel}(r)$ versus r for several downstream stations reveals

- a viscous sub-range $S_2 \propto r^2$ at $r \lesssim \eta$;
- an extended inertial sub-range with $2/3$ slope;
- a saturation towards $2u'^2$ as $r \rightarrow L$.

Fitting a line of slope $2/3$ on a log–log plot allows one to extract ε and hence collapsing data from different Reynolds numbers onto a single similarity curve.

Scientific significance of structure functions. Structure functions are indispensable because they diagnose how turbulent energy and intermittency are distributed *across scales* directly in physical space, without recourse to spectral transforms or the Taylor frozen-flow hypothesis. The longitudinal third-order structure function, for example, embeds the four-thirds Kolmogorov law and thus quantifies the mean energy flux through the inertial cascade, providing an experimental closure to the Kár-

mán–Howarth equation. Higher–order moments, $S_n(r)$, expose deviations from the $\frac{n}{3}$ K41 similarity exponent; those anomalous scalings are the empirical backbone of modern multifractal theories and reveal the degree of small-scale intermittency that any predictive model must reproduce. In large-eddy simulations, structure functions measured at filter scale determine whether the subgrid model supplies the correct backscatter and dissipation. In Lagrangian dispersion, the second-order structure function at the Kolmogorov scale enters directly into Richardson’s t^3 law for pair separation. Finally, because $S_n(r)$ is a difference statistic, it remains insensitive to slow drifts in mean velocity and can be measured robustly in mildly non-stationary environments such as the atmospheric surface layer. For all these reasons, structure functions constitute the primary real-space metric by which theoretical predictions, numerical simulations, and experimental data are judged for consistency with the fundamental physics of the turbulent cascade.

Chapter 8

Turbulence Theory

8.1 Kolmogorov's 1941 (K41) Similarity Hypotheses

Kolmogorov's 1941 theory (K41) rests on three central hypotheses:

H1 Global stationarity. In statistically steady turbulence, the mean energy-dissipation rate per unit mass

$$\varepsilon = 2\nu \langle s_{ij} s_{ij} \rangle$$

is constant in time, uniform in space, and, in the high-Reynolds number limit, independent of the molecular viscosity ν .

H2 Local isotropy. At sufficiently small scales ($\ell \ll L$), the statistics of the turbulent velocity field become independent of the anisotropy imposed by large-scale forcing, mean shear, or boundaries.

H3 Universality of small scales. In the inertial range ($\eta \ll \ell \ll L$), the statistical properties of velocity increments depend only on the mean dissipation rate ε and the scale ℓ , and are otherwise independent of the details of large-scale forcing or molecular

viscosity.

8.1.1 The Energy Cascade

Kolmogorov viewed fully developed turbulence as a *hierarchy of eddies* that transfers kinetic energy from the large scales at which it is injected, down through progressively smaller eddies, to the smallest scales where viscous dissipation dominates. This process is known as the *energy cascade*.

8.1.2 Energy-containing range ($\ell \sim L$)

: At scales $\ell = O(L)$ (the integral scale), eddies are directly driven by forcing (e.g. mean shear, buoyancy, pressure gradients). The flow here is typically anisotropic and geometry-dependent. The size of the largest eddies is comparable to the flow geometry. Let L denote the integral length scale and U (often $U \approx u'$) a large-eddy velocity scale. The large-eddy turnover time is

$$T_L \sim \frac{L}{U}. \quad (8.1)$$

Energy injection from the mean flow feeds the cascade at a rate that balances the dissipation:

$$\varepsilon \sim C_\varepsilon \frac{U^3}{L}, \quad C_\varepsilon = O(1). \quad (8.2)$$

8.1.3 Inertial Subrange ($\eta \ll \ell \ll L$)

Definition and physics. Between the forcing scale L and the Kolmogorov scale η lies the inertial subrange. Here nonlinear advection transfers energy conservatively from scale ℓ to smaller scales; forcing and viscosity are negligible at these intermediate scales.

Constant energy flux. Define the downscale flux $\Pi(\ell)$ (rate of transfer per unit mass). Both Π and ε have dimensions $L^2 T^{-3}$ ($\text{m}^2 \text{s}^{-3}$). In homogeneous, stationary

turbulence:

$$\Pi(\ell) = \varepsilon, \quad \eta \ll \ell \ll L. \quad (8.3)$$

Velocity increment scaling. Let $\delta_\ell u$ denote the characteristic velocity difference across separation ℓ . A scale-local transfer implies the inter-scale flux scales like

$$\varepsilon \sim \frac{(\delta_\ell u)^2}{\tau_\ell} \sim \frac{(\delta_\ell u)^3}{\ell} \implies \boxed{\delta_\ell u \sim (\varepsilon \ell)^{1/3}}. \quad (8.4)$$

This immediately gives the second-order structure-function scaling $S_2(\ell) = \langle |\delta_\ell u|^2 \rangle \sim C_2 (\varepsilon \ell)^{2/3}$.

8.1.4 The $-5/3$ Law for the Inertial-Range Energy Spectrum

In high-Reynolds-number, homogeneous and isotropic turbulence, the range of scales $\eta \ll \ell \ll L$ (between the Kolmogorov scale η and the energy-containing scale L) exhibits universal statistical behavior governed solely by the mean dissipation rate ε and the scale (or, equivalently, its wavenumber k). Kolmogorov's second similarity hypothesis then implies that the three-dimensional energy spectrum $E(k)$ depends only on ε and k :

$$E(k) = C_K \varepsilon^{2/3} k^{-5/3}, \quad (8.5)$$

the celebrated $-5/3$ law, where C_K is the (dimensionless) Kolmogorov constant (empirically $C_K \approx 1.5\text{--}1.7$).

The same hypothesis also yields the second-order structure function scaling.

$$S_2(r) \equiv \langle [\delta_r u]^2 \rangle = C_2 (\varepsilon r)^{2/3}, \quad (\eta \ll r \ll L), \quad (8.6)$$

with C_2 another universal constant (empirically $C_2 \approx 2.0\text{--}2.2$). The two constants C_K and C_2 are related by a

calculable transform between $S_2(r)$ and $E(k)$; in practice, they are determined from experiments or DNS.

8.1.5 Kolmogorov's Four-Fifths Law

A remarkable feature of turbulence theory is that, despite the apparent randomness and complexity of fluid motion, there exists a single exact, universal relation that connects velocity increments to the mean energy dissipation. This is the celebrated *Kolmogorov four-fifths law*, first derived in 1941.

Consider the longitudinal velocity increment

$$\delta_\ell u = [\mathbf{u}(\mathbf{x} + \boldsymbol{\ell}) - \mathbf{u}(\mathbf{x})] \cdot \hat{\boldsymbol{\ell}}, \quad \hat{\boldsymbol{\ell}} = \frac{\boldsymbol{\ell}}{|\boldsymbol{\ell}|}.$$

The p -th order longitudinal structure function is

$$S_p(\ell) = \langle [\delta_\ell u]^p \rangle.$$

Kolmogorov's law states that, in the inertial range of homogeneous, isotropic, high-Reynolds-number turbulence,

$$S_3(\ell) \equiv \langle [\delta_\ell u]^3 \rangle = -\frac{4}{5} \varepsilon \ell,$$

where ε is the mean kinetic-energy dissipation per unit mass.

This relation is noteworthy because:

- it is an *exact* result derived from the Navier–Stokes equations, not a dimensional or scaling argument;
- it involves no adjustable constants, in contrast with the Kolmogorov $-5/3$ spectrum which contains the empirical constant C_K ;
- it provides a direct way to measure the dissipation rate ε from experimental velocity measurements.

The four-fifths law thus serves as the cornerstone of turbulence theory: it bridges the deterministic Navier–Stokes equations and the statistical, universal properties of high–Reynolds-number flows.

The $-5/3$ spectrum is consistent with Kolmogorov’s exact $4/5$ law: a constant downscale energy flux $\Pi(k) = \varepsilon$ through the inertial range, with negligible direct influence of forcing and viscosity at those scales.

8.1.6 Dissipation Range (Kolmogorov Scales)

Definition and physics. At the smallest scales, viscosity dominates and dissipated the TKE. The scales from ν and ε are

$$\eta = \left(\frac{\nu^3}{\varepsilon} \right)^{1/4}, \quad u_\eta = (\nu \varepsilon)^{1/4}, \quad \tau_\eta = \left(\frac{\nu}{\varepsilon} \right)^{1/2}. \quad (8.7)$$

Spectra roll off more steeply than $k^{-5/3}$; a common fit is $E(k) \sim k^2 \exp[-\beta (k\eta)^{4/3}]$ with $\beta = O(1)$.

- 7. **Inertial subrange** ($\eta \ll \ell \ll L$): Intermediate eddies transfer kinetic energy conservatively without direct input or dissipation. Dynamics are universal and depend only on ε and ℓ .
- 8. **Dissipation range / Kolmogorov scale** ($\ell \sim \eta$): Smallest eddies, where viscosity ν balances inertial forces. Length, time, and velocity scales are

$$\eta = \left(\frac{\nu^3}{\varepsilon} \right)^{1/4}, \quad \tau_\eta = \left(\frac{\nu}{\varepsilon} \right)^{1/2}, \quad u_\eta = (\nu \varepsilon)^{1/4}.$$

Energy injected at large scales cascades through the inertial subrange and is finally dissipated at η by viscosity. This picture provides the physical basis for K41 scaling.

8.2 Kolmogorov–Obukhov Statistical Theory of Turbulence

Kolmogorov (1941a, 1941b) and Obukhov (1941) proposed a statistical theory of turbulence based on dimensional arguments. The central prediction was that the p th-order structure functions scale as

$$S_p(\ell) = \langle |u(x + \ell) - u(x)|^p \rangle \sim C_p \ell^{p/3}, \quad (8.8)$$

where ℓ is the separation and C_p are constants. This is the celebrated *K41 scaling hypothesis*.

Landau criticized this formulation because the constants C_p could depend on the large-scale flow structure and because intermittency in dissipation was ignored.

8.2.1 Kolmogorov–Obukhov 1962 Refined Similarity

To address Landau’s critique, Kolmogorov and Obukhov (1962) introduced the *refined similarity hypothesis*, which incorporates the coarse-grained dissipation:

$$\tilde{\varepsilon}_\ell = \frac{3}{4\pi\ell^3} \int_{|\mathbf{s}| \leq \ell} \varepsilon(x + \mathbf{s}) d\mathbf{s}. \quad (8.9)$$

The refined similarity form is then

$$S_p(\ell) = C'_p \langle \tilde{\varepsilon}_\ell^{p/3} \rangle \ell^{p/3}. \quad (8.10)$$

If $\langle \tilde{\varepsilon}_\ell^{p/3} \rangle \sim \ell^{\tau_p}$, the scaling exponents become

$$\zeta_p = \frac{p}{3} + \tau_p, \quad (8.11)$$

where τ_p are the *intermittency corrections*.

8.2.2 Intermittency and She–Leveque Correction

Log-normal models gave

$$\tau_p = \frac{\mu}{18} p(p - 3), \quad (8.12)$$

but disagreed with simulations and experiments for $p \gtrsim 6$.

She and Leveque (1994) proposed a log-Poisson cascade, yielding

$$\tau_p = -\frac{2p}{9} + 2 \left[1 - \left(\frac{2}{3} \right)^{p/3} \right], \quad \zeta_p = \frac{p}{3} + \tau_p. \quad (8.13)$$

This form preserves $\tau_0 = 0$ and $\tau_3 = 0$ (consistency with the 4/5-law) and matches DNS and experiments up to $p \approx 10$.

8.3 Buoyancy Dominated Flows: Turbulence Spectra

8.3.1 Bolgiano–Obukhov Scaling in Stratified Turbulence

Kolmogorov's 1941 theory (K41) describes turbulence in homogeneous, isotropic flows where the cascade is driven only by inertial transfer of kinetic energy. In buoyancy-driven turbulence (e.g. Rayleigh–Bénard convection, stably stratified turbulence), buoyancy forces couple velocity and temperature fluctuations. When turbulence is influenced by buoyancy forces, Bolgiano (1959) and Obukhov (1959) independently developed a scaling theory, now called the *Bolgiano–Obukhov (BO) scaling*.

8.4 Bolgiano–Obukhov (BO) Scaling:

We consider buoyancy-affected turbulence under the Boussinesq approximation, for velocity $\mathbf{u}(\mathbf{x}, t)$, pressure p , and temperature

fluctuation θ (with respect to a reference T_0):

$$\frac{\partial \mathbf{u}}{\partial t} + \mathbf{u} \cdot \nabla \mathbf{u} = -\frac{1}{\rho_0} \nabla p + \nu \nabla^2 \mathbf{u} + g\alpha \theta \hat{\mathbf{z}}, \quad (8.14)$$

$$\frac{\partial \theta}{\partial t} + \mathbf{u} \cdot \nabla \theta = \kappa \nabla^2 \theta + S_\theta, \quad (8.15)$$

$$\nabla \cdot \mathbf{u} = 0, \quad (8.16)$$

where ρ_0 is constant density, ν kinematic viscosity, κ thermal diffusivity, α thermal expansion coefficient, g gravity, and S_θ a large-scale source/sink.

8.4.1 BO hypotheses at scale ℓ

Let u_ℓ and θ_ℓ denote characteristic velocity and temperature increments over separation ℓ :

$$u_\ell \sim |\delta_\ell u|, \quad \theta_\ell \sim |\delta_\ell \theta|.$$

Define the turnover time $\tau_\ell \sim \ell/u_\ell$. In the BO inertial range we assume:

1. Inertia–buoyancy balance at scale ℓ :

$$\frac{u_\ell^2}{\ell} \sim g\alpha \theta_\ell. \quad (8.17)$$

2. Constant downscale flux of scalar variance:

$$\varepsilon_\theta \equiv \text{const} \sim \frac{u_\ell \theta_\ell^2}{\ell}. \quad (8.18)$$

Assumption (8.17) states that, at these scales, buoyancy does leading-order work on kinetic energy; (8.18) plays the role analogous to Kolmogorov's constant kinetic-energy flux, but for the scalar variance.

8.4.2 Scaling of u_ℓ and θ_ℓ

From (8.17),

$$u_\ell \sim (g\alpha)^{1/2} \theta_\ell^{1/2} \ell^{1/2}. \quad (8.19)$$

Insert (8.19) into (8.18):

$$\varepsilon_\theta \sim \frac{(g\alpha)^{1/2} \theta_\ell^{1/2} \ell^{1/2} \theta_\ell^2}{\ell} = (g\alpha)^{1/2} \theta_\ell^{5/2} \ell^{-1/2}.$$

Solve for θ_ℓ :

$$\theta_\ell \sim \varepsilon_\theta^{2/5} (g\alpha)^{-1/5} \ell^{1/5}. \quad (8.20)$$

Then, from (8.19),

$$u_\ell \sim \varepsilon_\theta^{1/5} (g\alpha)^{2/5} \ell^{3/5}. \quad (8.21)$$

Structure functions. The second-order longitudinal structure functions scale as

$$S_2^{(u)}(\ell) \equiv \langle (\delta_\ell u)^2 \rangle \sim u_\ell^2 \sim \ell^{6/5}, \quad S_2^{(\theta)}(\ell) \equiv \langle (\delta_\ell \theta)^2 \rangle \sim \theta_\ell^2 \sim \ell^{2/5}. \quad (8.22)$$

8.4.3 Spectral exponents in Bolgiano-Obukhov scaling

The goal is to connect the scale-dependent increments u_ℓ and θ_ℓ from Eq. (8.21) to the energy spectra in wavenumber space. Recall that in isotropic turbulence, the one-dimensional energy spectrum $E(k)$ is related to fluctuations at scale $\ell \sim 1/k$ via

$$E_u(k) \sim \frac{u_\ell^2}{k}, \quad E_\theta(k) \sim \frac{\theta_\ell^2}{k}, \quad \ell \sim \frac{1}{k}. \quad (8.23)$$

This scaling relation comes from dimensional analysis: velocity variance u_ℓ^2 represents the contribution from modes around wavenumber $k \sim 1/\ell$, and dividing by k spreads this contribution over the corresponding shell in spectral space.

Velocity spectrum. From Eq. (8.21), the velocity increment scales as

$$u_\ell \sim \ell^{3/5} \implies u_\ell^2 \sim \ell^{6/5}. \quad (8.24)$$

Substituting into Eq. (8.23):

$$E_u(k) \sim \frac{u_\ell^2}{k} \sim \frac{\ell^{6/5}}{1/\ell} \sim \ell^{11/5}.$$

Since $\ell \sim 1/k$, we obtain

$$E_u(k) \sim k^{-11/5}. \quad (8.25)$$

Thus the kinetic energy spectrum in the BO range is steeper than the K41 $k^{-5/3}$ law.

Temperature spectrum. From Eq. (??), the temperature increment scales as

$$\theta_\ell \sim \ell^{1/5} \implies \theta_\ell^2 \sim \ell^{2/5}. \quad (8.26)$$

Substituting into Eq. (8.23):

$$E_\theta(k) \sim \frac{\theta_\ell^2}{k} \sim \frac{\ell^{2/5}}{1/\ell} \sim \ell^{7/5}.$$

Since $\ell \sim 1/k$, we obtain

$$E_\theta(k) \sim k^{-7/5}. \quad (8.27)$$

This is shallower than the Obukhov–Corrsin $k^{-5/3}$ law for passive scalars in neutral turbulence.

Final dimensional form. Restoring the prefactors from the dimensional analysis (involving ε_θ and αg), the Bolgiano–Obukhov laws are

$$E_u(k) \sim C_u (\varepsilon_\theta (\alpha g)^2)^{2/5} k^{-11/5}, \quad (8.28)$$

$$E_\theta(k) \sim C_\theta \varepsilon_\theta^{4/5} (\alpha g)^{-2/5} k^{-7/5}. \quad (8.29)$$

Here C_u and C_θ are dimensionless constants of order unity.

- The velocity spectrum $E_u(k) \sim k^{-11/5}$ (–2.2) is steeper

than the Kolmogorov $k^{-5/3}$ (-1.67), reflecting the stronger damping influence of buoyancy on kinetic energy at large scales.

- The temperature spectrum $E_\theta(k) \sim k^{-7/5}$ (-1.4) is shallower than Obukhov–Corrsin’s passive-scalar $k^{-5/3}$, because temperature is now an *active scalar* injecting energy into the flow through buoyancy.
- These laws apply in the *Bolgiano range*, i.e. at scales $\ell > L_B$. At smaller scales ($\ell < L_B$), buoyancy effects weaken and the classical K41 inertial-range scaling is recovered.

8.4.4 Bolgiano length and Oztmidov scale

Let ε denote the kinetic-energy dissipation rate. The *Bolgiano length* ℓ_B (or wavenumber $k_B = 1/\ell_B$) marks the transition between buoyancy-controlled BO scaling at large scales and inertia-dominated K41 scaling at smaller scales. Matching the BO and K41 expressions for u_ℓ at $\ell = \ell_B$ yields the classical estimate

$$\ell_B \sim \frac{\varepsilon^{5/4}}{(g\alpha\varepsilon_\theta)^{3/4}}, \quad k_B \sim \frac{(g\alpha\varepsilon_\theta)^{3/4}}{\varepsilon^{5/4}}. \quad (8.30)$$

In stably stratified turbulence, the *Oztmidov scale*

$$\ell_O \equiv \left(\frac{\varepsilon}{N^3}\right)^{1/2}, \quad N \equiv \sqrt{g\alpha \frac{dT}{dz}}, \quad (8.31)$$

separates isotropic (smaller than ℓ_O) from anisotropic (larger than ℓ_O) motions; here N is the Brunt–Väisälä frequency.¹

¹In convective (unstably stratified) flows, one often uses ℓ_B for the BO/K41 crossover; in stable flows, ℓ_O controls isotropization. They arise from different balances: ℓ_B from buoyancy–inertia with scalar-flux constancy; ℓ_O from inertia–stratification ($\tau_\ell^{-1} \sim N$).

8.4.5 Contrast with Kolmogorov 1941 (K41)

Under K41 (homogeneous, isotropic, neutrally stratified turbulence with constant kinetic energy flux ε):

$$u_\ell^{(\text{K41})} \sim (\varepsilon \ell)^{1/3}, \quad E_u^{(\text{K41})}(k) \sim C_K \varepsilon^{2/3} k^{-5/3}. \quad (8.32)$$

For a passive scalar with constant scalar-variance flux ε_θ (Obukhov-Corrsin):

$$\theta_\ell^{(\text{OC})} \sim \varepsilon_\theta^{1/2} \varepsilon^{-1/6} \ell^{1/3}, \quad E_\theta^{(\text{OC})}(k) \sim C_\theta \varepsilon_\theta \varepsilon^{-1/3} k^{-5/3}. \quad (8.33)$$

Key differences. In BO, buoyancy does leading-order work at the inertial scales, replacing the constant kinetic-energy flux hypothesis by constant *scalar* flux; this steepens the velocity spectrum to $k^{-11/5}$ and yields $k^{-7/5}$ for temperature, cf. (8.25)–(8.27). Below ℓ_B (i.e. for $k \gg k_B$), buoyancy becomes negligible and the K41/OC scalings (8.32)–(8.33) are recovered.

8.4.6 Summary of BO scalings

$$\begin{aligned} u_\ell &\sim \varepsilon_\theta^{1/5} (g\alpha)^{2/5} \ell^{3/5}, & E_u(k) &\sim k^{-11/5}, \\ \theta_\ell &\sim \varepsilon_\theta^{2/5} (g\alpha)^{-1/5} \ell^{1/5}, & E_\theta(k) &\sim k^{-7/5}, \\ \ell_B &\sim \frac{\varepsilon^{5/4}}{(g\alpha \varepsilon_\theta)^{3/4}}, & k_B &\sim \frac{(g\alpha \varepsilon_\theta)^{3/4}}{\varepsilon^{5/4}}. \end{aligned}$$

In neutral (unstratified) turbulence, Kolmogorov's 1941 (K41) theory assumes that the inertial range is governed solely by the mean kinetic energy dissipation rate ε and the wavenumber k , leading to the well-known $k^{-5/3}$ spectrum.

In buoyancy dominated flows as the buoyancy forces play a leading role across a range of scales. This modifies the cascade: the kinetic energy flux is no longer constant, but instead the cascade of *temperature variance* (or potential energy) controls the inertial range. This is the *Bolgiano-Obukhov (BO) scaling*.

8.5 Connection to the -3 Spectra in LES of Buoyant Plumes

Large-eddy simulations (LES) of thermal and buoyant gas plumes by Chen & Bhaganagar report a robust k^{-3} kinetic-energy spectrum at low wavenumbers (“buoyancy range”), followed by a transition to the classical $k^{-5/3}$ inertial range at higher k . Their analyses also show positive helicity throughout plume development and identify baroclinic torque as a dominant source term in the vorticity dynamics.² ???

8.5.1 Governing balances: baroclinic torque and plume anisotropy

Under Boussinesq, the vorticity equation reads

$$\frac{D\boldsymbol{\omega}}{Dt} = (\boldsymbol{\omega} \cdot \nabla) \mathbf{u} - (\nabla \mathbf{u})^\top \cdot \boldsymbol{\omega} + \nu \nabla^2 \boldsymbol{\omega} + \underbrace{\frac{\nabla \rho \times \nabla p}{\rho^2}}_{\text{baroclinic}}, \quad (8.34)$$

so that misalignment between $\nabla \rho$ and ∇p (strong across the plume edge and in the rising cap region) injects vorticity and couples scalar and momentum. LES diagnostics show that this *baroclinic* term dominates plume vorticity production over broad regions and correlates with a spectral buoyancy range scaling as k^{-3} .?

The helicity density $h = \mathbf{u} \cdot \boldsymbol{\omega}$ is observed to be positive and to exhibit spectral fluxes mirroring those of TKE, consistent with an organization of motions into large, columnar, quasi-2D structures (“quasi-2Dization”) that favor enstrophy-like forward cascades in horizontal planes.?

²See Chen & Bhaganagar on plume vorticity dynamics and spectra, Phys. Fluids **33** (2021), and subsequent energetics/cascading studies showing a double cascade with a buoyancy -3 range and small-scale $-5/3$ range.

8.5.2 Why a -3 slope? Two complementary routes

(i) **Quasi-2D/potential-enstrophy cascade in horizontal planes.** At scales larger than a crossover but still within the plume body, horizontal motions are anisotropic and sheet-/column-like. If we consider horizontal wavenumbers k_h and assume a local, forward cascade of (potential) enstrophy with constant flux η_Q (as in 2-D and QG phenomenology), dimensional analysis yields

$$E_h(k_h) \sim C_Q \eta_Q^{2/3} k_h^{-3}, \quad (k_h \ll k_*), \quad (8.35)$$

where k_* marks the return toward fully 3-D isotropy (see below). This provides a natural *kinetic* -3 range without invoking K41 energy flux constancy, consistent with LES reports of a low- k -3 branch.??

(ii) **Buoyancy-range balance with baroclinic production.** Alternatively, at low k one can view the energy budget as

$$\underbrace{\mathcal{B}(k)}_{\text{buoyancy/baroclinic production}} \approx \underbrace{\Pi_E(k)}_{\text{spectral transfer}} \Rightarrow \Pi_E(k) \text{ set by } \mathcal{B}(k), \quad (8.36)$$

with \mathcal{B} dominated by the baroclinic work associated with $\theta-u$ correlations. If the effective enstrophy-like transfer controls the cascade rate in this buoyancy range, the same dimensional route as (8.35) recovers $E(k) \sim k^{-3}$, aligning with LES.?

8.5.3 Crossover to $-5/3$ and relation to BO

LES show a transition from the plume -3 buoyancy range to a small-scale $-5/3$ inertial range (K41-like) as k increases.? Define a buoyancy/anisotropy crossover wavenumber k_* (analogous in spirit to $k_B = 1/\ell_B$ or to Oztmidov/Zeman scales in

stably stratified/rotating flows):

$$k \ll k_* : E(k) \sim k^{-3} \quad \longrightarrow \quad k \gg k_* : E(k) \sim k^{-5/3}. \quad (8.37)$$

Note that the classical Bolgiano–Obukhov (BO) prediction for *isotropic* buoyancy-controlled ranges is $E_u(k) \sim k^{-11/5}$; the plume LES instead exhibit a *steeper* -3 at low k . This difference may be attributed to (i) strong anisotropy and coherent, columnar plume geometry (quasi-2Dization), (ii) dominant baroclinic vorticity production at large scales, and (iii) helicity-arrested dynamics shaping an enstrophy-like forward transfer in horizontal planes, all of which violate the BO hypotheses leading to $-11/5.???$

8.5.4 Practical identification in data

To diagnose this regime in simulations/experiments:

1. Compute $E(k)$ (or $E_h(k_h)$) and identify a low- k window with slope near -3 and a high- k window near $-5/3$.
2. Evaluate baroclinic alignment via $\cos \phi = \frac{\nabla \rho \cdot \nabla p}{|\nabla \rho| |\nabla p|}$ (PDFs peaking away from ± 1 indicate persistent misalignment), and correlate with regions of vorticity production.
3. Inspect helicity spectra/fluxes; similar trends to TKE spectra support quasi-2D, columnar organization and the enstrophy-like cascade picture.

These diagnostics reproduce the LES findings of a buoyancy -3 range and a double cascade, consolidating the physical origin of the observed spectra.??